

Journal of Architectural Research and Development

Honorary Editor-in-Chief

Pooya Lotfabadi

Eastern Mediterranean University, TRNC

Editors-in-Chief

Paolo Beccarelli

The University of Nottingham, UK

Rocio Maira Vidal

Spanish National Research Council, Spain

BIO-BYWORD SCIENTIFIC PUBLISHING PTY LTD

(619 649 400)

Level 10

50 Clarence Street

SYDNEY NSW 2000

Copyright © 2024. Bio-Byword Scientific Publishing Pty Ltd.

Complimentary Copy





Integrated Services Platform of International Scientific Cooperation

Innoscience Research (Malaysia), which is global market oriented, was founded in 2016. Innoscience Research focuses on services based on scientific research. By cooperating with universities and scientific institutes all over the world, it performs medical researches to benefit human beings and promotes the interdisciplinary and international exchanges among researchers.

Innoscience Research covers biology, chemistry, physics and many other disciplines. It mainly focuses on the improvement of human health. It aims to promote the cooperation, exploration and exchange among researchers from different countries. By establishing platforms, Innoscience integrates the demands from different fields to realize the combination of clinical research and basic research and to accelerate and deepen the international scientific cooperation.

Cooperation Mode



Clinical Workers



In-service Doctors



Foreign Researchers



Hospital



University



Scientific institutions

Table of Contents

- 1 Effect of Pore Structure on Purification of Pervious Concrete**
Xinping Li, Xiling Zhou
- 9 Research on the Application of Refined Management in Construction Industry Management**
Xuejun Ouyang
- 14 The Ecological Code of Landscape Cities: Traditional Feng Shui Patterns for Modern Sustainable Spatial Designs**
Bowen Dong
- 22 Research on Dam Safety and Risk Management in Water Conservancy Engineering**
Lihui Li, Dan Wu
- 28 Ecological Security Assessment and Risk Management Framework for Recycled Water Systems in Landscape Hydration**
Xinmiao Wang
- 32 The Influence of Coal Gangue Particle Gradation on the Performance of Inorganic Foamed Paste Backfill Materials**
Chonghui Fu, Chunwei Wang, Fengshun Zhang, Hucheng Chai, Liya Zhao, Xuemao Guan, Jianping Zhu, Haibo Zhang
- 52 Effect of Different Mineral Admixtures on the Dry Shrinkage and Mechanical Properties of Mortar**
Yanbin Zhu, Yi Wu, Linhui Wan, Xiling Zhou
- 60 Discussion on Smart Strategies for Barrier-Free Design of Outdoor Spaces in Healthcare and Wellness Buildings in Chongqing**
Linye Gao, Haihe Zhao
- 68 Atomic-Level Understanding of Contact Potential of Quartz Surface**
Lina Ma

Effect of Pore Structure on Purification of Pervious Concrete

Xinping Li, Xiling Zhou*

College of Water Conservancy and Civil Engineering, Hunan Agricultural University, Changsha 410128, Hunan, China

*Corresponding author: Xiling Zhou, zhouxiling@hunau.edu.cn

Copyright: © 2025 Author(s). This is an open-access article distributed under the terms of the Creative Commons Attribution License (CC BY 4.0), permitting distribution and reproduction in any medium, provided the original work is cited.

Abstract: By adding zeolite aggregate with good adsorption properties, different mix ratios of added zeolite pervious concrete (ZPC) were designed to compare the water purification effect of ordinary pervious concrete and water purification tests that were conducted. The pore characteristics of the pervious concrete were identified using three-dimensional reconstruction software and the relationship between pore structure and water purification performance was quantified by gray entropy correlation analysis. The results showed that the purification efficiency of zeolite-doped pervious concrete was 17.6%–22.3% higher than that of ordinary pervious concrete. The characteristic parameters of the pore structure of permeable concrete, i.e. planar porosity and tortuosity, were determined using three-dimensional reconstruction software. The correlation between the degree of tortuosity and the removal rate reached more than 0.90, indicating that the internal pore structure of pervious concrete has a good correlation with the water purification performance.

Keywords: Pervious concretes; Water purification; Pore structure characteristics; CT scanning

Online publication: April 4, 2025

1. Introduction

Numerous studies have demonstrated that pervious concrete exhibits excellent water purification properties and plays a significant role in treating pavement runoff^[1–3]. Given the severity of rural non-point source pollution, pervious concrete can effectively alleviate pollution loads. The pore structure characteristics play a crucial role in the removal of water pollutants, making it essential to explore the factors influencing its purification performance to provide guidance for improving its water purification capabilities.

Based on extensive research, pollutants purified by pervious concrete can be categorized into two types: organic nutrient pollutants, such as nitrogen and phosphorus, and heavy metal ions. Xie *et al.* investigated the water purification performance of sewage treatment using modified pervious concrete with varying biochar doping levels to evaluate its TN and TP removal capacities^[4]. Shang *et al.* introduced organoclay into pervious concrete to remove polycyclic aromatic hydrocarbons (PAHs) and other organic pollutants through isothermal adsorption experiments^[5]. Ali Yousefi *et al.* concluded that adding pumice aggregate to pervious concrete mixtures effectively removes heavy metals from aqueous solutions or urban runoff, with natural zeolites, silica fume, and iron oxides

also serving as heavy metal adsorbents and supplementary admixtures ^[6]. The aforementioned studies incorporated admixtures with adsorbent properties into pervious concrete to enhance its water purification performance.

The porous structure plays a crucial role in the functional performance of pervious concrete. The advantage of nondestructive scanning is that the distribution of aggregate and pore structure inside the ecological concrete specimen can be more accurately obtained without changing the morphology of the pervious concrete specimen and without affecting its internal aggregate and pore structure. CT scanning combined with digital image processing (DIP) techniques can quickly obtain microstructural images of pervious concrete. Zhang *et al.* used CT imaging technology to construct a visual virtual pervious concrete model, extracted and analyzed the pore structure characteristics of pervious concrete, and obtained a grid of connected pore models ^[7]. Zhou *et al.* used CT scanning and image processing technology to determine pore diameters and used code algorithms to compute pore geometric properties ^[8]. Wang *et al.* used X-CT scanning and image three-dimensional reconstruction technology to obtain a three-dimensional model of the internal pores of ceramic permeable pavement tiles, extracted the pore structure characteristic parameters, and carried out a correlation analysis of the pore structure characteristic parameters ^[9]. Thomas *et al.* evaluation by computerized axial tomography to understand the effect of continuous regeneration on concrete properties ^[10].

The complex pore structure inside pervious concrete plays a crucial role in its structure and properties. Characterizing the pore structure of pervious concrete and investigating its influence on its properties has become a current research trend. To further analyze the influence of pore structure characteristics of pervious concrete on water purification performance, this study constructs different pore structures by changing aggregate particle size gradation and scans the pervious concrete after curing and molding using CT technology for image identification and analysis. The static adsorption experiment was used to detect the water purification performance of permeable concrete for total nitrogen and the pore structure characteristic parameters were identified through three-dimensional reconstruction to obtain the key indexes for purifying pollutants. Gray correlation entropy analysis was used to analyze the degree of correlation between pore characteristic parameters and water purification performance.

2. Materials and methods

2.1. Materials

The cement used was P-O 42.5 ordinary silicate cement (OPC), the chemical composition of OPC is shown in **Table 1**. The crushed stone aggregate and zeolite aggregate were sieved through a square hole aggregate standard sieve. The crushed stone aggregate with a particle size of 10–15 mm and the zeolite aggregate with a particle size of 8–9 mm and 16–18 mm were selected.

Table 1. Chemical composition of OPC

Material	SiO ₂	CaO	Al ₂ O ₃	Fe ₂ O ₃	MgO	Na ₂ O	K ₂ O	SO ₃
Material content (by weight, %)	21.1	58.4	7.30	3.13	5.94	0.691	0.83	1.65

2.2. Mixing ratio

In this study, the aggregate grading of crushed stone of 10–15 mm and zeolite adsorbent aggregate of 8–9mm and 16–18mm were used first. The design ratio is shown in **Table 2**. According to the research of many scholars, it is known that the physical adsorbent property of zeolite-added permeable concrete (ZPC) will be improved by the increase of zeolite admixture ^[11–14].

Table 2. Mix proportion of pervious concrete

Number	Designed porosity(%)	Aggregate(g)	Zeolite(g)	Cement(g)	Water(g)
EC		1440	0		
ZPC-1	25	1296	144	500	130
ZPC-2		1152	288		
ZPC-3		1008	432		

2.3. Preparation and maintenance

This test employs the cement paste-wrapped stone method and considers two mixing techniques for pervious concrete: manual insertion pounding and mechanical vibration. Although mechanical vibration is relatively simple to operate, its vibration time and amplitude are difficult to control. Additionally, given the small overall volume of the test, this study uses the manual insertion pounding method.

The standard mold used was a three-link mold with dimensions of 100 mm × 100 mm × 100 mm. After 24 hours, the specimens were demolded and placed in a constant temperature and humidity curing box, maintained at 20 ± 2°C and 95 ± 2% relative humidity.

2.4. Water purification performance test

This experiment used static adsorption experiments to investigate the purification effect of different zeolite particle size content on the simulated water pollutants and the factors affecting them in the static water state. Water quality tests are conducted every 6 hours, relying on the removal rate to analyze the performance of water purification. The rate was calculated using the equation below and the permeable concrete test block ratios are recorded.

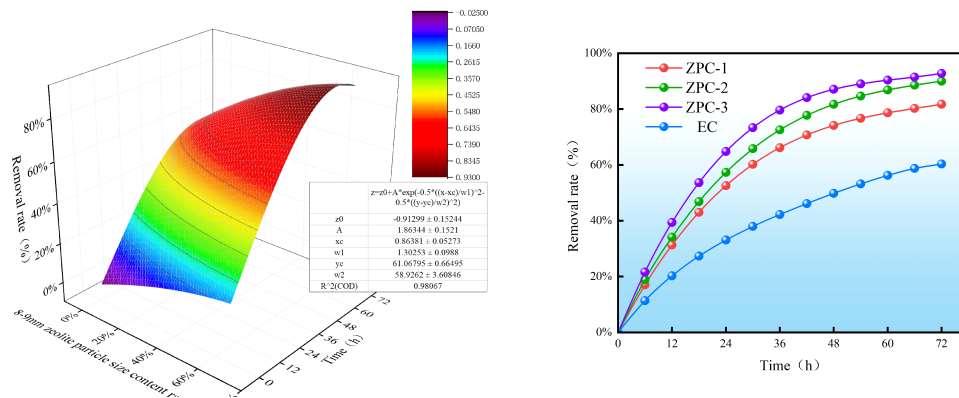
$$\eta = \frac{C_0 - C_i}{C_0}$$

In this equation, η is the removal rate of pollutants(%), C_0 is the raw water pollutant concentration(mg /L), and C_i is the pollutant concentration(mg /L).

3. Results and discussion

3.1. Water purification performance

The surface fitting method was used to establish the functional relationship between time, zeolite gradation percentage, and removal rate, and the R^2 reached 0.980. As shown in **Figure 1**, the fitting curves of time, 8–9mm zeolite particle size, and removal rate were obtained.

**Figure 1.** Three-dimensional/two-dimensional effect of total phosphorus purification with three mixing ratios

The corresponding fitting equations are as follows:

$$Rr = -0.864 + 11.023 \times \exp(-0.5 \times ((ZP_{8-9mm} - 13.972) / 6.992)^2 - 0.5 \times ((T + 76.607) / 74.427)^2)$$

In this equation, Rr denotes the removal rate of total phosphorus, ZP_{8-9mm} denotes 8–9 mm zeolite particle size content, and T denotes test time. The curve fitting results show that the increasing trend of the removal rate with the increase of 8–9 mm zeolite particle size content is more significant with the increase of test time. It is because with the increase of 8–9 mm zeolite particle size content, the internal surface area of concrete increases and the total phosphorus contacts more attachment points, thus improving the purification effect.

In the whole experiment, the results of zeolite-doped pervious concretes and ordinary concrete are shown in **Figure 1**. Ordinary pervious concrete has some ability to purify total phosphorus, but its effectiveness is lower compared to zeolite-doped pervious concrete. The removal rate of zeolite-doped pervious concrete is 21.4% to 32.45% higher than that of ordinary pervious concrete, demonstrating its superior ability to purify total phosphorus. This is because zeolite is a porous aluminum silicate crystal with a skeleton structure. In the initial stage of adsorption, the removal rate of total phosphorus increases significantly with time, and then gradually tends to slow down until the adsorption equilibrium, which shows the characteristics of “fast adsorption, slow equilibrium”. The effect of zeolite particle size and content on the adsorption equilibrium time is also relatively significant; the smaller the particle size of the zeolite content, the faster the adsorption, and the shorter the time required to reach the adsorption equilibrium. This is because the size of the particle on the specific surface area of phosphorus and adsorbate diffusion rate has an impact; the smaller the particle size, the larger the specific surface area, and the adsorbate diffusion rate is also larger, which is more favorable to the adsorption.

3.2. Analysis of planar porosity variation

To better reflect the influence of the internal pore structure of the pervious concrete on the water purification performance, the porosity of each layer cross-section was extracted equally spaced along the height direction of the specimen to obtain the planar porosity. **Figure 2** shows the two-dimensional porosity distribution of the specimens along the Z-axis, and its variance is shown in **Table 3**.

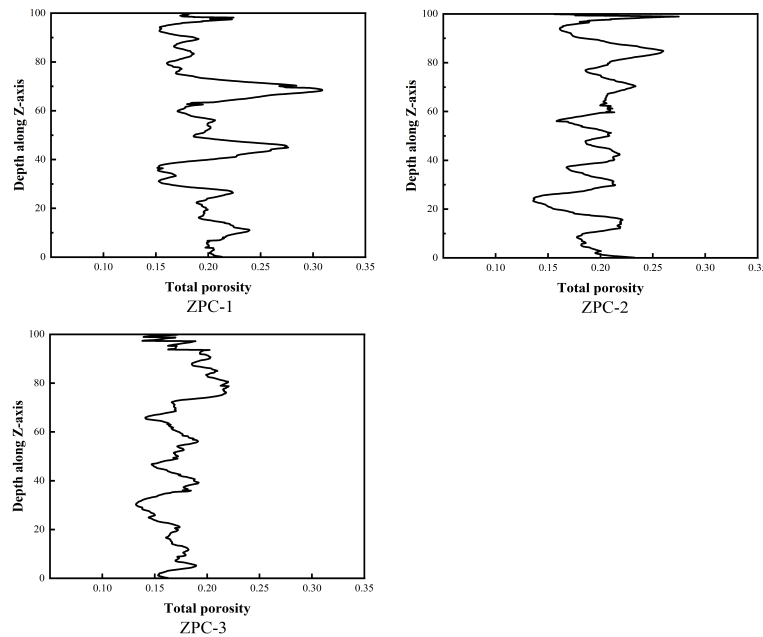


Figure 2. The porosity changes in different planes

Table 3. Results of 2D pore structure of ZPC.

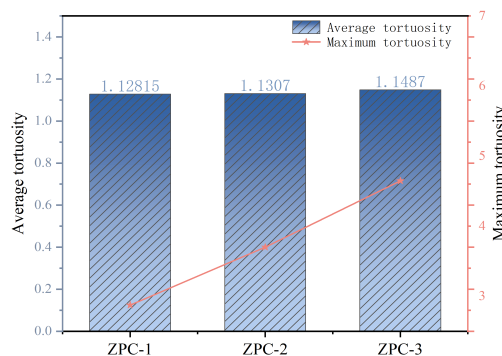
Number	ZPC-1	ZPC-2	ZPC-3
Variance	0.0011	0.0006	0.0004

The larger value of the variance of the two-dimensional porosity change indicates that the homogeneity of the planar porosity decreases. In ZPC-1, ZPC-2, and ZPC-3, the internal pore structure exhibits different trends. As the content of 8–9 mm zeolite particles increases, the variation in two-dimensional porosity with depth remains minimal. The variance of ZPC-1 is the highest at 0.0011, whereas ZPC-3 shows a significantly lower variance of 0.0004. This indicates that permeable concrete specimens prepared with smaller-sized aggregates have a more uniform pore distribution. Additionally, aggregate particle size plays a crucial role in influencing the uniformity of pore distribution. Additionally, the porosity remained relatively stable without significant fluctuations near the top and bottom surfaces of the specimens, indicating that the top-bottom tamping was effective during the casting process.

Overall, ZPC-3 exhibits the lowest planar porosity and the uniformity of pore distribution improves as the content of 8–9 mm zeolite particles increases. This is closely linked to water purification performance, as the smaller-sized aggregates fill the interior of the ZPC, reducing overall porosity while enhancing planar porosity uniformity. This improved uniformity allows for better contact with pollutants during adsorption, leading to more effective purification. Therefore, water purification performance is positively correlated with planar porosity uniformity.

3.3. Analysis of changes in tortuosity

A higher tortuosity indicates a more complex internal pore structure within the porous concrete, creating a more intricate and rugged path for artificial simulated pollutants to travel from the top to the bottom. Additionally, the reticulated structure of zeolite in ZPC, along with the surface characteristics of the pore holes, prolongs the retention time of the pollutant solution. The curved pore channels further enhance contact, allowing for more effective pollutant adsorption and filtration. As shown in **Figure 3**, the average tortuosity of ZPC-1, ZPC-2, and ZPC-3 exhibits an increasing trend. This suggests that as the content of 8–9 mm zeolite particles increases and the proportion of 16–18 mm zeolite particles decreases, the internal pore structure of ZPC becomes more complex. The maximum tortuosity of ZPC-3 reaches 4.65, which is higher than that of ZPC-1 and ZPC-2. Combined with the experimental results, it can be concluded that a higher average tortuosity correlates with improved purification performance of ZPC for total phosphorus.

**Figure 3.** Tortuosity parameter analysis diagram of specimen

3.4. Multivariate regression analysis

The one-dimensional linear analysis of planar porosity and average tortuosity versus removal rate can be concluded that there is a good correlation between the pore structure parameters and water purification performance, as shown in **Figure 4** and **Figure 5**. All of them can reach R^2 above 0.9.

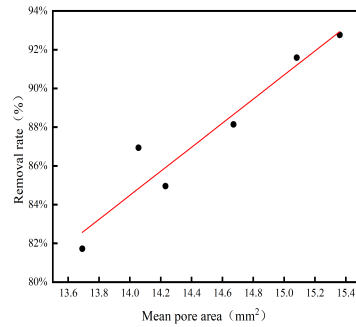


Figure 4. Fitting effect of plane porosity and removal rate

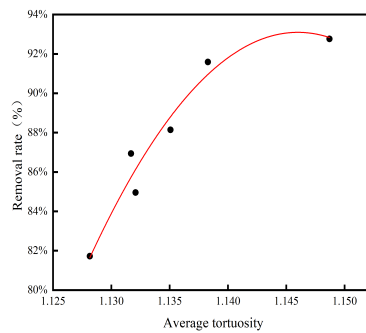


Figure 5. Fitting effect of average tortuosity and removal rate

The univariate linear regression equation obtained from the linear fit of mean pore area to removal rate is shown below:

$$R_1 = 0.0621x_1 - 0.02454$$

$$R_1 = -359.55711x_2 + 824.10217x_2 - 471.27802$$

In this equation, R_1 is the removal rate(%), x_1 is average pore area(mm^2), x_2 is average tortuosity. As seen in **Table 5** and **Table 6**, the planar porosity was linearly distributed with water purification performance, and the R^2 adjusted was 0.9042, which had a good fitting status. The results of polynomial fitting of mean tortuosity to water purification performance when R^2 is adjusted to 0.8691 are greater than the linear fitting results, indicating that for linear fitting, polynomial fitting is more suitable to characterize the tortuosity in relation to the permeability coefficient. The derived regression equation is as follows.

Table 5. One-dimensional linear fit of mean pore area to removal rate

	DF	Square sum	Mean square	F	Probability > F
Mould	1	0.00783	0.00783	48.19975	0.00226
Inaccuracies	4	6.50151E-4	1.62538E-4		
Total	5	0.00848			
Adjusted R^2	0.90421				

Table 6. One-dimensional linear fit of average tortuosity to removal rate

	DF	Square sum	Mean square	F	Probability > F
Mould	2	0.00376	0.00188	14.28322	0.06543
Inaccuracies	2	2.62909E-4	1.31454E-4		
Total	4	0.00402			
Adjusted R ²			0.86914		

4. Conclusion

In this paper, different mixing ratios of zeolite-doped pervious concrete specimens are prepared. Based on CT scanning technology, to obtain the microscopic internal pore structure characteristic parameters of pervious concrete and the method of multiple regression analysis, the main conclusions are as follows:

- (1) The porosity of zeolite-added pervious concrete with different mixing ratios at different heights is distributed in wave shape, the uniformity of planar porosity is positively correlated with the water purification performance, and the average tortuosity is positively correlated with the water purification performance.
- (2) The planar porosity and tortuosity have good correlation with the removal rate and this result indicates that there is a close relationship between the internal pore structure of zeolite-added pervious concrete and its water purification performance.

Funding

Hunan Provincial Department of Water Resources: Research on Formula Optimization and Performance Evaluation System of Ecological Concrete for River Water Quality Purification Based on the Dual Carbon Goal (Project No.: XSKJ2024064-44)

Disclosure statement

The authors declare no conflict of interest.

References

- [1] Azad A, Saeedian A, Mousavi SF, et al., 2020, Effect Of Zeolite And Pumice Powders On The Environmental And Physical Characteristics Of Green Concrete Filters. *Construction And Building Materials*, 240: 117931.
- [2] Kurtay M, Gerengi H, Kocak Y, et al., 2020, The Potency Of Zeolite And Diatomite On The Corrosive Destruction Of Reinforcing Steel In 1 M HNO₃ Environment. *Construction And Building Materials*, 236(3): 117572.
- [3] Yang S, Guo M, Duan S, et al., 2019, Study On Strength Variation Of Permeable Concrete Based On Differential Calorimetry Method And Multi-Index Test. *Advances In Materials Science And Engineering*, 2019(9): 1–9.
- [4] Jia J, Yu Y, Guo Y, et al., 2021, Study On Composition Design Of Water-Purifying Functional Pervious Concrete. *Bulletin Of The Chinese Ceramic Society*, 40(08): 2554–2563.
- [5] Shang H, Sun Z, 2019, PAHs (Naphthalene) Removal From Stormwater Runoff By Organoclay Amended Pervious Concrete. *Construction And Building Materials*, 200: 170–180.
- [6] Yousefi A, Matavos-Aramyan S, 2018, Mix Design Optimization Of Silica Fume-Based Pervious Concrete For

Removal Of Heavy Metals From Wastewaters. *Silicon*, 10(4): 1737–1744.

- [7] Zhang J, Ma G, Ming R, et al., 2018, Numerical Study On Seepage Flow In Pervious Concrete Based On 3D CT Imaging. *Construction And Building Materials*, 161: 468–478.
- [8] Zhou H, Li H, Abdelhady A, et al., 2019, Experimental Investigation On The Effect Of Pore Characteristics On Clogging Risk Of Pervious Concrete Based On CT Scanning. *Construction And Building Materials*, 212: 130–139.
- [9] Wang Y, Tan J, Li W, et al., 2024, Quantitative Relationship Model Research Between Pore Characteristic And Permeability Coefficient Of Permeable Pavement Brick. *Journal Of Building Materials*, 27(02): 174–180.
- [10] Liu S, Chen X, Li S, et al., 2021, Mesoscopic Structure Analysis Of Recycled Aggregate Ecological Porous Concrete Based On CT. *Water Resources And Hydropower Engineering*, 52(02): 174–183.
- [11] Liu J, Li Y, 2020, Runoff Purification Effects Of Permeable Concrete Modified By Diatomite And Zeolite Powder. *Advances In Materials Science And Engineering*, 2020(2): 1–11.
- [12] Sudagar AJ, Andrejkovicova S, Rocha F, et al., 2023, Compressive Strength And Heavy Metal Adsorption Of Cork Residue, Natural Zeolite, And Low-Grade Metakaolin-Based Geopolymers. *Construction And Building Materials*, 366: 130125.
- [13] Teymouri E, Wong KS, Tan YY, et al., 2023, Mechanical Behaviour Of Adsorbent Pervious Concrete Using Iron Slag And Zeolite As Coarse Aggregates. *Construction And Building Materials*, 388: 131720.
- [14] She X, Chen J, 2021, Research Progress On Preparation And Properties Of Zeolite Porous Concrete. *New Building Materials*, 48(10): 75–79 + 99.

Publisher's note

Bio-Byword Scientific Publishing remains neutral with regard to jurisdictional claims in published maps and institutional affiliations.

Research on the Application of Refined Management in Construction Industry Management

Xuejun Ouyang*

Jiangxi Provincial Tourism Group, Nanchang 330200, Jiangxi, China

*Corresponding author: Xuejun Ouyang, hdp816@163.com

Copyright: © 2025 Author(s). This is an open-access article distributed under the terms of the Creative Commons Attribution License (CC BY 4.0), permitting distribution and reproduction in any medium, provided the original work is cited.

Abstract: Refined management, as a management concept and method that pursues efficiency, quality, and low consumption, has been applied in various industries. Due to its particularity, the construction industry needs to strengthen management and refined management has become the primary choice for the industry, which is of great significance for its stable development. The article elaborates on the definition of refined management, analyzes the necessity of refined management in the construction industry, and explores the application measures of refined management in construction industry management, aiming to provide reference for improving the management level of the construction industry.

Keywords: Refined management; Construction industry; Cost management; Security management

Online publication: April 4, 2025

1. Introduction

Under the rapid development trend of the construction industry, the traditional extensive management mode is no longer able to meet the requirements of modern construction projects in terms of quality, cost, schedule, and other aspects. To make up for this deficiency, a refined management mode has emerged. As a new management concept, refined management requires enterprise managers to start from details and strengthen their attention to management processes and execution capabilities to improve the overall operational efficiency and competitiveness of construction enterprises. Therefore, the construction industry should attach importance to the introduction and application of refined management and maximize its application effect.

2. Definition of refined management

Fine management refers to the scientific and effective approaches employed by enterprise managers to implement refined and systematic control over various management processes. The goal is to enhance management efficiency, reduce costs, improve product quality, and strengthen the overall competitiveness of the enterprise. Refined management is characterized by a strong emphasis on details, processes, implementation, and results.

As an inevitable trend in enterprise management reform, it can inject vitality into the long-term development of enterprises.

3. Necessity of refined management in the construction industry

The construction industry, characterized by large project scales, long cycles, and extensive involvement, presents an inherently high level of management complexity. The traditional extensive management model often struggles to comprehensively and accurately control every aspect of the project, resulting in frequent problems and low efficiency during project execution. The introduction of refined management can help the construction industry solve this problem. Firstly, refined management breaks down a large construction project into several specific and actionable small projects or tasks by subdividing the management objects, making management more targeted and operable. Building on this foundation, each specific task can be further refined and broken down, with clear designation of responsible parties, timelines, and completion standards to ensure effective execution and monitoring. For the construction industry, this refined management approach can greatly improve the efficiency and quality of project execution^[1].

Secondly, refined management also refines various implementation links of management systems, ensuring that management systems can truly take root and play a role. In the process of refined management, construction enterprises establish a sound management system, clarify the responsibilities and authorities of management personnel at all levels, and form a hierarchical and interconnected management chain, making project management more standardized and orderly. Finally, refined management helps to improve the management level of construction enterprises and reduce management costs. Through refined management, construction enterprises can more effectively utilize resources, avoid waste and repetitive labor, and thus improve resource utilization efficiency. In the fierce market competition, construction enterprises can only improve their management level and reduce costs through refined management to win more market share and customer trust, thus occupying a favorable position in the market competition.

4. Application measures of refined management in construction industry management

4.1. Refined cost management

Cost management occupies a core position in the management of the construction industry and is a key link in ensuring project profitability. By implementing refined management, construction enterprises can gain a deeper understanding and grasp of the cost composition and dynamic changes of projects, thereby achieving precise cost control. To achieve refined cost management, construction enterprises need to take the following measures. Firstly, establish a scientific cost management system. The system should define the responsibilities of cost managers, establish clear cost control objectives, and ensure that all relevant personnel fully understand and prioritize cost management. By formulating detailed cost management systems and processes, construction enterprises can further standardize cost management practices and enhance overall management efficiency.

Secondly, strengthen the accuracy and scientificity of budget preparation. Construction enterprises should conduct sufficient market research and historical data analysis in cost budget management, predict project costs reasonably, and ensure the rationality and feasibility of the budget^[2]. Additionally, construction enterprises should establish a budget adjustment mechanism to promptly modify the budget based on the project's actual conditions, ensuring its flexibility and adaptability. Third, use information technology to monitor and analyze cost data in real-time. By introducing advanced cost management software, construction companies can track cost changes in real

time, detect and solve cost overruns in a timely manner, thereby improving the timeliness of cost management and reducing the risk of human errors. Moreover, strengthen the supervision and management of contract execution. Construction companies should ensure clear and concise contract terms to avoid cost disputes caused by vague contract terms. Based on this, a sound contract execution tracking mechanism should be established to promptly identify and resolve problems that arise during contract performance, ensuring effective control of contract costs ^[3].

4.2. Refined material management

The cost of materials plays a crucial role in the total cost of construction projects, therefore, implementing refined management of materials is essential for controlling project costs and improving material utilization efficiency. Firstly, to implement refined material management, construction enterprises should develop a comprehensive material list that includes essential details such as material name, specifications, quantity, and intended use. Additionally, a supplier information database should be established to thoroughly assess suppliers' qualifications, reputation, pricing, and supply capacity, ensuring timely delivery and reliable material quality. By understanding suppliers, construction companies can establish long-term cooperative relationships with high-quality suppliers, further reduce material procurement costs, and improve procurement efficiency. Secondly, in terms of inventory management, construction companies should strengthen the management of material warehousing, outbound, and inventory to ensure the accuracy and real-time nature of inventory data ^[4].

Based on a comprehensive understanding of inventory materials, construction companies can set reasonable safety stock levels to avoid material backlog and waste, while ensuring continuous supply of materials at the construction site. In addition, construction companies should regularly check and organize their inventory materials, promptly dispose of idle and expired materials, and reduce inventory costs. To standardize the use of materials, construction enterprises should also establish strict systems for material collection and use, clarify the process and approval authority for material collection, and ensure the rationality and necessity of material use. Moreover, utilize information technology to monitor and analyze the real-time usage of materials. To manage building materials reasonably, construction enterprises can introduce material management systems to track the flow and usage of materials in real time and promptly discover and solve material waste problems. In this process, construction companies can optimize material procurement plans and usage schemes by conducting in-depth analysis of material usage data, further improving material utilization efficiency ^[5].

4.3. Refined safety management

Safety is a prerequisite for the smooth progress of construction projects and a key factor in ensuring the safety of construction personnel. To achieve refined safety management, construction enterprises need to take a series of practical and effective measures to control safety risks at the lowest level. In the process of achieving this goal, construction enterprises need to start from the following aspects. Firstly, enterprises need to establish a sound safety management system and process system. For construction enterprises, in the process of safety management, it is necessary to clarify the division of safety responsibilities among management personnel at all levels, so that each link has a dedicated person responsible and accountable ^[6]. At the same time, detailed safety operating procedures should be formulated to regulate employee behavior and reduce safety hazards. In addition, construction companies need to develop comprehensive emergency plans to ensure that they can quickly activate response mechanisms and effectively control the development of the situation in the event of a safety accident.

Secondly, construction companies need to effectively strengthen safety education and training for construction personnel. Construction companies should regularly organize various safety training courses, systematically impart safety production knowledge, operating procedures and emergency response methods to construction personnel,

and ensure that construction personnel can comprehensively and proficiently master and correctly apply this knowledge through various forms such as case analysis and on-site demonstrations ^[7]. In addition, construction companies should actively create a safety culture atmosphere and encourage construction personnel to actively participate in various safety activities, such as safety knowledge competitions, emergency drills, etc., to enhance the safety responsibility and self-protection awareness of construction personnel and build a solid defense line for construction safety. Thirdly, strengthen the inspection and maintenance of construction equipment and tools. Construction companies should regularly inspect, repair, and maintain construction equipment and tools to ensure that they are in good working condition and avoid safety accidents caused by equipment failures. At the same time, construction enterprises should establish equipment management systems, clarify the responsibilities for the use, storage and maintenance of equipment, and ensure the safety and reliability of equipment ^[8].

4.4. Refined quality management

Quality is the lifeline of construction projects, directly related to the service life and safety of building products. To achieve refined quality management, construction enterprises need to take comprehensive and effective measures to ensure strict control of construction quality and significant improvement of building product quality ^[9]. Firstly, establish a scientific and comprehensive quality management system and process. When building a quality management system, construction enterprises should clarify the specific responsibilities of quality responsible persons at all levels, set clear and measurable quality control objectives, and provide clear direction for quality management work. Construction enterprises also need to establish detailed and comprehensive quality management systems and operating procedures, standardize quality management behavior, and ensure that every detail in the construction process is strictly executed following quality standards. This can effectively improve the overall construction quality and lay a solid foundation for the long-term development of construction enterprises.

Secondly, to grasp the construction quality status in real time, construction enterprises can use information technology to monitor and analyze the construction quality in real time. In this process, construction companies can introduce quality management software, install quality monitoring equipment, etc., to track quality data in real time during the construction process, discover and solve quality problems in a timely manner, and prevent the occurrence of quality accidents. Finally, strengthen the inspection and acceptance of the construction process and finished products. Construction enterprises should establish strict inspection and acceptance systems, clarify inspection standards and acceptance procedures, and ensure that the quality of the construction process and finished products meets relevant standards and specifications. At the same time, construction enterprises should strengthen the training and management of inspection and acceptance personnel, improve their professional quality and sense of responsibility, and ensure the accuracy and reliability of inspection and acceptance work ^[10].

5. Conclusion

In summary, as an advanced management method, the application of refined management in the construction industry has significant implications for improving enterprise management level, reducing management costs, and enhancing economic benefits. For the construction industry, in the process of applying refined management, measures such as cost management refinement, material management refinement, safety management refinement, and quality management refinement should be taken to improve their own management level, to adapt to the needs of the times. With the continuous development of the construction industry and the intensification of market competition, refined management will become the key to enhancing the core competitiveness of construction enterprises. Therefore, construction enterprises should actively introduce refined management concepts and methods, continuously improve and optimize their management systems, and inject new impetus into the

sustainable development of the enterprise.

Disclosure statement

The author declares no conflict of interest.

References

- [1] Zhang Z, 2025, The Application of Refined Management in Construction Project Management. *Development Orientation of Building Materials*, 23(2): 94–96.
- [2] Wang L, 2025, The Application of Refined Management in Construction Project Management. *Engineering Construction and Design*, 2025(1): 246–248.
- [3] Wang Q, Ding X, 2024, Fine-Tuned Construction Strategy Design Combining BIM Technology and Fuzzy Comprehensive Evaluation. *Journal of Heilongjiang Institute of Technology (Comprehensive Edition)*, 24(8): 123–128.
- [4] Jiang X, 2024, Application of Fine Management in Real Estate Construction Project Management. *Residential and Real Estate*, 2024(34): 109–111.
- [5] Zhao X, 2024, Application of Fine Management in Housing Construction Project Management. *Residential and Real Estate*, 30(23): 119–122.
- [6] Cai D, 2024, Research on the Application of Fine Management Mode in Construction Project Management. *Real Estate World*, 32(9): 92–94.
- [7] Wang J, 2024, The Application of Refined Management Mode in Construction Project Management. *Residential Industry*, 2024(11): 193–195.
- [8] Huang N, 2023, Practical Research on Fine Management in Construction Management Work. *Building Materials Development Direction*, 21(24): 162–164.
- [9] Tong J, 2024, The Effective Application of Refined Management Concept in Material Management of Construction Enterprises. *China Logistics and Procurement*, 2024(17): 69–70.
- [10] Wang X, 2024, Application of BIM Technology in Fine Management of Construction Stage in Building Engineering. *Urban Architecture*, 21(24): 219–222.

Publisher's note

Bio-Byword Scientific Publishing remains neutral with regard to jurisdictional claims in published maps and institutional affiliations.

The Ecological Code of Landscape Cities: Traditional Feng Shui Patterns for Modern Sustainable Spatial Designs

Bowen Dong*

University of Liverpool, Liverpool, United Kingdom

**Corresponding author:* Bowen Dong, Bowen.Dong21@gmail.com

Copyright: © 2025 Author(s). This is an open-access article distributed under the terms of the Creative Commons Attribution License (CC BY 4.0), permitting distribution and reproduction in any medium, provided the original work is cited.

Abstract: The traditional Feng Shui pattern embodies rich ecological wisdom and philosophical thoughts, which are of great significance to the modern sustainable space design. The core concepts of Feng Shui patterns from traditional civilization can provide a theoretical foundation and research framework for this study. By integrating these principles, such as “hiding the wind and gathering the Qi” and “backing the mountain and facing the water”, a functional relationship between urban structures can be established. This approach can help optimize the spatial layout of urban elements, minimize energy consumption, and enhance environmental comfort. It also examines the influence of the ShanShui City pattern in traditional Feng Shui on guiding the development of modern urban ecological networks, as well as its role in protecting and restoring biodiversity through ecological corridors and ecological nodes. The modern urban design of traditional Feng Shui culture focuses on the inheritance and innovation of riotous things and the combination of traditional Feng Shui concepts and modern design concepts to form ecological spaces with cultural connotation. This paper hopes to give some inspiration or methods for contemporary urban design and to reconcile the relationship between human and nature through these thoughts.

Keywords: ShanShui City; Ecological code; Traditional Feng Shui pattern; Modern sustainable space design; Ecological balance

Online publication: March 28, 2025

1. Introduction

As urbanization continues to accelerate, cities are gradually maturing while also facing many ecological and habitat problems and how to achieve ecological harmony in urban design has become an important issue. Traditional Feng Shui pattern, as a form of ancient ecological wisdom, emphasizes the harmonious coexistence of human and nature, and contains rich ecological significance and philosophical thoughts. The analysis of the influence of traditional Feng Shui patterns on the modern urban design can optimize the spatial layout of cities and buildings, improving the ecological resilience of cities and the quality of life of residents. This paper will discuss the inspiration of traditional Feng Shui pattern for modern sustainable space design, analyze how it is applied in space layout optimization, ecological network construction, cultural inheritance and innovation, and give new

ideas and methods for modern city design.

2. Traditional Feng Shui patterns —core concepts

2.1. The essence of Feng Shui

(1) The aiming concept: The four “Qi”, “wind” and “water” of Feng Shui and their ecological implications

Qi is the fundamental principle behind Feng Shui and the life force of the universe understood to be omnipresent and constantly moving. This flow and gathering of Qi also has a direct impact on a person’s fortune and health. In the context of ecology, Qi can be interpreted as the flow of energy within the natural environment, including air, sunlight, and geothermal heat. By harnessing these energy sources as potential generators and maximizing their synergy across a broad area, a stable and sustainable regional ecological environment can be formed. According to Fengshui, “hiding the wind and gathering the Qi”, that is to say, a reasonable environmental layout can help gather and maintain auspicious Qi and avoid the influence of bad factors.

The wind is considered one of the factors that is always dispersed Qi in the Feng Shui, so it is necessary to avoid an excessive wind frontal impacted to the living environment. In ecology, the effect of wind in nature is ultimately reflected in air circulation and climate regulation. Moderative wind can supply fresh air, but too strong wind can stimulate energy loss and environment instability.

Water in Feng Shui represents the flow of wealth and fortune, and clear, meandering rivers are believed to impart prosperity and vitality to the surrounding area. Water in ecology is the origin of life. Water bodies can moderate the climate, enrich the land, and sustain different life forms. As an example, Hong Kong Victoria Harbor, the asymmetric bay shape not only brings landscape beauty to the city, but also relieves the heat island effect of the city through the regulating effect of water body, which improves the quality of the city’s ecological environment.

(2) Analyzing how Feng Shui patterns influence the energy flow and material circulation in the environment

Feng Shui patterns focus on optimizing spatial layouts to ensure the free flow and accumulation of Qi, aligning with the principles of energy (material) circulation in the environment. For example, mountain ranges are believed to channel and guide the Earth’s Qi, influencing its movement and enhancing the surrounding environment. Among natural elements, large bodies of water, where Qi tends to accumulate, are considered the most beneficial, followed by wind, which plays a secondary role. Rational architectural planning and directional collection can lure and settle good Qi, avoid bad factors, and serve the goal of improving the living and working environment.

Ecology, in this configuration supports air flow, climate, soil and water retention, and encourages living organisms. Essentially, for a design closer to the water source, but not facing directly to the water flow, it is helpful to regulate the microclimate, reduce the occurrence of diseases, reasonable distribution of vegetation, taking terrain design into consideration to maintain soil and water, and effective propulsion of material circulation. For instance, with the Hakka roundhouses in southern China, the layouts of the buildings are typically designed to face the paddy field and have their back toward the hilly area, forming a good ecological circulation system. The grasses on the hills help stabilize the soil, preventing erosion, while paddy fields and mulched farmland contribute to a life-supporting environment by enhancing moisture levels through evaporation. These agricultural landscapes also regulate local climates and support diverse ecosystems, promoting ecological balance.

2.2. Elements of traditional Feng Shui layout

(1) Landscape, topography, and vegetation as well as their importance in Feng Shui layout

From a Feng Shui perspective, the mountains, topography, and vegetation are natural elements that help

the layout arrangement. Mountains are considered as the head of Feng Shui, symbolizing stability, solidity, and longevity. The height, shape, and orientation of mountains affect the landscape and well-being of the inhabitants. For example, having a dominant high peak and symmetrical peak on the left and right in a mountain range is the most ideal Feng Shui pattern for positive energy gathering.

According to Bagua theory and the Five Elements, the orientation of the mountains determines the fortune of the occupants. The height can be the height of the land, the height of the slope near the building, and the shape of the valley surrounding the environment. An environment of high ground is often a territory of talent, whereas low-lying areas might just be graced by riches and fortune.

Feng Shui also sees the importance of vegetation. The greenery on the hills must be dense and flourishing, which will increase the gathering of energy. On the other side, mountains with barren and dry plants may produce bad energy, which leads to a bad impact on the inhabitants. Based on Shen *et al*, Huangshan Mountain located in Anhui Province of China, the unique of the mountain shape and superb vegetation not only provides rich tourism resources for the area but also maintains soil and water and regulates the climate through the ecological function of vegetation, which provides an important base support for the ecological environment of the adjacent areas.

(2) Balanced relationship among the buildings and the nature

The most crucial one of traditional Feng Shui patterns considers the nature of the relationship between buildings and nature as harmonious and symbiotic and believes that the perfect combination of the two is a core principle that needs to be pursued. These principles, particularly the layout concepts of “backing the mountain and facing the water” and “hiding wind and gathering Qi”, exemplify the ancient people’s deep understanding of natural laws and their enduring pursuit of an ideal living environment.

The pattern of “back to mountains and front to water” carries profound cultural significance and practical value. In Feng Shui concepts, the mountain serves as a steadfast protector, shielding the back of the house. This not only provides structural support but also blocks cold northern winds and potential natural disasters, such as landslides and mudslides, ensuring a stable and undisturbed living environment. At the front, flowing water symbolizes vitality and prosperity. The movement of water represents the continuous cycle of life, while its shimmering presence enhances the visual beauty of the surroundings. Beyond aesthetics, water is believed to bring fortune and abundance. Many ancient village houses reflect this ideal layout, nestled against picturesque mountains with clear streams flowing in front. In such environments, villagers have long experienced harmony and prosperity, deeply connected to nature.

The principle of gathering wind and Qi should not be overlooked when creating an ideal living environment. A well-balanced space should be designed to shield against harsh winds while allowing Qi to circulate smoothly and accumulate rather than disperse. This fosters an atmosphere of stability, prosperity, and auspicious energy. From a practical perspective, if a home’s front door directly aligns with a window or a back door, Qi flows straight through without settling, making it difficult to form a harmonious energy field. To counteract this, traditional courtyard designs often incorporate strategically placed walls, screens, or partitions. These elements not only maintain spatial ventilation but also guide airflow in a way that allows Qi to twist and circulate within, effectively achieving the feng shui principle of “hiding wind and gathering Qi”.

The orientation of a building is important for creating a comfortable living space. Sunlight, wind direction, and temperature affect different directions in different ways. A well-placed building can stay warm in winter by absorbing sunlight and cool in summer by using natural breezes. Choosing the right orientation helps make a home more comfortable and energy-efficient. A good example is Wuzhen in Zhejiang Province, China, where traditional houses are built to fit the natural landscape. With mountains and water nearby, and tall trees and hills behind, the layout creates a peaceful and eco-friendly environment.

3. Key elements of modern sustainable space design

3.1. Ecological balance and biodiversity

It is vital to protect and restore the integrity of natural ecosystems in urban design. The natural heritage of the city must be protected, not only for the current benefit of mankind but also to maintain the potential needed for future generations. Specifically, the protection, maintenance, sustainable use, restoration, and enhancement of the environment are key to achieving this goal. For example, protecting natural areas such as natural river basins, coastlines, and forests ensures that these ecosystems can continue to fulfill their ecological functions. In addition, by rationally planning urban space and avoiding overdevelopment and destruction of natural habitats, pressure on ecosystems can be effectively reduced, thereby maintaining ecological balance. Taking Singapore as an example, the country attaches great importance to the protection of natural ecosystems in its urban planning. By establishing several nature reserves and national parks, such as the Gardens by the Bay and the U Min Island Nature Reserve, the country protects the rich biodiversity and at the same time provides opportunities for urban residents to get close to nature.

Green infrastructures, such as urban parks and green space networks, are effective means to promote biodiversity. These green spaces not only provide urban residents with places for leisure and recreation but also provide habitats for a variety of organisms. For example, urban parks and green space networks can serve as corridors for biological migration, connecting different natural areas and promoting species exchange and genetic diversity. In addition, green infrastructure can support the survival and reproduction of different species by providing diverse ecological environments. For example, Barcelona provides important support for biodiversity through a complex resource of green spaces, each type with its own characteristics and functions, such as protecting nature, reducing air pollution, and regulating temperature. According to statistics, Barcelona's network of urban parks and green spaces provides habitats for more than 200 species of birds, 50 species of mammals, and thousands of plant species, greatly enriching the city's biodiversity.

3.2. Efficient utilization of resources

In cities, recycling of water resources and energy is a key strategy for achieving sustainable development. In terms of water resource management, rainwater harvesting systems can effectively reduce the burden of urban drainage and, at the same time, be used for non-potable water purposes, such as garden watering and toilet flushing. For example, rooftop rainwater harvesting tanks with filtration devices ensure that the water quality is basically clean and then stored in underground cisterns for secondary use.

In addition, the choice of water-saving appliances, such as low-flow toilets and shower heads, can drastically cut down on daily water consumption and, in the long run, will greatly reduce the cost of water supply. Taking the city of Freiburg in Germany as an example, the city has reduced the city's per capita water consumption to less than 100 liters per day, well below the national average in Germany, through an extensive rainwater collection system and the use of water-saving appliances.

The application of green building technologies is an important means of improving resource utilization efficiency. For example, passive solar design reduces energy consumption through rational layout and technological innovation to achieve the purpose of energy saving and emission reduction. Large south-facing windows with sun-shading facilities allow full sunlight to reach the interior in winter while blocking too much direct light in summer to maintain a comfortable room temperature.

High-performance insulated windows and an Intelligent Building Management System (IBMS) automatically adjust lights, curtains, and HVAC (heating, ventilation, and air conditioning) to optimize energy allocation based on actual occupancy rates and weather forecasts, enabling refined management and avoiding waste. In addition, LED lighting systems are favored for their high efficiency and long lifespan, saving more than 75% of electricity

compared to traditional light sources with no mercury pollution. Take Seattle in the United States as an example; many of the city's new buildings have adopted passive solar design and intelligent building management systems, reducing the building's energy consumption by more than 30%, thus greatly improving the city's energy efficiency.

3.3. Green infrastructure construction

Planning and designing green infrastructures, such as urban green spaces and water systems, are essential for the modern sustainable design of spaces. Urban green spaces consist of parks, green spaces along city roads, rooftops of buildings, and many other forms, which not only offer a space to rest and play for the urban inhabitants but also grant habitats for numerous types of organisms. As canonical examples, the intersections between urban parks and green infrastructure or hydrological systems can function as biological corridors, enabling the migration of organisms across fragmented landscapes into "natural" systems and allowing species to move and mix for genetic diversity and adaptable evolution. On the other hand, planning water systems incorporates the conservation and rehabilitation of water bodies (like rivers, lakes, and wetlands), which are vital to climate regulation, water storage, and air purification.

Restoring the natural shape and ecological function of rivers can significantly reduce urban flooding and improve the microclimate of cities, for instance. Moreover, when planning green infrastructure, it should also be the coordination of other functional areas in the city, such as transportation, residential, and commercial areas, to achieve a comprehensive optimization of urban space. For example, the design of extensive green spaces and water systems in Amsterdam, Netherlands not only lays a good ecological foundation for the ecological environment of the city but also integrates green infrastructure with the transportation, residential, and other functional areas of the city, improving the overall quality of the city.

Green infrastructure serves in multiple ways, making the city more ecologically resilient and residents' life quality more pleasant than the engineered infrastructure. Firstly, green infrastructure can help to improve the recovery of the city in natural disasters. Green spaces and water systems, for example, can serve as urban "sponges" by absorbing and storing rainwater during heavy rains to mitigate flooding risk and releasing water during droughts to support ecosystem stability. Second, green infrastructure has the potential to enhance urban microclimate. Evaporation and transpiration from green spaces and water bodies help lower urban temperatures and reduce the heat island effect; they also absorb airborne pollutants and improve air quality.

Green infrastructure also gives residents a chance to engage with nature, which can improve their physical and mental well-being and their quality of life. For example urban parks and green space can provide a space for residents to relax, exercise, and socialize, improving community cohesion and sense of well-being for residents. For example, in Tokyo, Japan, by creating plenty of urban parks and green spaces, including Ueno Park and Yoyogi Park, the city not only effectively improved the ecological environment in the city, but also provided people with a wealth of recreation and leisure places, which indirectly improved people's quality of life.

4. Implications of traditional Feng Shui patterns for modern sustainable space design

4.1. Optimization of spatial layout

The feng shui concept of "hiding wind and gathering Qi" has important inspiration significance to modern city and building spatial layout. Therefore, the idea of Feng Shui has always been on collecting and leading the flow of Qi through reasonable spatial layout, which creates a harmonious and stable environment. The orientation and layout of buildings can be optimized, reducing energy consumption and improving environmental comfort through the use of natural wind and sunlight in modern urban planning. To reduce the use of air conditioning and artificial

lighting, for example, buildings can be built in a north-south orientation to utilize natural light and ventilation.

A rational building layout can also create natural ventilation corridors, guiding the flow of tide air to facilitate smooth airflow and optimizing the microclimate in the city. Taking Beijing as an example, many traditional courtyard architectural settings fully reflect the principle of “hiding the wind and gathering the Qi” through reasonable orientation and layout to create good ventilation and lighting conditions inside the courtyard, to enhance the comfort of living.

Proper building orientation and design is an effective means to reduce energy consumption and improve envelope comfort. Zero energy building(ZEB) design comes from passive strategies based on site analysis, such as integration and building orientation and layout to make the most of natural light and ventilation to avoid using light and mechanical cooling systems. Additionally, the rational building layouts can serve as natural ventilation corridors to smoothen the airflow and enhance the microclimate of cities. For instance, by using certain spatial arrangements of buildings, we could increase air circulation and reduce heat accumulation, resulting in the reduction of heat island effect in the city.

These designs not only just preserve energy and limit emissions, but they help state residents live better, too. Taking Hamburg in Germany as an example, there are several natural ventilation corridors formed by rational building layout and orientation design in city planning advantages, which can effectively alleviate the urban heat island effect and improve the environmental comfort degree of the city.

4.2 Construction of Ecological Network

The ShanShui pattern of traditional Feng Shui provides a guiding significance for the construction of the ecological network in modern cities. In Feng Shui, emphasizing the environment of mountains and water, refracting wind and gathering Qi, which symbolizes Fengqi and can be formed through the rational layout of ecological network and the landscape resources in modern urban planning. Water bodies like rivers, lakes, and wetlands can act as ecological corridors of the city and can integrate ecological patches that enable population migration and gene exchange. Furthermore, mountains and green lands can be ecological knots, providing habitation and ecological works for the ecological resilience of cities. For example, in Hangzhou, China, the beautiful water bodies, surrounding mountain ranges, and greenery are reasonably distributed to form a complete ecological network to ensure the protection of rich biodiversity and improve the quality of the city’s ecological environment.

Biodiversity can be protective and restored through ecological corridors and ecological nodes. Ecological axes can connect different ecological patches to form a continuous ecological network and promote the migration of species and gene exchange. Rivers, green spaces, and parks, for example, can provide ecological corridors in cities, serving as migratory corridors for birds, insects, and other organisms.

Ecological nodes, in contrast, can serve as habitats for many life forms and help the reproduction and growth of multiple species. For example, parks and recreational sites can be captured as habitats to host a variety of plants and animals to enhance the biodiversity. Ecological networks provide not only support to protect biodiversity but also contribute to enhancing the ecological resilience of cities and the quality of life of urban residents. Taking Portland in the United States as an example, through the construction of several ecological corridors and ecological nodes, such as the Willamette River Ecological Corridor and Forest Park Ecological Node, the city has effectively protected and restored the city’s biodiversity and improved its ecological quality.

4.3. Cultural inheritance and innovation

The inheritance and innovation of traditional Feng Shui culture in modern urban design is of great significance.

Feng Shui culture contains rich ecological wisdom and philosophical ideas, which can provide new ideas for modern urban design. For example, the principles of Feng Shui, such as “hiding the wind and gathering the Qi” and “facing the mountain and the water”, can be applied to modern architectural design to create a harmonious and comfortable living environment.

At the same time, the symbols and elements of traditional Feng Shui culture can also be integrated into modern design to increase cultural connotation and artistic value. Taking Shanghai in China as an example, many modern buildings have incorporated elements of traditional Feng Shui in their design, such as the building layout of the Lujiazui area, which fully considers the ShanShui City pattern in Feng Shui and forms a unique cityscape. Combining traditional Feng Shui concepts with modern design concepts can create ecological spaces with cultural connotations. For example, modern architectural design can incorporate the landscape pattern in Feng Shui to form an ecological network through the rational layout of landscape resources.

At the same time, symbols and elements in Feng Shui, such as dragons, phoenixes, Bagua, etc., can be used in modern design to increase the cultural connotation and artistic value. This combination not only helps to pass on and promote traditional culture but also enhances the ecology and artistry of modern urban design. In Guangzhou, China, for example, many modern buildings combine traditional Feng Shui concepts with modern design concepts in their design, such as the Canton Tower, which was designed with full consideration of the ShanShui City pattern and cultural symbols in Feng Shui, and has become a cultural landmark of the city.

5. Conclusion

As an ancient ecological wisdom, traditional Feng Shui patterns provide valuable insights for modern sustainable spatial design. By drawing on the concept of “hiding wind and gathering Qi” in traditional feng shui, the spatial layout of cities and buildings can be optimized, energy consumption can be reduced, and environmental comfort can be improved. At the same time, the ShanShui City pattern in traditional Feng Shui provides guidance for the construction of modern city ecological network, through the construction of ecological corridors and ecological nodes, can effectively protect and restore biodiversity. In addition, the inheritance and innovation of traditional Feng Shui culture in modern urban design, combining traditional Feng Shui concepts with modern design concepts, can create ecological space with cultural connotations. In conclusion, the traditional Feng Shui pattern provides new ideas and methods for modern urban design, promotes the harmonious coexistence of man and nature, and provides important theoretical and practical guidance for sustainable development.

Disclosure statement

The author declares no conflict of interest.

References

- [1] Chen J, Wen Y, 2022, Design Inspiration for Mountain-Water Cities Under the Aesthetic Characteristics of Urban Landscape Painting. *Industrial Buildings*, 52(6): 40–46.
- [2] Chen X, 2023, The Application and Practice of Landscape Painting Elements in the Construction of Mountain-Water Cities. *Architectural Science*, 39(9): 175.
- [3] Fang H, 2024, Research on the Mountain-Water Space Design of Yangzhou MixC Art Museum, thesis, Changchun University of Technology.
- [4] He F, Song Y, 2023, Low-Carbon Renewal Design of Public Spaces in Urban Residential Areas Based on Carbon

Cycle Theory: A Case Study of the Shanshui Renjia Residential Community in Chuzhou. *Residence*, (27): 88–91.

- [5] Huang L, Fan M, 2024, Research on the Interactive Smart Home Design Based on the Elements of Guangxi's Traditional Chinese Landscape Paintings. *Residence*, 2024(2): 10–12.
- [6] Li L, Chen L, Jiang P, 2025, Urban Waterfront Space Planning and Design Under the Concept of Mountain-Water Cities: A Case Study of the Lakeside Block in Chumen Town, Yuhuan City. *Urban Architecture*, 22(3): 142–145.
- [7] Jiang N, Bi J, 2023, Research on Planning Strategies from Mountain-Water Cities to Park Cities. *Urban Architecture Space*, 30(6): 49–52.
- [8] Liu W, 2024, The Application and Enlightenment of Traditional Ritual Culture in Modern Interior Design. *Ceramics*, (12): 88–89 + 93.
- [9] Li X, Gao Y, 2024, Research and Application of New Chinese-Style Interior Design in Modern Interior Spaces. *Footwear Craft and Design*, 4(23): 102–104.
- [10] Li Y, Zhou X, 2024, Research on the Protection and Design of Mountain-Water-Forest-Farmland Spaces in Xujiazha Village Based on Ecological Wisdom. *Industrial Design*, 2024(11): 70–73.
- [11] Qiu H, 2024, Inheritance and Development of Traditional Garden Art in Modern Rural Landscape Planning and Design. *Rural Science and Technology*, 15(12): 119–122.
- [12] Song Z, 2024, Reflections on the Model of Mountain-Water City Construction. *Urban and Rural Construction*, (21): 56–58.
- [13] Tao X, 2023, Research on the Spatial Construction of Huaqing Palace Garden, thesis, Xi'an University of Architecture and Technology.
- [14] Tie Z, 2023, What Is the Connotation of Mountain-Water Cities?—Reading Qian Xuesen's Scientific Thoughts on Mountain-Water Cities. *China Ecological Civilization*, 2023(2): 86–87.
- [15] Wang C, Wei D, 2025, The Application of Karesansui Art in Japanese Garden Landscape Design. *Modern Horticulture*, 48(2): 121–122 + 125.
- [16] Xu Q, Qiu F, 2024, Application of Blue-and-White Porcelain Elements in Spatial Design. *Jiangsu Ceramics*, 57(6): 18–19.
- [17] Yao J, Li Q, 2023, Landscape Bridge Design Based on the Narrative of Landscape Poetry. *Art Research*, 2023(5): 166–169.
- [18] Zhai B, 2023, Research on the Application of Color in Modern Architectural Design. *Real Estate World*, 2023(21): 37–39.
- [19] Zhang Z, 2024, Research on the External Space Design of Science and Innovation Parks Under the Guidance of Mountain-Water Imagery, thesis, Harbin Institute of Technology.
- [20] Zhao Y, Lü J, Zhan W, et al., 2024, Design and Application of Bamboo Materials in Modern Living Room Spaces. *World Forestry Research*, 37(6): 154.

Publisher's note

Bio-Byword Scientific Publishing remains neutral with regard to jurisdictional claims in published maps and institutional affiliations.

Research on Dam Safety and Risk Management in Water Conservancy Engineering

Lihui Li¹, Dan Wu^{2*}

¹Hohai University, Nanjing 210024, Jiangsu, China

²Shenzhen Zhiyuan Space Innovation Technology Co., Ltd., Shenzhen 518000, Guangdong, China

*Corresponding author: Dan Wu, 380121422@qq.com

Copyright: © 2025 Author(s). This is an open-access article distributed under the terms of the Creative Commons Attribution License (CC BY 4.0), permitting distribution and reproduction in any medium, provided the original work is cited.

Abstract: As the country with the highest number of dams in the world, China's dam safety management and risk control are crucial to public safety and economic development. This paper systematically analyzes the current status of dam safety in China, explores the causes of accidents such as design and construction defects, poor operation management, the impact of natural disasters, and proposes comprehensive dam safety management measures based on these analyses.

Keywords: Dam safety; Risk management; Water conservancy engineering; Risk assessment; Emergency response

Online publication: April 3, 2025

1. Introduction

With the rapid development of society and economy, China has achieved remarkable success in water conservancy construction, with a continuous increase in the number of dams and diversification of types. However, some dams built in the early stages have potential safety hazards due to low design standards and limited construction technologies. Therefore, methods to effectively evaluate dam risks and take scientifically reasonable management measures has become an urgent issue. This article aims to systematically review the current status of dam safety, analyze the causes of accidents, and explore effective methods for risk assessment and management, providing reference for ensuring the safe and stable operation of dams.

2. Analysis of dam safety status

2.1. General status of dam safety in China

2.1.1. Number and types of dams

According to the latest statistics, China has more than 98,000 dams of various types, making it the country with the most dams in the world. These dams include traditional types such as concrete gravity dams, arch dams, and earth-rock dams, as well as new types developed in recent years to meet different geographical environments and functional needs, such as panel rockfill dams and asphalt concrete core wall dams. Each type of dam exhibits significant differences in safety performance due to its structural characteristics, construction materials, and

construction methods.

2.1.2. Current status of dam safety

Dam safety management in China's water conservancy projects faces multiple challenges. On one hand, some older dams suffer from varying degrees of safety hazards due to low design standards, limited construction technologies, or structural aging caused by long-term operation. On the other hand, extreme weather events caused by climate change, such as heavy rainstorms and floods, pose new threats to dams. Although relevant government departments have formulated relatively complete dam safety regulations and technical standards and strengthened daily monitoring and maintenance work, a small number of dams still fail to meet current safety requirements.

2.2. Causes of dam accidents

2.2.1. Design and construction defects

In the design phase, factors such as insufficient geological surveys, inaccurate hydrological condition estimates, or inappropriate selection of structural calculation models may cause design parameters to deviate from actual conditions, thereby affecting the safety of dams. During construction, issues such as poor material quality control, non-compliance with construction standards, and neglecting quality due to tight schedules can all lead to potential defects. Additionally, if specific natural factors in special environments (such as earthquake-prone areas or cold regions) are not fully considered, potential safety hazards may arise.

2.2.2. Poor operation management

An effective operation management system should include sound rules and regulations, professional technical personnel, and advanced monitoring equipment. However, in practice, some dams may experience situations where management systems are not properly implemented or operating procedures are not strictly followed. Moreover, inadequate personnel training makes it difficult to identify and handle abnormal situations in a timely manner. Aging or malfunctioning monitoring systems or incorrect data interpretation can also render early warning mechanisms ineffective, preventing preemptive preventive measures. Long-term lack of necessary maintenance and repair work accelerates the aging and degradation of dam facilities, increasing the risk of accidents ^[1].

2.2.3. Impact of natural disasters

Natural disasters pose significant external threats to dam safety. Extreme weather events such as heavy rains causing floods or sudden precipitation after prolonged droughts may exceed the design capacity of dams, leading to overflow in spillways or damage to the dam body. Earthquakes generate strong vibrations and ground deformations that compromise the structural integrity of dams, especially in earthquake-prone areas where such risks are more prominent. The pressure changes caused by freezing and thawing processes can also affect the stability of the dam body and surrounding soil masses. These natural factors often have suddenness and unpredictability, increasing the difficulty of prevention and requiring scientific planning and engineering measures to mitigate their adverse effects on dam safety.

3. Methods for dam risk assessment

3.1. Risk identification

3.1.1. Risk source identification

Risk source identification is the foundation of dam risk management, aiming to determine all potential sources that may threaten dam safety. This includes internal and external aspects; internal risk sources mainly refer to

factors related to the dam's own structure, material properties, and construction quality, such as concrete cracks and foundation settlement; external risk sources cover changes in the natural environment (such as floods and earthquakes) and human activities (such as illegal sand mining and nearby construction). By analyzing historical data, conducting field investigations, and utilizing remote sensing technology for monitoring, all types of risk sources can be comprehensively and systematically identified, providing a basis for subsequent risk factor analysis.

3.1.2. Risk factor analysis

Risk factor analysis focuses on deeply analyzing the specific influencing factors behind each identified risk source. For different types of internal risk sources, it is necessary to assess their occurrence probability and impact on the dam's structural integrity and functionality under specific conditions. For external risk sources, the mechanism, intensity, and frequency of their actions must be examined. Additionally, the interrelationships between various risk factors and the possibility of chain reactions must be considered.

3.2. Risk analysis

3.2.1. Qualitative analysis

Qualitative analysis is primarily used to preliminarily judge the nature and likelihood of risks without involving specific numerical calculations. This method relies on expert experience and engineering intuition, combined with relevant theories and technical standards, to categorically describe risk sources and factors. By constructing risk event trees or causal diagrams, the logical path from risk sources to potential accidents can be intuitively displayed. Furthermore, qualitative analysis helps identify risk factors that are difficult to quantify but are crucial to dam safety, such as public awareness and emergency response capabilities. Although qualitative analysis results have a certain degree of subjectivity, they provide necessary background information and support for more precise quantitative analysis.

3.2.2. Quantitative analysis

Quantitative analysis uses mathematical models and statistical tools to estimate the probability and consequences of risks numerically. This process typically relies on extensive historical data, monitoring records, and experimental test results, employing methods such as fault tree analysis (FTA), event tree analysis (ETA), and Monte Carlo simulation to quantify uncertainties and variabilities. By calculating expected loss values (ELV) and risk indices (RI), the harm levels of different types of risks can be accurately measured, providing scientific evidence for decision-makers. It is important to note that the effectiveness of quantitative analysis depends on the quality of data and the rationality of model assumptions, so careful handling of input parameter selection and uncertainty analysis is essential.

3.3. Risk evaluation

3.3.1. Risk level classification

Risk level classification involves categorizing and prioritizing identified risks according to their severity and urgency based on the results of risk analysis. Generally, both the likelihood of risk occurrence and the consequences once it occurs are comprehensively considered, using two-dimensional matrixes or three-dimensional cube models for evaluation. For example, high-probability and high-consequence risks are classified as Level 1 risks, requiring immediate action to control them. While, low-probability and low-consequence risks are categorized as Level 4 risks, serving as long-term monitoring targets. This grading approach not only facilitates the rational allocation of resources but also lays the foundation for formulating targeted risk management strategies.

3.3.2. Risk evaluation methods

Risk evaluation methods refer to systematic procedures and technical means for comprehensively assessing the risk levels faced by dams and guiding corresponding management actions. Common methods include Analytic Hierarchy Process (AHP), Fuzzy Comprehensive Evaluation (FCE), and Grey Relational Analysis^[2]. These methods address different aspects of complexity and multidimensionality in risk evaluation. For instance, AHP is suitable for comparing the relative importance of risk elements with clear hierarchical structures, while FCE performs well in handling fuzzy information and uncertain conditions. Choosing appropriate risk evaluation methods is critical to ensuring the objectivity and reliability of evaluation results, while also considering the operability and cost-effectiveness in practical applications.

4. Dam safety management measures and emergency response plans

4.1. Dam safety management measures

4.1.1. Safety management during design and construction stages

In the design phase, national and industry standards must be strictly followed, fully considering the influence of geological and hydrological conditions, and adopting advanced computational models and technical means for structural optimization. During construction, a sound quality management system should be established to strengthen control over raw material quality, construction techniques, and procedures, implementing full-process supervision. Additionally, introducing third-party independent review mechanisms ensures the reasonableness of design schemes and compliance of construction quality with safety requirements. Conducting risk assessments to identify and address potential safety hazards in advance is also essential.

4.1.2. Safety management during operation stage

Safety management during the operation stage focuses on combining routine maintenance with emergency management. A comprehensive operation management system should be established, clearly defining operational procedures and responsibility divisions, ensuring strict adherence to norms in all operations. Regular comprehensive inspections of dams and their ancillary facilities should be conducted to promptly identify and repair defects or damages that could affect safety. Detailed emergency response plans should be formulated for different types of emergencies (such as floods and earthquakes), and drills should be carried out to enhance emergency response capabilities^[3].

4.1.3. Monitoring and testing

Monitoring and testing are key components of dam safety management, aimed at continuously tracking changes in the dam's condition through scientific means. Modern sensor technologies and satellite remote sensing tools should be adopted to construct a comprehensive, multi-level monitoring network, enabling real-time monitoring of key parameters such as deformation, seepage, and stress. Specialized tests, including concrete strength testing and crack depth measurement, should be conducted regularly to obtain accurate data support. In data analysis, statistical principles and machine learning algorithms should be employed to uncover hidden patterns and predict future trends, providing scientific evidence for decision-making.

4.2. Emergency response plan compilation

4.2.1. Emergency response plan system

An emergency response plan system refers to a complete organizational structure and procedural arrangement for responding to dam emergencies. This system covers all levels of government and relevant functional departments

from central to local levels, forming a responsibility chain that extends vertically and horizontally. Core content includes the establishment of command coordination institutions, division of responsibilities among departments, smooth communication channels for information reporting, and the improvement of public participation mechanisms. Cross-regional cooperation needs should also be considered to ensure rapid mobilization of resources and coordinated operations in emergencies. Regular updates to the plan content and joint drills should be organized to continuously improve the operability and adaptability of the plan ^[4].

4.2.2. Content of emergency response plans

Emergency response plans specify the steps and measures to be taken when specific types of emergencies occur. First, the event level should be determined based on the scale of the disaster and its impact range to define the response level. Second, evacuation plans should be established, clearly specifying evacuation routes, assembly points, and transportation arrangements to ensure the safety of affected populations. Third, detailed rescue plans should be listed, including inventories of emergency supplies, professional team assembly locations, and on-site handling methods. Finally, an information release mechanism should be included to promptly inform the public about the progress of the situation, avoiding panic caused by rumors. All this content should undergo expert review and be continuously optimized and adjusted based on actual circumstances.

4.2.3. Implementation and evaluation of emergency response plans

The implementation and evaluation of emergency response plans are critical steps in testing their effectiveness. Once the emergency response plan is activated, all relevant departments must act swiftly according to predetermined procedures, ensuring accurate instruction transmission and resource allocation. Afterward, a comprehensive review and summary of the entire emergency response process should be conducted to analyze existing problems and deficiencies, particularly focusing on weak links in communication coordination, resource allocation, technical support, and proposing improvement suggestions ^[5].

5. Conclusion

In summary, dam safety management is a complex and systematic project that requires strict control throughout the entire lifecycle from design and construction to operation and maintenance, as well as precise risk assessment and prevention measures for potential risk sources. By establishing a sound monitoring and early warning mechanism and optimizing the compilation and implementation process of emergency response plans, the ability to respond to emergencies can be significantly improved. In the future, continued investment in scientific research, promotion of technological innovation, improvement of legal frameworks, and promotion of multi-department collaboration will be necessary to achieve the modernization transformation of dam safety management, thereby better protecting people's lives and property and promoting sustainable social and economic development.

Disclosure statement

The authors declare no conflict of interest.

References

- [1] Xu Y, Yuan M, Bao T, et al., 2023, Reservoir Dam Safety Operation Management from an Engineering Ethics Perspective. *Dams and Safety*, 2023(6): 4–8.

- [2] Li M, 2023, Analysis of Safety Monitoring Technology for Water Conservancy Engineering Dams. *Engineering Research and Practice*, 4(4), 199–201. DOI: 10.37155/2717-5316-0404-66.
- [3] Zhu Q, Sha H, Jiang J, 2023, Research on Safety Risk Analysis of Small Reservoir Dam Groups Based on Safety Semantic Features. *Proceedings of the 2023 China Water Conservancy Academic Conference (5)*, 2023.
- [4] Wu Y, 2021, Safety Inspection and Strategy for the Operation of Reservoir Dam Projects. *Hydropower and Water Conservancy*, 5(2): 33–34.
- [5] Comfort LK, 2007, Crisis Management in Hindsight: Cognition, Communication, Coordination, and Control. *Public Administration Review*, 67(s1), 189–197.

Publisher's note

Bio-Byword Scientific Publishing remains neutral with regard to jurisdictional claims in published maps and institutional affiliations.

Ecological Security Assessment and Risk Management Framework for Recycled Water Systems in Landscape Hydration

Xinmiao Wang*

China University of Geosciences (Beijing), Beijing 100083, China

*Corresponding author: Xinmiao Wang, wangxinmiaos@163.com

Copyright: © 2025 Author(s). This is an open-access article distributed under the terms of the Creative Commons Attribution License (CC BY 4.0), permitting distribution and reproduction in any medium, provided the original work is cited.

Abstract: Against the backdrop of intensifying global water scarcity, reclaimed water reuse has emerged as a critical strategy for ecological replenishment of landscape water bodies. However, its potential ecological risks remain underexplored. This study aims to establish a multidimensional ecological safety evaluation framework for reclaimed water replenishment systems and propose hierarchical risk prevention strategies. By integrating ecotoxicological assays (algae growth inhibition, *Daphnia* behavioral anomalies, zebrafish embryo toxicity), multimedia exposure modeling, and Monte Carlo probabilistic simulations, the risk contributions and spatial heterogeneity of typical pollutants are quantitatively analyzed. Results revealed that sulfamethoxazole (RQ = 2.3) and diclofenac (RQ = 1.8) posed high ecological risks, with their effects nonlinearly correlated with hydraulic retention time (HRT < 3 days) and nutrient loading (TN > 1.2 mg/L). A three-tier risk prevention system was developed based on the “source-pathway-receptor” framework: ozone-activated carbon pretreatment achieved 85% removal efficiency for pharmaceutical contaminants, ecological floating beds enhanced nitrogen and phosphorus retention by 40%–60%, and hydraulic regulation (flow velocity > 0.1 m/s) effectively suppressed pathogen proliferation. The innovation of this study lies in establishing a chemical-biological-hydrological coupled risk quantification model for reclaimed water reuse scenarios. The hierarchical prevention standards have been incorporated into local reclaimed water management regulations, providing a scientific foundation and technical paradigm for sustainable landscape water replenishment.

Keywords: Recycled water systems; Landscape hydration; Ecological security assessment; Risk management framework

Online publication: April 4, 2025

1. Introduction

Rapid urbanization and escalating water stress have positioned reclaimed water reuse as a vital strategy to alleviate water shortages. Landscape water bodies, integral to urban ecosystems, increasingly rely on reclaimed water due to its stable supply and cost-effectiveness^[1]. However, residual chemical pollutants (e.g., pharmaceuticals and personal care products, PPCPs), pathogens, and nutrients in reclaimed water may threaten aquatic ecosystems through bioaccumulation and synergistic toxicity^[2]. For instance, elevated concentrations of sulfonamide antibiotics and

endocrine-disrupting chemicals (EDCs) in urban landscape waters across China have triggered algal blooms and degraded aquatic biodiversity. Thus, scientifically assessing ecological risks and constructing adaptive prevention systems are pivotal for sustainable water resource management.

Existing research has advanced in optimizing water reclamation processes and evaluating single-pollutant toxicity. Conventional ecological risk assessments often focus on compliance with standard water quality parameters (e.g., BOD, TN, TP) using hazard quotient (HQ) methods [3]. Recent studies highlight the combined effects of emerging pollutants, such as antibiotic-heavy metal co-toxicity [4]. Technologically, constructed wetlands and membrane bioreactors (MBRs) demonstrate efficacy in pollutant removal [5]. Nevertheless, three critical gaps persist: (1) insufficient dynamic analysis of pollutant fate and biological responses in “reclaimed water–landscape water” systems; (2) overreliance on single-species laboratory tests, failing to reflect ecosystem-level cascading effects; and (3) fragmented prevention strategies focusing on end-of-pipe treatment rather than integrated “source reduction–process interception–endpoint remediation” systems.

Key challenges in this field include the complex quantification of pollutant risks, as the long-term, low-dose effects of trace pharmaceutical and personal care products (PPCPs) and pathogens are still unclear, with nutrient interactions potentially exacerbating these risks. Additionally, limitations in model integration pose a significant hurdle, as weak coupling between hydrological and ecotoxicological models hampers the dynamic prediction of pollutant fate across sediment–water–biota interfaces. Furthermore, there are gaps in technology adaptability, with conventional processes showing limited efficiency for emerging pollutants and lacking risk-tiered prevention strategies.

This study proposes a “chemical-biological-hydrological” coupled framework for ecological safety evaluation. Innovations include a hierarchical prevention system based on “source–pathway–receptor” analysis, incorporating ozone-catalytic oxidation pretreatment, ecological floating beds, and hydraulic regulation for targeted risk mitigation. By elucidating risk drivers in reclaimed water reuse, this work addresses theoretical gaps in multimedia risk assessment and informs revisions to standards such as China’s Water Quality Standard for Scenic Environment Use of Reclaimed Water (GB/T 18921) [1].

2. Materials and methods

Quantitative analysis of target pollutants was performed using ultra-performance liquid chromatography coupled with triple quadrupole mass spectrometry (UPLC-MS/MS, Agilent 6420). Separation occurred on an Agilent Zorbax SB-C18 column (100 mm × 2.1 mm, 1.8 μm) with a gradient mobile phase (0.1% formic acid in water [A] and acetonitrile [B]): 0–2 min (5% B), 2–10 min (5%–95% B), 10–12 min (95% B), followed by re-equilibration. Column temperature: 40°C; flow rate: 0.3 mL/min; injection volume: 5 μL.

Mass spectrometry was employed with electrospray ionization (ESI) in positive mode, using key parameters such as a capillary voltage of 3500 V, nebulizer gas (N₂) flow at 10 L/min and 300°C, and sheath gas flow at 12 L/min and 350°C. Multiple reaction monitoring (MRM) transitions were optimized, for example, sulfamethoxazole with m/z 254.1→156.1, and a collision energy of 20 eV.

For risk assessment, risk quotients (RQ) were calculated using the formula $RQ = MEC/PNEC$, where MEC represents the measured environmental concentration and PNEC is the predicted no-effect concentration derived from ECOTOX acute toxicity data (from the most sensitive species), divided by an assessment factor of 100. Statistical significance was determined via ANOVA ($P < 0.05$) using Agilent MassHunter and OriginPro 2022 [2].

3. Results

3.1. Spatial-temporal distribution of target pharmaceuticals

Five PPCPs were detected in landscape waters (**Table 1**). Carbamazepine (CBZ) and caffeine (CAF) showed the highest detection frequencies (98% and 100%), with mean concentrations of 12.3 ± 3.8 ng/L and 85.6 ± 22.1 ng/L, respectively. CAF exhibited 1.5-fold higher concentrations during wet seasons ($P < 0.05$), linked to hydrophilic properties and runoff inputs. Azithromycin (AZM) and metoprolol (MET) ranged from ND–9.2 ng/L and 2.1–15.4 ng/L, peaking 50 m downstream of replenishment points. Sulfamethoxazole (SMX) concentrations (8.7–32.5 ng/L) exceeded other antibiotics, attributable to intensive veterinary use and environmental persistence.

Table 1. The physicochemical properties of 5 model PPCPs.

NO.	Name	Function	CAS	Molecular Weight
1	Azithromycin	Antibiotic	83905-01-5	748.99
2	Caffeine	Analgesic	58-08-2	194.19
3	Carbamazepine	Anticonvulsant	298-46-4	236.27
4	Metoprolol	β 1-blocker	37350-58-6	267.37
5	Sulfamethoxazole	Antimicrobial	723-46-6	253.28

3.2. Pollutant occurrence patterns

Two distinct temporal patterns emerged: CBZ and SMX exhibited stable persistence (coefficient of variation $< 25\%$), while CAF and AZM displayed pulse fluctuations correlated with rainfall ($R^2 = 0.67$). MET concentrations remained stable post-replenishment, suggesting sediment-water exchange. Compared to global data, SMX levels were higher than European urban rivers but lower than Chinese industrial zones, reflecting regional usage and treatment disparities.

3.3. Preliminary ecological risk assessment

SMX posed the highest risk ($RQ = 0.8$ – 2.3), with 23% of sampling sites exceeding high-risk thresholds ($RQ > 1$), primarily in hydraulic ($HRT > 5$ days). CBZ ($RQ = 0.1$ – 0.3) and MET ($RQ = 0.05$ – 0.2) showed moderate-to-low risks, while CAF ($PNEC = 1000$ ng/L) posed negligible risks. AZM ($RQ = 0.4$ – 0.9) exhibited moderate risks, amplified under hypoxia ($DO < 3$ mg/L).

3.4. Key drivers of risk

Redundancy analysis (RDA) indicated that HRT positively correlated with SMX and AZM ($p = 0.002$), while sediment organic matter ($TOC > 2.5\%$) reduced aqueous MET by 30% via adsorption^[3].

4. Analysis

4.1. Hydrochemical coupling

SMX concentrations exceeded 20 ng/L in dry seasons but dropped below 10 ng/L during wet seasons due to dilution and microbial degradation. Conversely, CBZ peaked at 18.6 ng/L in wet seasons, driven by sediment resuspension. Post-replenishment spikes (15%–30%) confirmed reclaimed water as a key pollutant source.

4.2. Spatial heterogeneity

SMX followed a first-order decay model ($R^2 = 0.89$), peaking 50 m downstream and declining due to photolysis. CBZ exhibited minimal spatial attenuation ($< 10\%$) due to photostability (half-life > 100 days).

4.3. Temporal risk dynamics

SMX RQ exceeded 1.5 in dry seasons but dropped to 0.4–0.8 in wet seasons. At > 20 ng/L, SMX inhibited *Selenastrum capricornutum* growth by 50%. CBZ sediment accumulation (45 ng/g) warrants long-term monitoring^[4].

5. Discussion

5.1. Pollutant behavior mechanisms

SMX's high risk stems from persistence (half-life > 30 days) and toxicity. Prolonged HRT (> 5 days) reduced photodegradation by 60%, while hypoxia ($DO < 3$ mg/L) impaired microbial degradation. CBZ's sediment accumulation aligns with suggesting benthic food chain risks.

5.2. Limitations and future directions

Unaddressed benthic organism responses and model uncertainties (e.g., sediment-water partitioning coefficients) require refinement. Future work should integrate metagenomics and metabolomics to elucidate microbial adaptation and validate prevention systems via pilot-scale studies^[5].

6. Conclusions

This study establishes a hierarchical risk prevention framework for reclaimed water reuse. SMX is the priority risk driver ($RQ_{max} = 2.3$), requiring dry-season in high-HRT zones. CBZ poses long-term sediment accumulation risks (45 ng/g), necessitating benthic monitoring. The three-tier system (ozone-activated carbon + ecological floating beds + hydraulic regulation) reduced SMX risks by 72%, demonstrating technical feasibility. By bridging micro-scale toxicology and macro-scale management, this work advances global paradigms for sustainable water reuse. Future interdisciplinary efforts must translate theoretical insights into policy and practice.

Disclosure statement

The author declares no conflict of interest.

References

- [1] Yuan X, 2014, Selection of Water Quality Objectives and Treatment Processes for Recharging Large Urban Landscape Water Bodies. *China Water & Wastewater*, 30(06): 14–16.
- [2] Kong Y, Gu W, Duan F, et al., 2021, Removal Characteristics of Organic Pollutants in Cephalosporin Pharmaceutical Wastewater. *Chemical Industry and Engineering Progress*, 40(4): 2357–2364.
- [3] Yang Z, Li H, Li N, 2024, Research Progress on the Risk Assessment of Antibiotics in the Agricultural Environment. *Environmental Science*, 45(06): 3468–3479.
- [4] Xie J, Jiang M, Zhang H, et al., 2022, Study on the Co-selection Mechanism of Antibiotic and Heavy Metal Resistance in the Aquaculture Environment. *Asian Journal of Ecotoxicology*, 17(06): 213–224.
- [5] Jiang L, Liu J, Qian Z, et al., 2010, Treatment of Rural Domestic Sewage by MBR/Constructed Wetland Process. *China Water & Wastewater*, 26(04): 29–31+41.

Publisher's note

Bio-Byword Scientific Publishing remains neutral with regard to jurisdictional claims in published maps and institutional affiliations.

The Influence of Coal Gangue Particle Gradation on the Performance of Inorganic Foamed Paste Backfill Materials

Chonghui Fu, Chunwei Wang, Fengshun Zhang, Hucheng Chai, Liya Zhao, Xuemao Guan, Jianping Zhu, Haibo Zhang*

Henan Key Laboratory of Materials on Deep-Earth Engineering, School of Materials Science and Engineering, Henan Polytechnic University, Jiaozuo 454003, China

*Corresponding author: Haibo Zhang, zzhb@hpu.edu.cn

Copyright: © 2025 Author(s). This is an open-access article distributed under the terms of the Creative Commons Attribution License (CC BY 4.0), permitting distribution and reproduction in any medium, provided the original work is cited.

Abstract: The issue of top contact in paste backfill materials is a common technical challenge in coal mine filling processes, and overcoming this problem has become a significant research direction in current studies and engineering practices. This paper utilizes coal gangue as aggregate and hydrogen peroxide as a foaming agent to prepare foamed paste backfill materials. Three close-packing theories were employed to investigate the effects of different coal gangue particle gradations on the mechanical properties, expansion ratio, water absorption, and dry density of foamed paste backfill materials under the same foaming agent content. The hydration mechanism and pore structure evolution were analyzed using XRD, SEM, and OSM techniques. The results indicate that when the hydrogen peroxide addition is 5%, the foamed paste backfill material regulated by MAA gradation theory exhibits the best comprehensive performance, achieving a 28-day compressive strength of 0.89 MPa, an expansion ratio of 155.5%, and a dry density of 1.24 g/cm³. The regulation of coal gangue aggregate particle gradation not only improves the foaming efficiency but also allows the formation of CH to fill the material pores, enhancing the overall structural support capacity and forming a closer microstructure. This research provides new insights into controlling the properties of foamed paste backfill materials.

Keywords: Particle gradations; Coal gangue; Foamed paste backfill materials; Cement; Coal ash

Online publication: April 4, 2025

1. Introduction

Coal is a crucial energy source for humanity, with high demand and intensive extraction processes^[1,2]. However, coal mining generates significant waste and underground voids, leading to issues such as land subsidence and groundwater pollution^[3-8]. Currently, paste backfill technology is one of the effective technologies widely applied in recent years to manage underground voids, as illustrated in **Figure 1**^[9]. Compared to traditional filling materials, paste backfill materials offer excellent flowability and high compressive strength, making them adaptable to various geological conditions and engineering environments^[10]. Paste backfill materials is composed

of cementitious materials, supplementary cementitious materials (such as fly ash and slag), aggregates (such as coal gangue and slag), additives (such as retarders and water reducers), and water, mixed uniformly ^[11–17]. After mixing on the surface, paste backfill materials are typically transported by gravity or pumping. The hydrated paste backfill materials not only provide support to the surrounding rock but also ensure a safe working environment for miners.

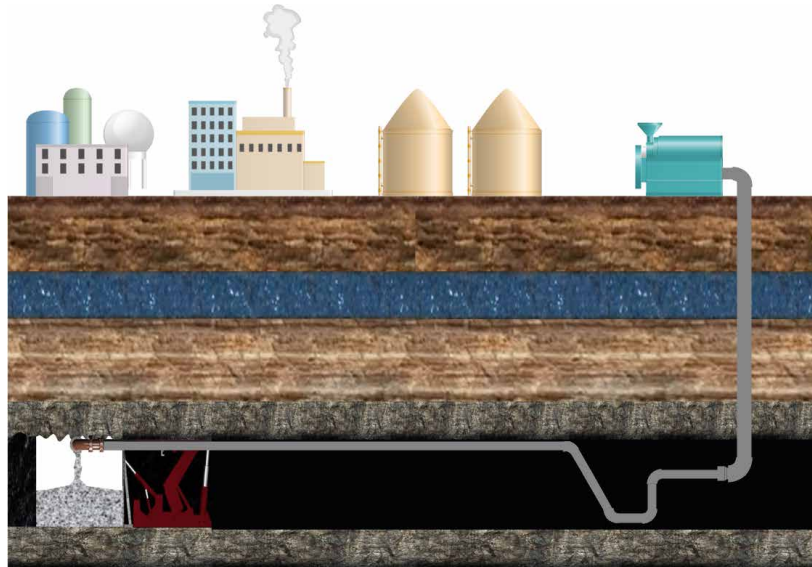


Figure 1. Paste backfill process

However, paste backfill materials typically require good fluidity during the pumping process, which results in a high water-to-binder ratio. This often leads to water loss and bleeding during placement and hydration. Additionally, the high proportion of aggregate in paste backfill materials can cause aggregate settlement, creating voids between the paste backfill material and the roof, preventing a compact contact with the roof and making it difficult to completely fill the goaf, thereby reducing the stability of the underground filling area, as shown in **Figure 2** ^[18, 19]. To date, several techniques have been proposed to overcome this issue, such as artificial roof-contacted, forced roof-contacted, and multi-point discharging ^[20]. These techniques can significantly improve the poor contact between paste backfill materials and the roof, but their high costs make them difficult to implement. Therefore, finding a cost-effective solution to the problem of poor roof contact has become a key research direction for paste backfill materials.



Figure 2. Gaps occurring in paste backfill roof contact

Foamed concrete is characterized by its advantages of volume expansion and minimal shrinkage, while its porous structure helps reduce local stress concentration, effectively addressing the aforementioned issues. Inspired by foamed concrete, incorporating foaming agents into paste backfill materials to create foamed paste backfill materials is an effective approach. Due to the high porosity of foamed paste backfill materials, they have lower density and poorer mechanical properties compared to traditional paste backfill materials. To enhance performance, current research on foamed paste backfill materials primarily focuses on mineral additives, dosage, and types and amounts of foam [21–25]. However, for coal gangue-based foamed paste backfill materials, cost constraints typically result in coal gangue aggregates comprising over 70% of the material. The content and gradation of these aggregates are decisive factors affecting the compaction performance and compressive strength of coal gangue-based foamed paste backfill materials [26].

This study systematically evaluates the impact of different coal gangue particle gradations on foamed paste backfill materials based on three-particle packing theories (Talbot gradation theory, MAA gradation theory, and the I method). The mechanical properties of the foamed paste backfill materials were assessed using a pressure testing machine, and the pore structure, microstructure, and phase composition were investigated using SEM, XRD, TG-DTG, and MIP techniques. The foaming mechanism and top contact process issues were theoretically analyzed, providing theoretical guidance for improving the stability and safety of goaf areas. **Figure 3** illustrates the effects achieved by the foaming top contact process.

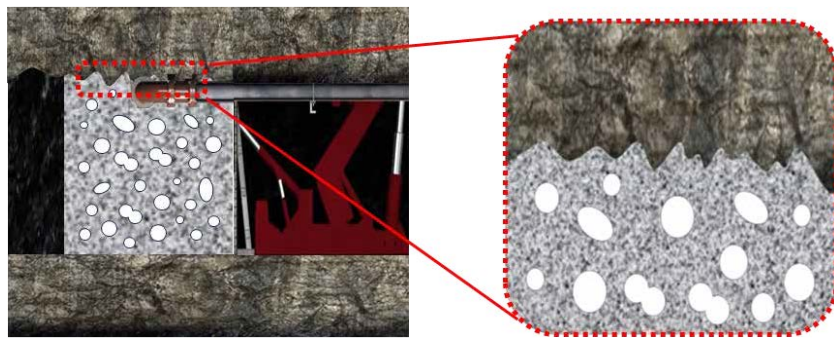


Figure 3. Foam-based roof contact process

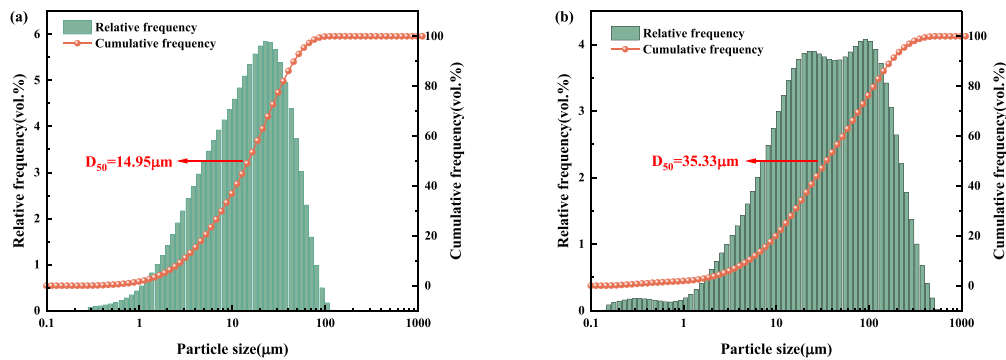
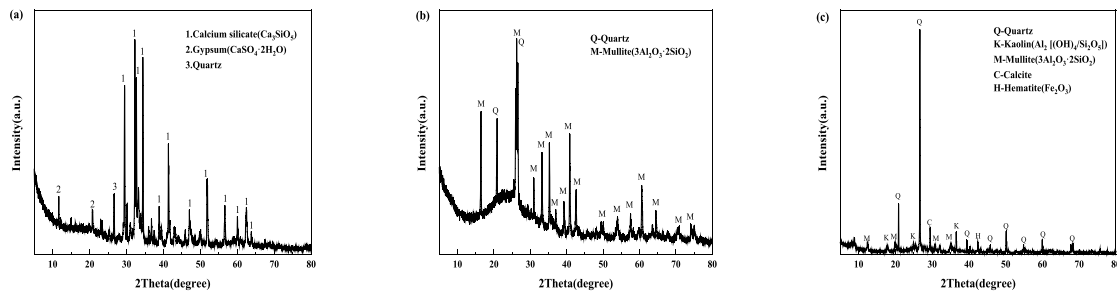
2. Experimental procedure

2.1. Raw materials

This study utilizes various raw materials to formulate foamed paste backfill materials. The primary raw materials include P·O 42.5 ordinary Portland cement (sourced from Jiaozuo Qianye Cement Co., Ltd.), industrial-grade fly ash, and coal gangue (both sourced from Shanxi Lu'an Environmental Energy Development Co., Ltd.). The admixture used is a water-reducing agent produced by Shanxi Sangmus Building Materials and Chemical Co., Ltd., and the foaming agent is hydrogen peroxide produced by Yantai Shuangshuang Chemical Co., Ltd. (with a density of 1.11 g/cm^3 and a concentration of 30%). The XRF analysis of the raw materials is presented in **Table 1**. The particle size distribution of the raw materials is shown in **Figure 4** and the XRD results are depicted in **Figure 5**.

Table 1. Chemical composition of raw materials(%)

Chemical composition	Cement	Fly ash	Coal gangue
SiO ₂	21.95	49.33	57.59
Al ₂ O ₃	7.99	30.15	21.31
Fe ₂ O ₃	2.81	6.09	6.51
CaO	58.03	4.78	6.42
K ₂ O	0.88	1.15	3.51
TiO ₂	0.41	1.08	1.24
Na ₂ O	0.57	0.73	1.03
MgO	3.44	0.70	0.99
SO ₃	3.54	1.22	0.73
LOI	3.92	6.6	11.4

**Figure 4.** Particle size distribution of raw materials: (a) Cement; (b) Fly ash.**Figure 5.** XRD result of raw materials(a) Cement;(b) Fly Ash;(c) Coal gangue.

2.2. Sample preparation

2.2.1. Preparation of foamed paste backfill material

The preparation process of paste backfill materials is illustrated in **Figure 6**. According to the proportions listed in **Table 2**, accurately weigh the raw materials (the amount of each particle size of coal gangue is calculated based on different close packing theories, with results shown in **Table 3**, **Table 4**, and **Table 5**). Sequentially add coal gangue, fly ash, and cement into the mixer, and dry mix them thoroughly. Gradually add water and a water-reducing agent over a period of 90 seconds. After all the water has been added, continue mixing for an additional 120 seconds. Then, pour hydrogen peroxide into the mixing bowl and stir for 6–8 seconds. Pour the mixture into

molds with dimensions of 100 mm × 100 mm × 100 mm for shaping. The molded samples are then placed in a standard curing room (20°C, 95% humidity) for curing.

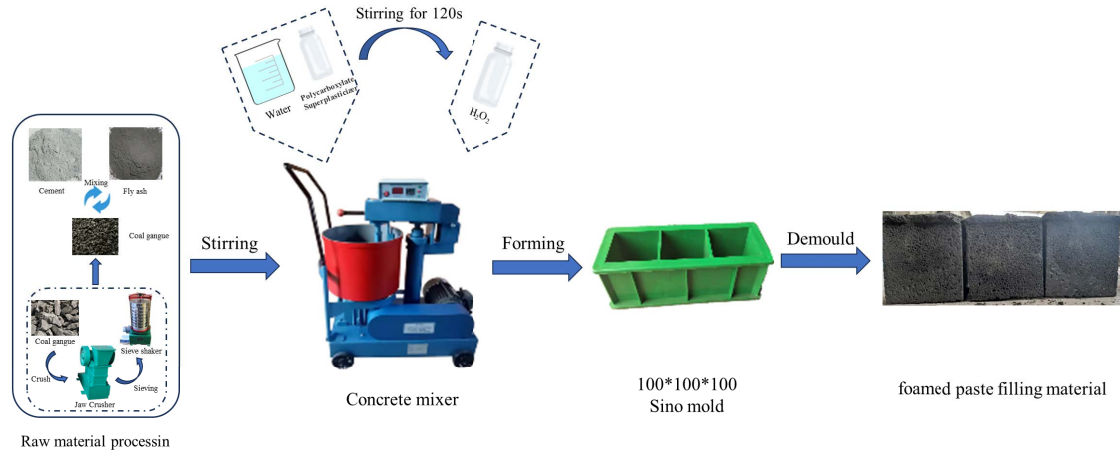


Figure 6. Detail steps for the preparation of paste backfill materials

Table 2. Paste backfill material proportion design(kg/m³).

Cement	Fly ash	Coal gangue	Water reducer	Water	H ₂ O ₂
180	270	1320	1.26	312	22.5

Based on the investigation of Fuller, a minimal porosity can be theoretically achieved by an optimal particle size distribution (PSD) of all the applied particle materials in the mix^[27, 28]. Talbot also proposed a fitting equation based on the trend of the curve, as shown in Equation 1 below:

$$Y = 100 \left(\frac{D_0}{D_{\max}} \right)^n \quad (1)$$

In this equation, $P(D)$ is a fraction of the total solids being smaller than size D , D is the particle size (μm), D_{\max} is the maximum particle size (μm) and q is the distribution modulus.

Table 3. Percentage of cumulative sieve residue for Talbot theory

Label	n	Mass content (%) of particles passing through the following sieve pores (mm)							
		16	9.5	4.75	2.36	1.18	0.6	0.3	0.15
1	0.38	100.00	82.03	63.03	48.32	37.13	28.72	22.07	16.96
2	0.42	100.00	80.34	60.05	44.76	33.45	25.18	18.82	14.07
3	0.44	100.00	79.50	58.60	43.08	31.76	23.58	17.38	12.81
4	0.46	100.00	78.68	57.20	41.46	30.14	22.08	16.05	11.67
5	0.5	100.00	77.06	54.49	38.41	27.16	19.36	13.69	9.68

Dinger and Funk., through experimentation, suggested that in reality, there must be a finite lower size limit. Hence, they proposed a modified model based on the Andreasen and Andersen Equation, as shown in Equation 2^[29].

$$\text{CPFT}(\%) = 100 \left(\frac{D^q - D_S^q}{D_L^q - D_S^q} \right) \quad (2)$$

In this equation, CPFT(%) represents the cumulative percentage finer than a given particle size D ; D_L denotes the maximum particle size in the system; D_S represents the minimum particle size in the system; D is the known particle size; q is the distribution coefficient.

Table 4. Percentage of cumulative sieve residue for MAA grading theory

Label	q	Mass content (%) of particles passing through the following sieve pores (mm)							
		16	9.5	4.75	2.36	1.18	0.6	0.3	0.15
1	0.17	100.00	85.84	68.86	53.64	40.24	28.60	17.98	8.54
2	0.21	100.00	84.68	66.73	51.09	37.69	26.38	16.33	7.64
3	0.25	100.00	83.47	64.58	48.56	35.22	24.25	14.78	6.82
4	0.29	100.00	82.23	62.41	46.06	32.82	22.23	13.33	6.06
5	0.33	100.00	80.97	60.24	43.61	30.52	20.33	11.99	5.36

Based on the study of the maximum packing density curve theory, particle interference theory, and related grading algorithms, a calculation formula was proposed using the percentage passing decrement rate i as a parameter, known as the I method, as shown in Equation 3^[30]:

$$P_i = 100(i)^{(x)} \quad (3)$$

In this equation, P_i represents the percentage passing through the x -th sieve size (%); i is the decrement rate of the particle passing percentage, ranging from 0.7 to 0.8; the series x , where dx is the corresponding square sieve opening size for each particle grade (e.g., 16, 13.2, 9.5, ..., 0.075 mm).

Table 5. Percentage of cumulative sieve residue for i-method theory

Label	i	Mass content (%) of particles passing through the following sieve pores (mm)							
		16	9.5	4.75	2.36	1.18	0.6	0.3	0.15
1	0.7	100.00	76.48	53.55	37.37	26.16	18.48	12.94	9.06
3	0.72	100.00	78.12	56.26	40.39	29.09	21.11	15.21	10.95
5	0.74	100.00	79.75	59.02	43.56	32.24	24.04	17.79	13.17
7	0.76	100.00	81.36	61.84	46.89	35.64	27.27	20.73	15.76

2.2.2. Preparation of test samples

The preparation of samples is illustrated in **Figure 7**. The preparation process of test samples is as follows: The paste backfill blocks are precisely cut into different sizes for various microstructural analyses. For XRD testing, one-sixteenth of the block is taken, crushed, and hydration is terminated using alcohol. The sample is then dried at a constant temperature of 50°C until a stable mass is achieved. The dried sample is ground to pass through a 200-mesh standard sieve. MIP test samples are prepared as regular rectangular prisms with dimensions of 10mm ± 1mm in length and width and a height not exceeding 20mm ± 1mm. All samples are soaked in anhydrous ethanol for 48 hours to terminate hydration reactions, followed by drying at 50°C.

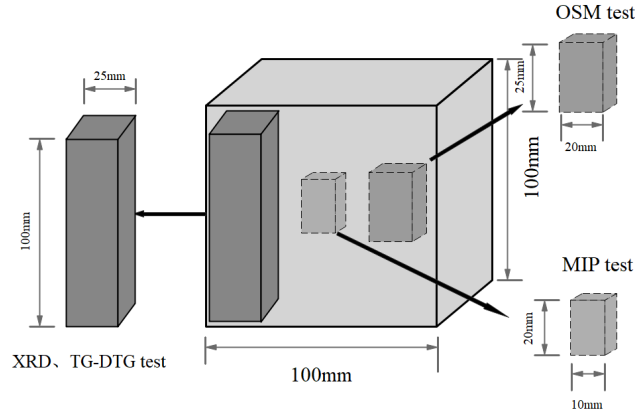


Figure 7. Schematic diagram of microscopic sample preparation.

2.3. Test methods

2.3.1. Bulk density and expansion ratio

Using a plastic measuring cup, weigh the mass M of 1000 ml of paste with the foaming agent, and record the volume V after foaming ceases. The weight of the plastic measuring cup is m . The bulk density is calculated as shown in Equation 4. The expansion ratio is the ratio of the final volume to the initial volume of 1000 ml.

$$\gamma = \frac{M-m}{V} \quad (4)$$

2.3.2. Dry density

Three test blocks are taken, and the length, width, and height of each block are measured in three directions. The average of six measurements is used as the length value in each direction. The volume V of each test block is calculated. The three blocks are placed in a drying oven at a temperature of $(60 \pm 5)^\circ\text{C}$ until the mass difference between two consecutive measurements, 4 hours apart, is no more than 1g. After removal, the dry mass m_0 of the test block is weighed, accurate to 1g. The dry density is calculated as shown in Equation 5. The dry density is the average of the three blocks, accurate to 1 kg/m^3 .

$$\rho_0 = \frac{m_0}{V} \quad (5)$$

2.3.3. Water absorption

The immersion process for determining dry density uses a graded immersion method. The test block is placed in a constant temperature water environment at $(20 \pm 5)^\circ\text{C}$, proceeding in three stages: first, immersed to 1/3 of the block height for 24 hours, then water is added to 2/3 height for another 24 hours, and finally, water is added to exceed the block surface by 30mm for a further 24 hours. After immersion, the block is removed, surface free water is wiped off with a damp cloth, and the mass m_g is immediately weighed (accuracy 1g). The water absorption rate W is calculated as shown in Equation 6. The water absorption rate should be the average of the three test blocks, accurate to 0.1%.

$$W = \frac{m_g - m_0}{m_0} \times 100\% \quad (6)$$

2.3.4. Compressive strength

The samples continue standard curing to the predetermined age (3, 7, 28 days) to test the compressive strength of the paste cubes. A universal testing machine is used to test the mechanical properties of the samples, with a loading

rate of 0.5mm/s during testing. The test results are determined by the average of three samples.

2.3.5. Mercury intrusion porosimetry (MIP)

The mercury intrusion porosimetry (MIP) method is used to measure the cumulative porosity and pore size distribution of the samples. MIP characterizes pores larger than 3nm, with a pressure range of 0.1–30000 psia, using a full scan mode and a contact angle of 130°.

2.3.6. Scanning electron microscope (SEM)

After curing to the specified age, the test blocks are crushed, and the flaky paste material is soaked in anhydrous ethanol to terminate hydration for 48 hours, then dried in a 50°C oven. A scanning electron microscope (SEM) from Carl Zeiss NTS GmbH, Merlin Compact, is used for SEM testing. Before testing, the samples are vacuumed and gold-sputtered. Secondary electron testing is conducted at 10kV.

2.3.7. X-ray Diffraction(XRD)

X-ray diffraction (XRD) is used to analyze phase changes in samples as the proportion of coal gangue powder increases. Prepared powder samples are analyzed using a high-resolution powdered X-ray diffractometer (XRD, Cu target). The test voltage is 45 KV, the current is 150 mA, the scan step is 0.02°, the scan speed is 5°/min, and the test range is 5–80°.

2.3.8. Thermogravimetric analysis(TGA)

Thermogravimetric analysis (TGA) is used to analyze the decomposition process of samples at high temperatures. Approximately 20mg of sample powder is weighed, and thermal analysis is conducted using an STA8122/H comprehensive thermal analyzer. The test is conducted under a nitrogen atmosphere, with a heating rate of 10°C/min, a temperature range of 25–1000°C, and a gas flow rate of 20 mL/min.

2.3.9. Optical super depth-of-field microscope (OSM)

The pore structure of the foamed paste backfill material is observed using a Leica DVM6 ultra-depth-of-field microscope from Leica Microsystems. The treated samples are placed on a microscope carrier with a magnification of 30× for observation.

3. Results

3.1. Water absorption, expansion ratio, dry density, and compressive strength

Figure 8 illustrates the effects of different coefficients in three close packing theories on the water absorption, expansion ratio, dry density, and compressive strength of foamed paste backfill materials.

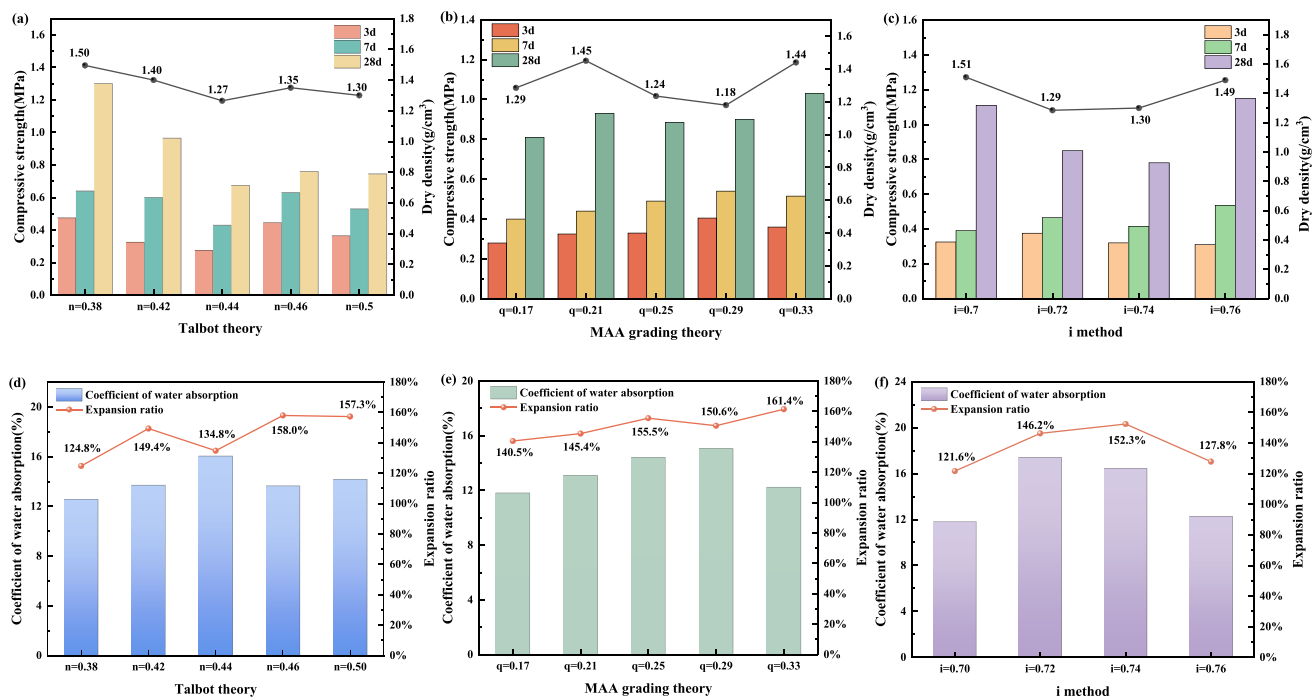


Figure 8. The influence of different close packing theories on macroscopic properties: (a–c) the influence of Talbot theory, MAA grading theory, and i method on compressive strength and dry density; (d–f) the effects of Talbot theory, MAA grading theory, and i method on water absorption and expansion ratio.

Figure 8 (a) and **(d)** show that in the Talbot theory, as the coefficient n increases, the dry density and compressive strength initially decrease and then increase, while the water absorption first increases and then decreases, and the expansion ratio exhibits a stepwise increase. This is because, in the Talbot theory, with an increase in n , the proportion of coarse coal gangue (16mm–4.75mm) increases, while the proportion of fine coal gangue (4.75mm–0.15mm) decreases. The overall specific surface area of the coal gangue decreases with increasing n , allowing the same amount of hydrogen peroxide to achieve a greater expansion ratio. The change in aggregate particle gradation provides more reaction interfaces for hydrogen peroxide, facilitating bubble diffusion and expansion in the paste. When $n = 0.44$, the expansion ratio decreases while water absorption increases, due to the agglomeration of coal gangue observed during foaming. The generation of bubbles causes partial aggregation of coarse coal gangue, increasing the number of open pores and thus reducing compressive strength. At $n = 0.46$ and $n = 0.50$, both the expansion ratio and dry density increase because these groups have a higher proportion of coarse coal gangue compared to the previous groups, resulting in a heavier overall material.

Figure 8 (b) and **(e)** indicate that in the MAA gradation theory, as the coefficient q increases, the dry density and compressive strength first increase, then decrease, and increase again, while the water absorption first increases and then decreases. The expansion ratio shows a trend of first increasing, then decreasing, and increasing again. In the MAA gradation theory, both compressive strength and expansion ratio are relatively better compared to the other two close packing theories. As shown in **Table 4**, the lower content of coal gangue powder results in a relatively higher free water content in the paste, making bubble generation easier. However, higher fluidity is not always beneficial. In the MAA gradation theory, the proportion of coal gangue powder (0.15mm–0.074mm) is less than in the other two theories. As q increases, the proportion of coal gangue powder decreases, making it difficult for the paste to encapsulate the coal gangue, reducing the cohesiveness of the foamed paste backfill material,

leading to aggregate settlement and segregation. After adding the foaming agent, newly formed bubbles cause the aggregate to float. Due to the relatively high density of the aggregate, those initially at the top layer gradually move downward, but bubbles may burst during the movement of coal gangue, explaining why the expansion ratio increases while the dry density rises at $q=0.33$.

Figure 8 (c) and (f) demonstrate that in the i method theory, the macroscopic performance trends are similar to those in the Talbot theory. As the coefficient i increases, the proportion of coarse coal gangue decreases, while the proportion of fine coal gangue increases, leading to an initial rise and subsequent fall in the expansion ratio. This phenomenon occurs because a higher proportion of coal gangue powder results in less free water in the paste, reducing the foaming effect. The results indicate that in foamed paste backfill materials, the paste must have a certain cohesiveness to effectively encapsulate bubbles, preventing their escape and avoiding aggregate settlement^[31]. Good particle gradation can also enhance compressive strength^[32]. On the other hand, an excessive proportion of coal gangue powder can lead to poor paste fluidity, making bubble generation difficult and failing to achieve effective top contact^[33].

3.2. MIP

Figure 9 illustrates the impact of different coefficients of three close-packing theories on the porosity of foamed paste backfill materials.

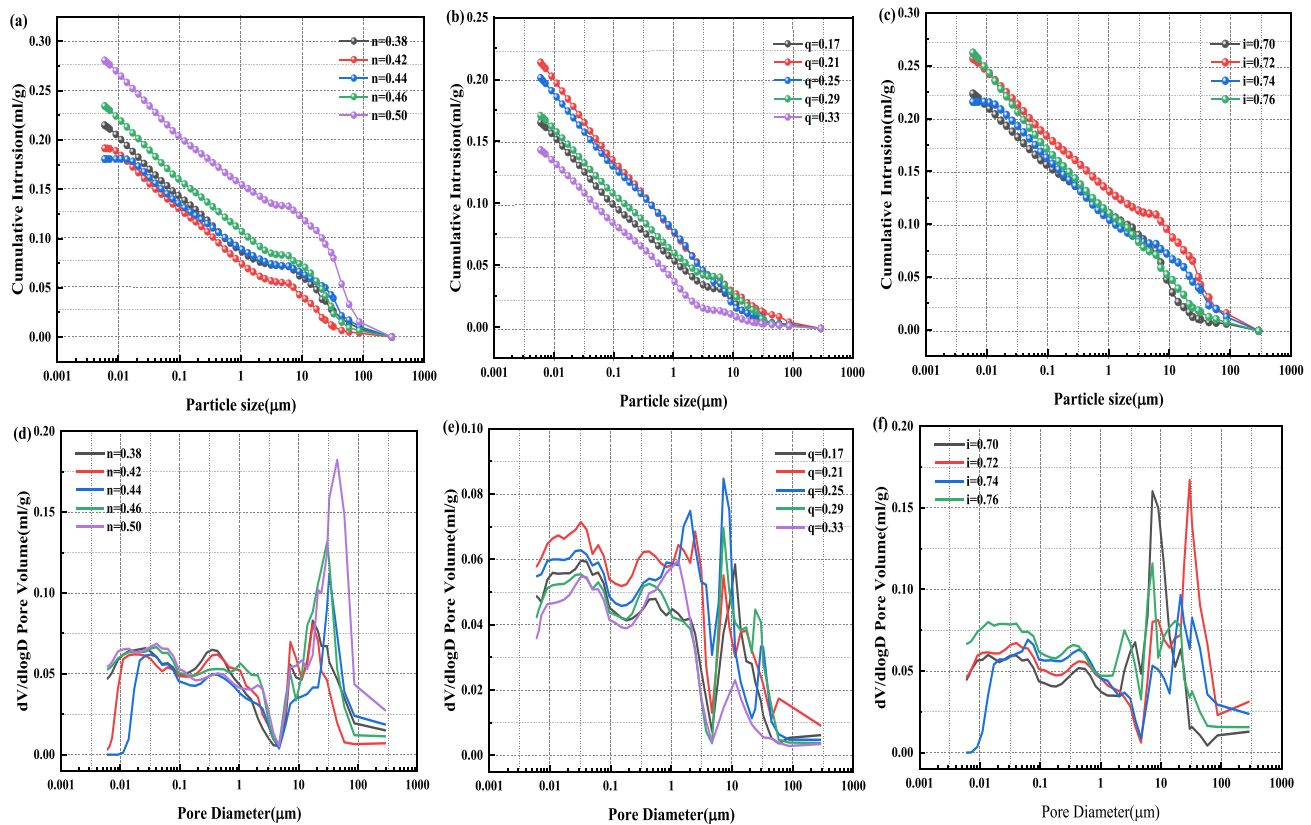


Figure 9. MIP curves of sample with different close packing theories: (a–c) cumulative pore distribution of Talbot theory, MAA grading theory and i method theory, respectively. (d–f) $dV/d\log D$ pore volume of Talbot theory, MAA grading theory and i method theory, respectively.

It can be observed from the figure that changes in the gradation of coal gangue aggregate particles significantly affect pores larger than $10\mu\text{m}$ within the cementitious system. In **Figure 9(a)** and **(d)**, the overall porosity change according to the Talbot theory is not significant. However, as the coefficient n increases from 0.38 to 0.50, there is a trend where pores larger than $10\mu\text{m}$ first decrease and then increase. This is because, at

$n = 0.38$, the higher proportion of coal gangue powder results in less free water within the paste, reducing its fluidity and thus the foaming efficiency of the foaming agent. Additionally, due to the closer cementitious system, bubbles generated by the foaming agent cannot diffuse into the surrounding area, and the high viscosity of the paste prevents bubble coalescence, leading to most pores being smaller than $10\mu\text{m}$. As the coefficient n increases, the proportion of coarse coal gangue rises while that of fine coal gangue decreases, reducing the overall specific surface area of the coal gangue. This increases the free water content in the paste, allowing bubbles generated by the foaming agent to diffuse more easily. Furthermore, the decreased viscosity of the paste increases the likelihood of bubble coalescence, resulting in more bubbles larger than $10\mu\text{m}$. At $n = 0.5$, the paste's viscosity is insufficient to stabilize the bubbles, leading to a collapse. In **Figure 9(b)** and **(e)**, the overall pore distribution according to the MAA gradation theory is more uniform compared to the other two theories, with the overall porosity first increasing and then decreasing. This phenomenon is mainly attributed to the uniform distribution of aggregate particle sizes in the MAA gradation theory, along with a relatively low content of coal gangue powder, which prevents excessive paste viscosity and uneven foaming, thereby enhancing overall strength and bubble stability. In **Figure 9(c)** and **(f)**, the pore size distribution according to the i method is similar to that of the Talbot theory, with a larger proportion of pores over $10\mu\text{m}$. This can lead to decreased bubble stability and increased water absorption of the foamed paste backfill material, which may result in material failure under conditions such as coal mine goafs. For foamed paste backfill materials, a good pore size distribution can reduce stress concentration and improve the overall strength and durability of the material ^[34, 35].

3.3. Sectional view

Figure 10, **Figure 11**, and **Figure 12** illustrate the effects of different coefficients in three close-packing theories on the aggregate distribution in foamed paste backfill materials. Based on the analysis, the coefficients selected for the study were $n = 0.42, 0.44, 0.46$ in the Talbot theory, $q = 0.17, 0.21, 0.25, 0.29$ in the MAA gradation theory, and $i = 0.72, 0.74, 0.76$ in the i method.

From **Figure 10**, it can be observed that under the Talbot theory, as the coefficient changes, the overall aggregate distribution is more uniform when $n = 0.46$. This is because as n increases, the viscosity of the paste decreases. On one hand, this facilitates the generation and diffusion of bubbles within the paste, forming a uniform bubble structure, but it can also lead to bubble coalescence, resulting in larger bubbles. On the other hand, coal gangue aggregates are more evenly dispersed in the paste, significantly enhancing the fluidity of the paste and reducing aggregate agglomeration.

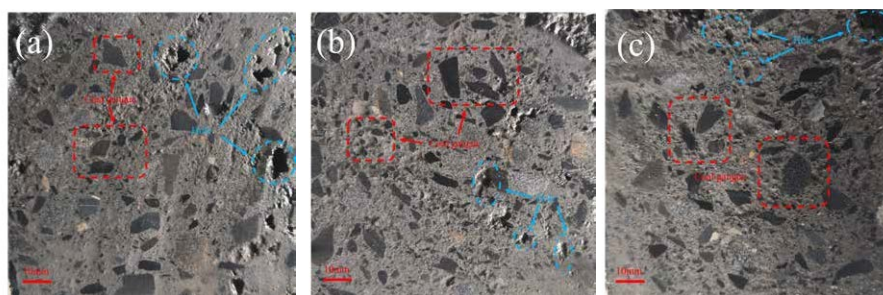


Figure 10. Cross-sectional images of samples with Talbot theory: (a) $n = 0.42$; (b) $n = 0.44$; (c) $n = 0.46$.

Figure 11 shows that under the MAA gradation theory, when $q = 0.25$, the aggregate distribution within the cross-section exhibits a high degree of uniformity. In the MAA gradation theory, the content of coal gangue powder is relatively low, and as the coefficient increases, the viscosity of the paste gradually decreases. This not only causes aggregates to potentially settle under gravity, leading to stratification, but also causes bubbles to

rise and burst rapidly. When $q = 0.29$, it is evident that aggregates concentrate in certain areas, which can lead to uneven physical and mechanical properties, affecting the performance of the foamed paste backfill material.

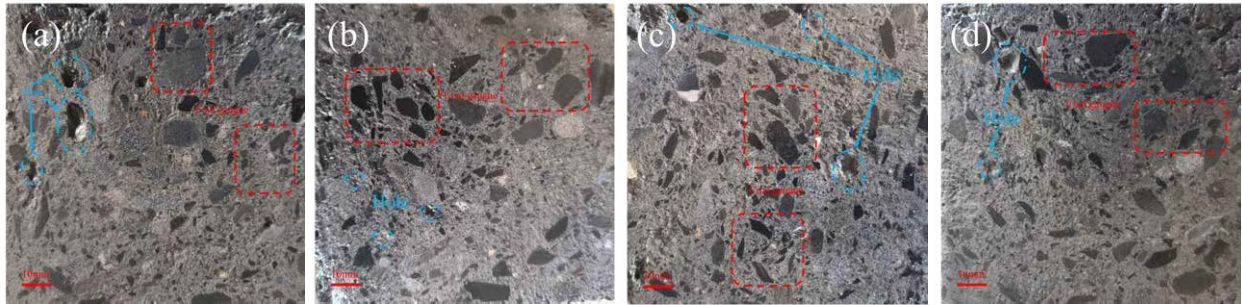


Figure 11. Cross-sectional images of samples with MAA grading theory: (a) $q = 0.17$; (b) $q = 0.21$; (c) $q = 0.25$; (d) $q = 0.29$.

From **Figure 12**, it is evident that in the I method, when $i = 0.74$, the aggregate distribution is more uniform compared to the other two groups. This phenomenon occurs because, as the coefficient i changes, the content of coarse coal gangue in the paste gradually decreases while the content of fine coal gangue increases, leading to increased paste viscosity. An appropriate paste viscosity can prevent aggregates from settling or floating, ensuring their uniform distribution.

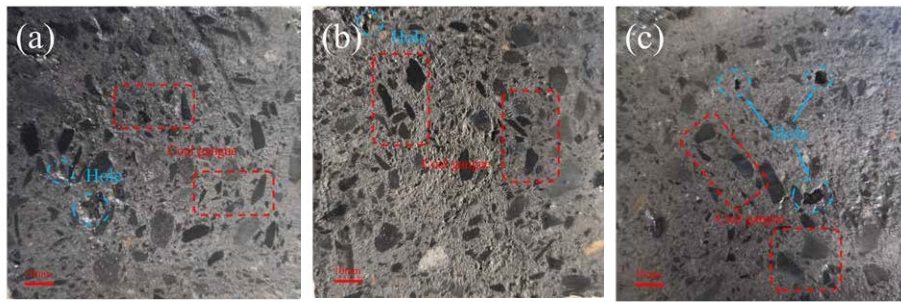


Figure 12. Cross-sectional images of samples with i method theory: (a) $i = 0.72$; (b) $i = 0.74$; (c) $i = 0.76$.

The above results indicate that in foamed paste backfill materials, uniformly distributed aggregates can effectively support the foamed structure, while also helping to reduce material deformation and aggregate settlement, thereby enhancing structural stability.

3.4. OSM

The impact of three close-packing theories on the pore structure of foamed paste backfill materials is illustrated in **Figure 13**. Based on the aforementioned analysis, three sample groups with superior comprehensive performance were selected from the three close-packing theories. Due to the rough surface of the samples and the tendency for some coal gangue aggregates to be mistaken for bubbles, Image Pro Plus was used to process the images and calculate the average pore size, as shown in **Table 6**.

Figure 13 reveals that bubbles smaller than 1mm constitute a significant proportion and numerous irregular bubbles appear in the coal gangue foamed paste materials. This phenomenon arises because, during the foaming process, the high density of coal gangue causes it to move within the paste, while external forces acting on the bubbles lead to uneven foaming and deformation. The average pore size also indicates that when $q = 0.25$, the average pore size is relatively the smallest, which helps form a more uniform and stable foam structure, enhancing the overall strength and stability of the material and reducing the risk of material fracture. This is partly due to changes in aggregate particle gradation, which alter the viscosity of the paste, affecting bubble formation and

stability. Higher viscosity aids bubble stability but may inhibit bubble formation. Lower viscosity allows bubbles to form and spread more easily within the paste but can lead to thinner bubble walls, increasing the risk of bubble rupture. It also affects the paste's flowability, thereby influencing bubble formation and distribution.

Additionally, changes in aggregate particle gradation affect the material's compactness; coarse aggregates can form an aggregate structure, while fine aggregates fill the voids between coarse aggregates, creating a more stable matrix structure that supports bubble stability. Furthermore, aggregate particle gradation may influence the distribution and effectiveness of the foaming agent within the paste, thereby affecting the foaming outcome. Therefore, by reasonably adjusting particle gradation, the foaming effect can be optimized, enhancing the material's performance and quality ^[36].

Table 6. Average pore size of samples with different close packing theories.

Sample	$n = 0.46$	$q = 0.25$	$i = 0.74$
Average pore size/ μm	744.9	504.3	672.0

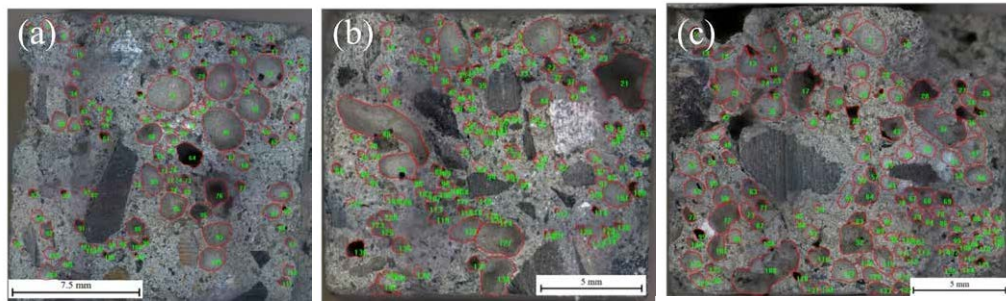


Figure 13. Pore structure of samples with different close packing theories: (a) $n = 0.46$; (b) $q = 0.25$; (c) $i = 0.74$.

3.5. SEM

Figure 14 illustrates the impact of three close packing theories on the microstructure of 28-day foamed paste backfill materials. It can be observed that variations in particle gradation significantly affect the distribution of hydration products. In **Figure 14(a)**, most of the cement hydration products are encapsulated on the surface of coal gangue, with a considerable amount of unreacted fly ash particles present internally. The internal microstructure in **Figure 14(c)** is quite similar to that in **Figure 14(a)**. In **Figure 14(b)**, the C-S-H gel produced by cement hydration connects the surrounding coal gangue and fly ash particles, forming a closer structure. A uniform particle gradation facilitates the formation of close C-S-H gel, thereby enhancing the material's strength.

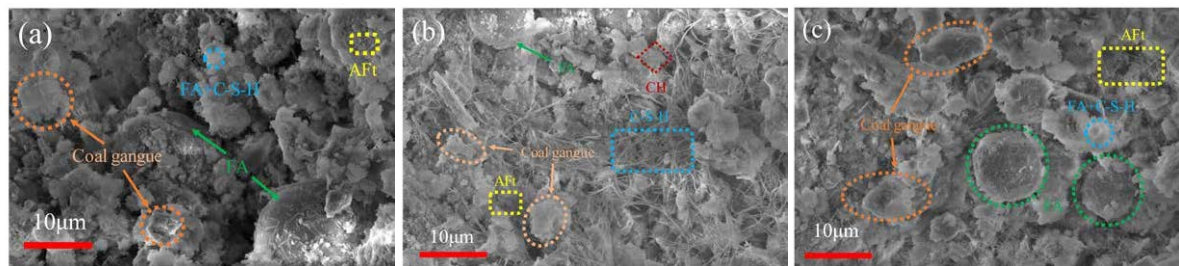


Figure 14. SEM image of samples with different close packing theories: (a) $n = 0.46$; (b) $q = 0.25$; (c) $i = 0.74$.

3.6. XRD

Figure 15 shows the effect of three close packing theories on the hydration products of 28-day foamed paste backfill materials.

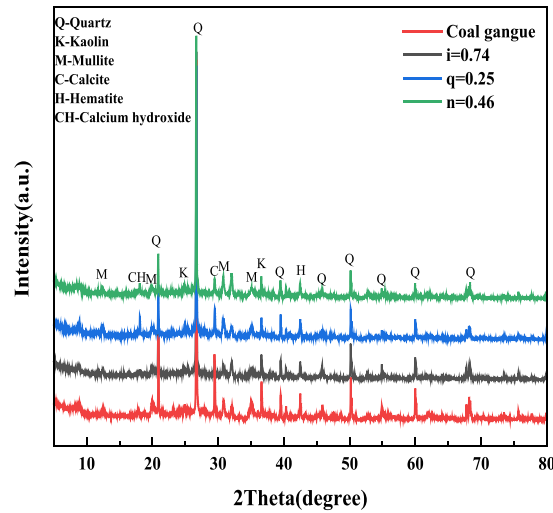


Figure 15. XRD of samples with different close packing theories.

It is evident that changes in particle gradation have a significant impact on the phase composition. After adding cement and fly ash to the specimens, diffraction peaks of minerals such as quartz and mica are still present, but their heights have decreased, indicating a reduction in the relative content of quartz and mica, leading to a decrease in their XRD peak intensity. Additionally, different particle gradations result in corresponding changes in the calcium hydroxide content within the specimens. This is because variations in particle gradation affect the foaming efficiency of hydrogen peroxide.

Firstly, the particle gradation of coal gangue influences the pore structure of the mixture. A better gradation may provide a more uniform pore distribution, thereby affecting the decomposition of hydrogen peroxide and bubble formation. Secondly, particle gradation may affect the contact area between hydrogen peroxide and the cement paste, influencing its decomposition rate and foaming efficiency. Finally, the foaming efficiency of hydrogen peroxide impacts the hydration reaction of cement (e.g., by altering the pore structure or moisture distribution), and the increase in water released from hydrogen peroxide decomposition increases the solubility of calcium hydroxide, affecting its content in the specimens.

3.7. TG-DTG

Figure 16 presents the TG-DTG curves of paste materials based on three close packing theories.

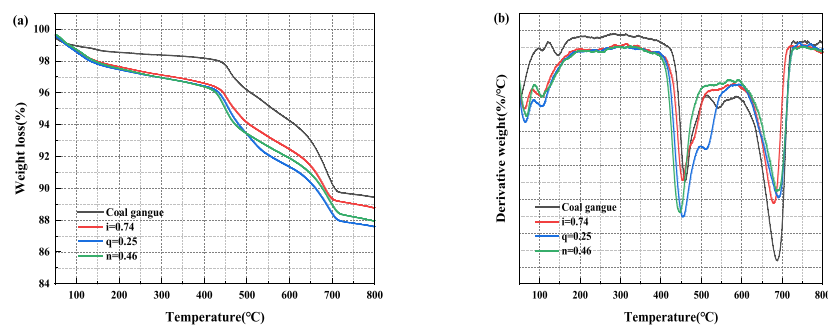


Figure 16. TG and DTG curves of samples with different close packing theories: (a) mass loss curves; (b) derivative of mass loss curves.

Each group of specimens exhibits a small absorption peak between 60–200°C, accompanied by a certain amount of mass loss, corresponding to the loss of free water, adsorbed water, and weakly bound water in the gel ^[37, 38]. In the 200–400°C range, the mass loss mainly results from the continued dehydration of the gel ^[39]. Between 400–600°C, the dissociation of large molecular functional groups in coal gangue, hydroxyl removal, and calcium hydroxide decomposition occurs ^[40]. In the 600–800°C range, a significant endothermic peak is observed, indicating the presence of calcium carbonate ^[41].

By comparing the different close packing theories, variations in coal gangue particle gradation lead to shifts in the weight loss peaks at each stage. In the 60–200°C range, there are differences in the gel content. In the 400–600°C range, the decomposition of calcium hydroxide produced by cement hydration causes a shift in the weight loss peak, indicating differences in calcium hydroxide content, consistent with the XRD analysis results.

4. Discussion

4.1. Effect of aggregate particle size on foam backfill material

The intermolecular forces on the surface of liquid-phase substances create surface tension. When the surface tension is too high, molecules cannot overcome this force to form bubbles ^[42].

Upon adding a foaming agent to the cement paste, gases produced by chemical reactions accumulate within the paste, causing volume expansion. Eventually, the bubbles solidify to form a porous filling material.

The formation mechanism of foamed materials can be summarized as the evolution process of foam cells, as shown in **Figure 17**. This process mainly includes three stages:

- (1) Nucleation: gas is introduced or generated by the decomposition of the foaming agent.
- (2) Bubble growth: the initial gas nuclei gradually expand.
- (3) Structure stabilization: the configuration of bubbles stabilizes during the hardening of the cement paste.

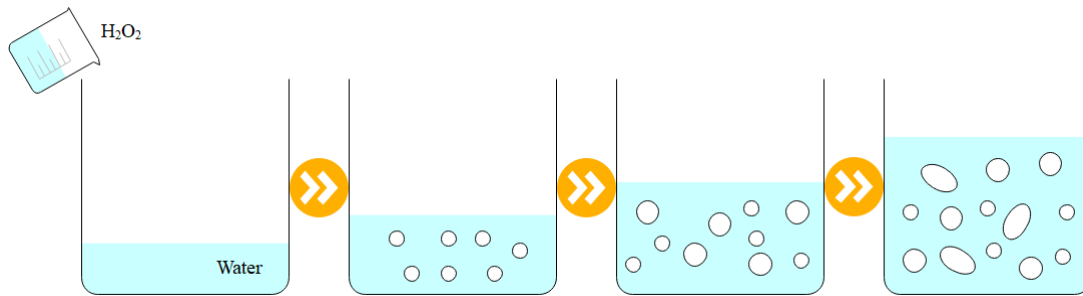
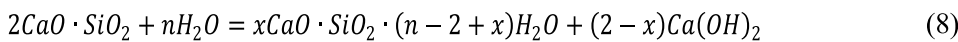
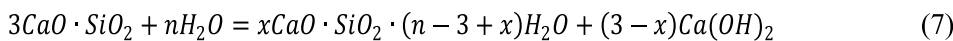


Figure 17. Hydrogen peroxide foaming process

Due to the presence of peroxide bonds and low symmetry, hydrogen peroxide easily undergoes decomposition reactions. When hydrogen peroxide is added to the cement paste, the alkaline environment within the paste accelerates its decomposition. The reactions of cement are shown in Equation 7 and Equation 8.



From these chemical reaction equations, it can be seen that the cement paste becomes alkaline due to the calcium hydroxide produced by the reaction between cement and water. At this point, the reaction of hydrogen peroxide is shown in Equation 9, Equation 10, and Equation 11.



As shown in Equation 10, the reaction is reversible, and a stronger alkaline environment in the cement paste increases the hydroxide ion concentration, driving the reaction to the right, thereby increasing the concentration of $[HOO^-]$. According to Equation 11, the increased $[HOO^-]$ accelerates the decomposition of hydrogen peroxide, creating the necessary conditions for foaming in the paste. However, in the process of accelerating the reaction rate of hydrogen peroxide, it is not sufficient to merely pursue faster reactions, as bubbles are thermodynamically unstable systems^[43]. The bubbles produced cannot be preserved permanently and may collapse.

The formation and stability of bubbles are mainly influenced by two factors: Firstly, the surface tension of the liquid plays a decisive role in bubble formation. Excessive surface tension hinders the process of water molecules detaching from the liquid surface to encapsulate gas. Increasing the viscosity of the solution can effectively reduce surface tension, creating conditions for the stable existence of bubbles.

Secondly, the gravitational drainage effect of the liquid film significantly affects bubble stability. Due to the density difference between liquid and gas, the liquid moves downward under gravity, causing the upper part of the liquid film to thin and eventually rupture. Additionally, the presence of large particles in the system can move downward due to gravity, accelerating the bubble rupture process. Therefore, controlling the viscosity of the paste and optimizing particle stability are key to maintaining the bubble structure.

Figure 18 illustrates the foaming behavior when hydrogen peroxide is added to coal gangue paste. Under identical conditions, the proportion of coarse to fine coal gangue plays a crucial role in the foaming effect. A high proportion of coarse coal gangue can lead to a decrease in paste viscosity and an increase in surface tension, directly affecting the stability and distribution of bubbles. Although the presence of coarse coal gangue can promote bubble generation, the reduced viscosity of the paste prevents bubbles from being fully encapsulated, causing them to easily escape from the paste. This hinders the bubbles from performing their intended function, affecting foam generation and stability.

Due to the higher density of coal gangue, its gravitational effect causes it to settle at the bottom of the paste. During this settling process, coal gangue may collide with bubbles, leading to bubble rupture, which further reduces the foaming ratio. The instability and collapse of bubbles can result in a loose paste structure, decreasing overall strength and stability. This not only affects production efficiency but may also lead to subsequent process issues. Conversely, an excessively high proportion of fine coal gangue may overly increase the paste's viscosity, affecting its flowability and causing uneven foaming. A balanced proportion of coarse and fine coal gangue can enhance the strength of the foamed paste, help form a stable bubble structure, and prevent bubble rupture or uneven distribution.

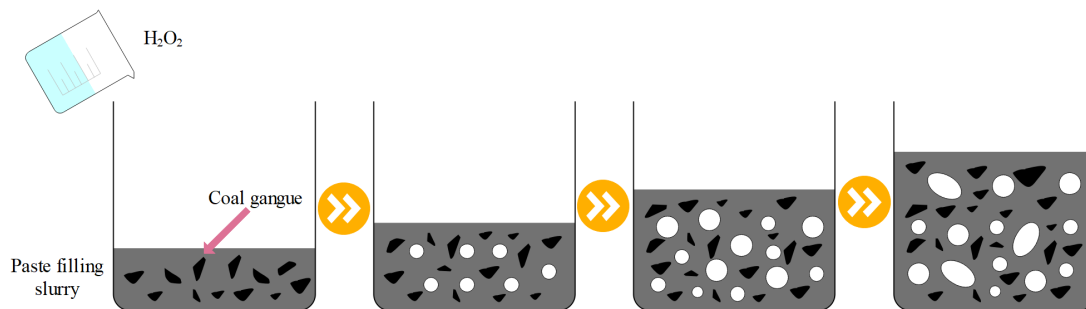


Figure 18. The foaming process of hydrogen peroxide in paste backfill paste.

4.2. Engineering application

Currently, the issue of top contact in paste backfill presents a common technical challenge in coal mine filling processes, primarily involving the contact and support effectiveness between the filling system and the roof. Insufficient fluidity of the paste, uneven roof surfaces, and paste settlement are key reasons for the failure of paste backfill to achieve top contact. **Figure 19** illustrates the phenomenon of paste backfill failing to achieve top contact. The inability of paste backfill to achieve top contact impacts mine safety in several ways:

- (1) The filling system cannot closely contact the roof, leading to inadequate support and increasing the risk of roof collapse or caving incidents.
- (2) The filling system that fails to achieve top contact cannot effectively bear and distribute ground pressure, resulting in pressure concentration in localized areas.
- (3) The filling system that fails to achieve top contact cannot fully perform its supporting function, leading to wastage of filling materials.



Figure 19. Diagram of paste backfill material failing to reach the roof

Figure 20 shows the condition of paste backfill materials achieving top contact after the addition of a foaming agent. To enhance the overall strength of paste backfill, a portion of non-foamed paste is first injected, followed by the addition of a foaming agent at the pipeline outlet. The mixing device at the pipeline outlet mixes the foaming agent with the paste, and the mixed foamed paste is then injected into the area requiring top contact. The spontaneous action of the foaming agent allows the paste material to achieve close top contact, thereby enhancing structural stability and safety. This method reduces costs, effectively fills irregular voids, ensures close contact with the roof, enhances the overall load-bearing capacity of the structure, and reduces the risk of roof collapse.

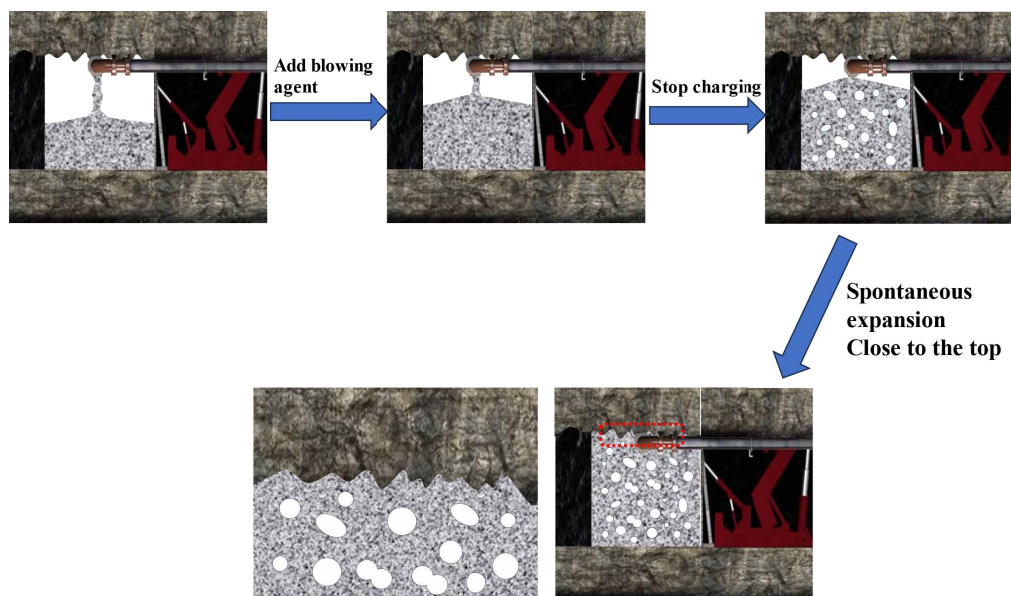


Figure 20. Foaming roof contact process

5. Conclusion

The above study demonstrates that employing different close packing theories to regulate the gradation of coal gangue aggregates significantly impacts the performance of foamed paste backfill materials. Based on the mechanical properties and microstructure of these materials, the main conclusions are as follows:

- (1) In the Talbot theory, the performance of foamed paste backfill with coal gangue is optimal when the coefficient $n = 0.46$. The 28-day compressive strength is 0.76 MPa, the expansion ratio is 158.0%, and the dry density is 1.35 g/cm³.
- (2) In the MAA gradation theory, the performance is optimal when the coefficient $q = 0.25$. The 28-day compressive strength is 0.885 MPa, the expansion ratio is 155.5%, and the dry density is 1.24 g/cm³.
- (3) In the i method theory, the performance is optimal when the coefficient $i = 0.74$. The 28-day compressive strength is 0.78 MPa, the expansion ratio is 152.3%, and the dry density is 1.3 g/cm³.
- (4) When considering only the particle gradation of coal gangue aggregates, the results derived from the three close packing theories differ. Comparing the optimal results of these theories reveals that the foamed paste backfill material regulated by the MAA gradation theory exhibits a more uniform distribution of aggregates and pores within the material, with a relatively smaller average pore size.
- (5) The impact of different particle gradations on performance varies. It not only affects the foaming efficiency of the foaming agent but also influences the hydration reaction. Specifically, particle gradation affects the internal CH content, which contributes to enhancing the overall structural support capacity of the material. An appropriate amount of CH helps fill the voids, improving the volumetric stability of the material.
- (6) Currently, the issue of top contact in paste backfill presents a common technical challenge in coal mine filling processes. The development of foamed paste backfill materials not only addresses the problem of inadequate contact with the roof but also enhances the overall load-bearing capacity of the structure, thereby reducing the risk of roof collapse and lowering costs.

Funding

National Natural Science Foundation of China (Project No.: U1905216).

Disclosure statement

The authors declare no conflict of interest.

References

- [1] Song G, Du K, Zhang Y, et al., 2023, Study of the Overlying Strata Movement Law for Paste-Filling Longwall Fully Mechanized in Gaohe Coal Mine. *Applied Sciences*, 13(14): 8017.
- [2] Du Z, Chen D, Li X, et al., 2024, Study on the Partial Paste Backfill Mining Method in a Fully Mechanized Top-Coal Caving Face: Case Study from a Coal Mine, China. *Sustainability*, 16(11): 4393.
- [3] Hu Y, Hu R, Zhang B, et al., 2024, Research on Mechanical Properties and Mix Proportion Design of Solid Waste-Based Cemented Paste Backfill. *Case Studies in Construction Materials*, 21: e03618.
- [4] Wang H, Chen D, Guo R, et al., 2023, A Preliminary Study on the Improvement of Gangue/Tailing Cemented Fill by Bentonite: Flow Properties, Mechanical Properties and Permeability. *Materials*, 16(20): 6802.
- [5] Li L, Huang Q, Zuo X, et al., 2022, Study on the Slurry Diffusion Law of Fluidized Filling Gangue in the Caving Goaf

of Thick Coal Seam Fully Mechanized Caving Mining. *Energies*, 15(21): 8164.

- [6] Wu P, Zhao J, Jin J, 2023, Similar Simulation of Overburden Movement Characteristics under Paste Filling Mining Conditions. *Scientific Reports*, 13(1): 12550.
- [7] Hou C, Zhu W, Yan B, et al., 2018, Influence of Binder Content on Temperature and Internal Strain Evolution of Early Age Cemented Tailings Backfill. *Construction and Building Materials*, 189: 585–593.
- [8] Yang L, Yilmaz E, Li J, et al., 2018, Effect of Superplasticizer Type and Dosage on Fluidity and Strength Behavior of Cemented Tailings Backfill with Different Solid Contents. *Construction and Building Materials*, 187: 290–298.
- [9] Wang Y, Fall M, Wu A, 2016, Initial Temperature-Dependence of Strength Development and Self-Desiccation in Cemented Paste Backfill that Contains Sodium Silicate. *Cement and Concrete Composites*, 67: 101–110.
- [10] Emad MZ, Mitri H, Kelly C, 2018, Dynamic Model Validation Using Blast Vibration Monitoring in Mine Backfill. *International Journal of Rock Mechanics and Mining Sciences*, 107: 48–54.
- [11] Yin S, Yan Z, Chen X, et al., 2022, Effect of Fly-Ash as Fine Aggregate on the Workability and Mechanical Properties of Cemented Paste Backfill. *Case Studies in Construction Materials*, 16: e01039.
- [12] Wang B, Yang L, Li Q, et al., 2024, Mechanical Behavior, Acoustic Emission and Principal Strain Field Evolution Properties of Layered Cemented Paste Backfill under Unconfined Compression. *Construction and Building Materials*, 415: 135111.
- [13] Xu B, Li Y, Li J, et al., 2024, Nonlinear Stress Growth and Failure Characteristics of Gangue-Cemented Backfill. *Construction and Building Materials*, 424: 135938.
- [14] Wang Z, Wu A, Wang S, et al., 2024, Effect and Mechanism of Time-Dependent and Economical Expansion Materials in Improving the Active Roof-Contact for Cemented Paste Backfill. *Construction and Building Materials*, 439: 137339.
- [15] Li Q, Wang B, Wei Z, et al., 2024, Experiment and Numerical Simulation Study of Polycarboxylate Superplasticizer Modified Cemented Ultrafine Tailings Filling Slurry: Rheology, Fluidity, and Flow Properties in Pipeline. *Construction and Building Materials*, 438: 137041.
- [16] Yunpeng K, Guangbo L, Zepu S, et al., 2024, Experimental Study on the Evolutive Shear Fracture Behaviour and Properties of Cemented Paste Backfill. *Construction and Building Materials*, 423: 135780.
- [17] Zhang C, Wang J, Song W, et al., 2024, Study on Shear Behavior and Microstructure of Rock and Cemented Paste Backfill Interface. *Construction and Building Materials*, 443: 137834.
- [18] Hefni M, Hassani F, 2020, Experimental Development of a Novel Mine Backfill Material: Foam Mine Fill. *Minerals*, 10(6): 564.
- [19] Li MY, Guo LJ, Zhao Y, et al., 2024, A State-of-the-Art Review on Delayed Expansion of Cemented Paste Backfill Materials. *Rare Metals*, 43(8): 3475–3500.
- [20] Kouame KJA, Feng Y, Jiang F, et al., 2015, A Study of Technical Measures for Increasing the Roof-Contacted Ratio in Stope and Cavity Filling. *Journal of Materials Science Research*, 5(1): 54–60.
- [21] Ercikdi B, Cihangir F, Kesimal A, et al., 2010, Utilization of Water-Reducing Admixtures in Cemented Paste Backfill of Sulphide-Rich Mill Tailings. *Journal of Hazardous Materials*, 179(1): 940–946.
- [22] Koohestani B, Belem T, Koubaa A, et al., 2016, Experimental Investigation into the Compressive Strength Development of Cemented Paste Backfill Containing Nano-Silica. *Cement and Concrete Composites*, 72: 180–189.
- [23] Fall M, Pokharel M, 2010, Coupled Effects of Sulphate and Temperature on the Strength Development of Cemented Tailings Backfills: Portland Cement-Paste Backfill. *Cement and Concrete Composites*, 32(10): 819–828.
- [24] Ngo I, Ma LQ, Zhao ZY, et al., 2024, Sol–Gel-Stabilized CO₂ Foam for Enhanced In-Situ Carbonation in Foamed Fly Ash Backfill Materials. *Geomechanics and Geophysics for Geo-Energy and Geo-Resources*, 10(1): 80.
- [25] Xu XCA, Sun XG, Yao W, et al., 2021, Strength and Ultrasonic Characteristics of Cemented Paste Backfill Incorporating Foaming Agent. *MINERALS*, 11(7): 681.

- [26] Li H, Wang H, Bai L, 2024, Effect of Coal Gangue Grading Characteristics on Cemented Paste Backfill Rheology. *Case Studies in Construction Materials*, 21: e03694.
- [27] Fuller WB, Thompson SEJ, 1907, THE LAWS OF PROPORTIONING CONCRETE. 59: 67–143.
- [28] Xiang JC, Liu LP, Cui XM, et al., 2019, Effect of Fuller-Fine Sand on Rheological, Drying Shrinkage, and Microstructural Properties of Metakaolin-Based Geopolymer Grouting Materials. *Cement and Concrete Composites*, 104: 103381.
- [29] Yu R, Spiesz P, Brouwers HJH, 2014, Mix Design and Properties Assessment of Ultra-High Performance Fibre Reinforced Concrete (UHPFRC). *Cement and Concrete Research*, 56: 29–39.
- [30] Peng B, 2005, Gradation Design Method Based on Method of i Change. *Journal of Wuhan University of Technology(Transportation Science and Engineering)*, 29(5) 751–754.
- [31] Xiang G, Song D, Li H, et al., 2023, Investigation on Preparation and Compressive Strength Model of Steel Slag Foam Concrete. *Journal of Building Engineering*, 72: 106548.
- [32] Han S, Zhang P, Zhang H, et al., 2023, Physical and Mechanical Properties of Foamed Concrete with Recycled Concrete Aggregates. *Frontiers in Materials*, 10: 01–14.
- [33] Ni K, Shi Y, Hu Z, et al., 2020, Effect of Coal Gangue Grain Size on Strength of Foam Concrete. *Journal of Physics: Conference Series*, 1635(1): 012080.
- [34] Wei H, Liu Y, Wu T, et al., 2020, Effect of Aggregate Size on Strength Characteristics of High Strength Lightweight Concrete. *Materials*, 13(6): 1314.
- [35] Chung SY, Abd Elrahman M, Kim JS, et al., 2019, Comparison of Lightweight Aggregate and Foamed Concrete with the Same Density Level Using Image-Based Characterizations. *Construction and Building Materials*, 211: 988–999.
- [36] Abd Elrahman M, El Madawy ME, Chung SY, et al., 2019, Preparation and Characterization of Ultra-Lightweight Foamed Concrete Incorporating Lightweight Aggregates. *Applied Sciences*, 9(7): 1447.
- [37] Deboucha W, Leklou N, Khelidj A, et al., 2017, Hydration Development of Mineral Additives Blended Cement Using Thermogravimetric Analysis (TGA): Methodology of Calculating the Degree of Hydration. *Construction and Building Materials*, 146: 687–701.
- [38] Fordham CJ, Smalley IJ, 1985, A Simple Thermogravimetric Study of Hydrated Cement. *Cement and Concrete Research*, 15(1): 141–144.
- [39] Carriço A, Real S, Bogas JA, et al., 2020, Mortars with Thermo Activated Recycled Cement: Fresh and Mechanical Characterisation. *Construction and Building Materials*, 256: 119502.
- [40] Romano RCdO, Bernardo HM, Maciel MH, et al., 2019, Using Isothermal Calorimetry, X-ray Diffraction, Thermogravimetry and FTIR to Monitor the Hydration Reaction of Portland Cements Associated with Red Mud as a Supplementary Material. *Journal of Thermal Analysis and Calorimetry*, 137(6): 1877–1890.
- [41] Jin J, Li M, Liu T, et al., 2024, Insights into Factors Influencing Coal Gangue-Filled Backfill Cemented by Self-Consolidating Alkali-Activated Slag Grouts. *Construction and Building Materials*, 411: 134422.
- [42] Hu N, Liu Y, Ke L, et al., 2023, Preparation and Frothing Mechanism of Froth Concrete Based on Solid Waste: A Review. *Construction and Building Materials*, 401: 132831.
- [43] Hou L, Li J, Lu Z, et al., 2021, Influence of Foaming Agent on Cement and Foam Concrete. *Construction and Building Materials*, 280: 122399.

Publisher's note

Bio-Byword Scientific Publishing remains neutral with regard to jurisdictional claims in published maps and institutional affiliations.

Effect of Different Mineral Admixtures on the Dry Shrinkage and Mechanical Properties of Mortar

Yanbin Zhu, Yi Wu, Linhui Wan, Xiling Zhou*

College of Water Conservancy and Civil Engineering, Hunan Agricultural University, Changsha 410128, China

*Corresponding author: Xiling Zhou, zhouxiling@hunau.edu.cn

Copyright: © 2025 Author(s). This is an open-access article distributed under the terms of the Creative Commons Attribution License (CC BY 4.0), permitting distribution and reproduction in any medium, provided the original work is cited.

Abstract: In this paper, the effects of four different mineral ginseng materials on the mechanical properties of mortar were studied, and the results showed that high territory, fly ash, and silica fume had an inhibitory effect on the drying shrinkage of mortar, and mineral powder increased the drying shrinkage of mortar. The high territory in the mineral admixture has the best effect on the inhibition of mortar drying shrinkage. The compressive strength and flexural strength of the mortar can be improved by adding a certain amount of mineral admixture, which increases the compressive strength by about 20%-40% and the flexural strength by about 20%-30% compared with the control group, and the improvement effect difference between different components is not large.

Keywords: Mineral admixtures; Dry shrinkage performance; Mechanical properties; Polymer mortar

Online publication: March 28, 2025

1. Introduction

Cement mortar, one of the most widely used building materials in construction, is considered to be the most economically practical material due to its low cost and wide application. However, with its widespread use, a series of performance defects have also been exposed, such as low bonding strength, high brittleness, significant shrinkage, and poor crack resistance^[1-4]. Therefore, how to improve the performance of cement mortar has become a widely concerned issue. Many scholars at home and abroad have found that mineral admixtures can improve its working performance. Research by Zhou et al. showed that when the ratio of metakaolin to mineral powder is appropriate, the geopolymer has a denser structure and when the content of metakaolin is higher, the resulting geopolymer gel has stronger acid resistance^[5]. Properly increasing the mineral powder can enhance the durability of the repair material by improving the density of the structure. Liu et al. found that the compressive strength of fly ash mortar with a large amount of silica fume increases and then decreases with the increase of silica fume content and the pattern of single mineral powder addition is similar to that of silica fume^[6]. Both silica fume and mineral powder have a good strengthening effect on fly ash mortar with a large amount of addition. Therefore, this paper comprehensively studies the effects of four different mineral admixtures on the drying shrinkage performance and mechanical properties of cement mortar, aiming to provide a certain reference for the in-depth study of mortar performance improvement.

2. Overview of the trial

2.1. Mix design

Metakaolin (MK), fly ash (F), ore powder (Slag) and silica fume (SF) were used to replace 5%, 10%, 15% and 20% of cement in mass fractions. **Table 1** illustrates the fits.

Table 1. Mineral admixture mixture

Component	Cement/g	Sand/g	Water/ml	MK/g	F/g	Slag/g	SF/g	Water reducer/g
Control	500	1000	325	—	—	—	—	1
MK5	475	1000	325	25	—	—	—	1
MK10	450	1000	325	50	—	—	—	1
MK15	425	1000	325	75	—	—	—	1
MK20	400	1000	325	100	—	—	—	1
F5	475	1000	325	—	25	—	—	1
F10	450	1000	325	—	50	—	—	1
F15	425	1000	325	—	75	—	—	1
F20	400	1000	325	—	100	—	—	1
Slag5	475	1000	325	—	—	25	—	1
Slag10	450	1000	325	—	—	50	—	1
Slag15	425	1000	325	—	—	75	—	1
Slag20	400	1000	325	—	—	100	—	1
SF5	475	1000	325	—	—	—	25	1
SF10	450	1000	325	—	—	—	50	1
SF15	425	1000	325	—	—	—	75	1
SF20	400	1000	325	—	—	—	100	1

2.2. Test method

Dry shrinkage, flexural strength, and compressive strength: tested in accordance with JGJ/T 70-2009 “Test Method for Basic Properties of Construction Mortar”, as shown in **Figure 1**.



Figure 1. Test device and test process

3. Test results and analysis

3.1. Effect on the dry shrinkage properties of mortar

Mortar drying shrinkage refers to the volume shrinkage and deformation of cement mortar due to water loss in an environment with low relative humidity, referred to as dry shrinkage. Due to the lack of maintenance or

insufficient maintenance in the early stage, the surface exuded water evaporates and is lost in the surrounding dry environment, resulting in surface drying, the appearance of surface dryness, the continuous diffusion and migration of internal moisture to the outer surface, and the reduction of internal moisture causes the phenomenon of drying and shrinkage^[7]. Therefore, this chapter explores the effects of materials with different components and different dosages on the dry shrinkage of mortar and compares the improvement effects of fibers, mineral admixtures, and polymer emulsions on the dry shrinkage properties of mortars.

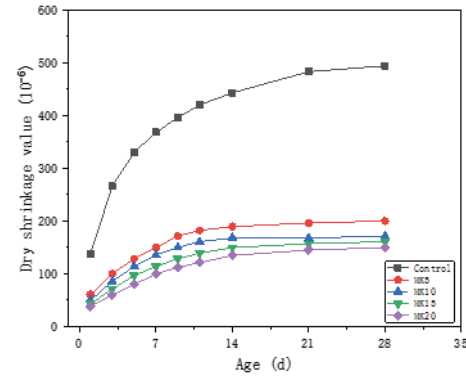


Figure 2. Effect of metakaolin on mortar drying

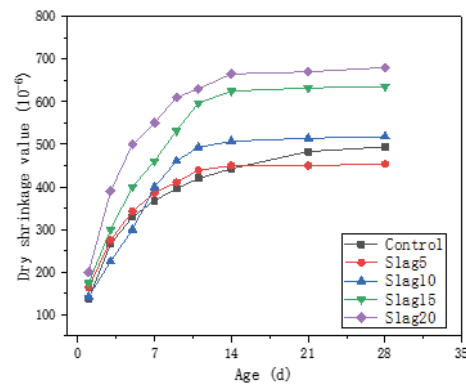


Figure 3. Effect of fly ash on mortar shrinkage

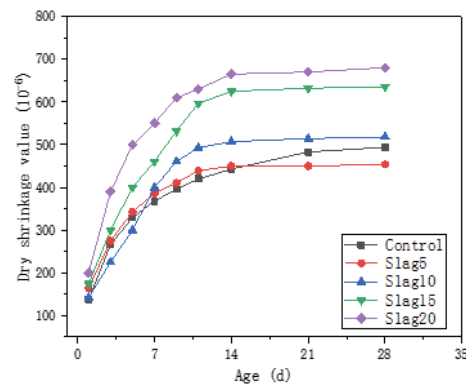


Figure 4. Effect of mineral powder on mortar dry shrinkage

Figure 2 shows the influence of metakaolin on the shrinkage and deformation of special mortar, and on the whole, a certain amount of high territory mixed with mortar has a certain inhibitory effect on the dry shrinkage of mortar. In the territory with high substitution rates of 5%, 10%, 15% and 20% of cement mass fraction, the dry shrinkage of mortar in 28 days was 200×10^{-6} , 171×10^{-6} , 161×10^{-6} and 150×10^{-6} , which were significantly lower than those in the control group (494×10^{-6}). This is because metakaolin can reduce the content of pores and capillaries in the mortar, and it has a large amount of active Al_2O_3 , which promotes the formation of related products in the reaction and inhibits the drying shrinkage of the mortar.

Figure 3 is the influence of fly ash on the shrinkage and deformation of special mortar, on the whole, a certain amount of fly ash in the mortar has a certain inhibitory effect on the dry shrinkage of the mortar. Mixed with fly ash with 5%, 10%, 15% and 20% of the cement mass fraction substitution rate, the dry shrinkage of the mortar in 28 days was 239×10^{-6} , 207×10^{-6} , 178×10^{-6} and 162×10^{-6} , which were significantly lower than those in the control group (494×10^{-6}). On one hand, the amount of cement is reduced after being mixed with fly ash, the hydration rate of fly ash is slow, and the unreacted fly ash plays a role in stabilizing and inhibiting the deformation of the slurry^[8]. On the other hand, the fine particles of fly ash are evenly distributed in the matrix phase of the cement slurry, just like fine aggregates. It binds well to the gel, which reduces the dry shrinkage of the mortar^[9].

Figure 4 shows the influence of mineral powder on the shrinkage and deformation of special mortar. On the whole, a certain amount of mineral powder in the mortar has a certain

inhibitory effect on the dry shrinkage of the mortar. The 28-day dry shrinkage of the mortar was 454×10^{-6} , 518×10^{-6} , 636×10^{-6} , and 682×10^{-6} , which were significantly higher than those in the control group (494×10^{-6}). As the amount of mineral powder increases, the proportion of cement in the cementitious material decreases. In the early stages, the hydration products generated by the mineral powder are relatively limited. With the evaporation and loss of water, the porosity of the slurry increases, making it more prone to significant shrinkage and deformation.

Figure 5 shows the influence of silica fume on the shrinkage and deformation of mortar. The dry shrinkage of the mortar has a certain inhibitory effect. The 28-day dry shrinkage of the mortar was 186×10^{-6} , 204×10^{-6} , 236×10^{-6} , and 279×10^{-6} , which were significantly lower than that of the control group (494×10^{-6}). This is mainly due to the small particle size of silica fume, which can reduce the content of pores and capillary pores while increasing the content of gel pores. At the same time, the drying shrinkage of mortar is usually caused by water loss from fine capillary pores and large gel pores, so silica fume can increase the difficulty of water migration and reduce the drying shrinkage of cement mortar ^[10].

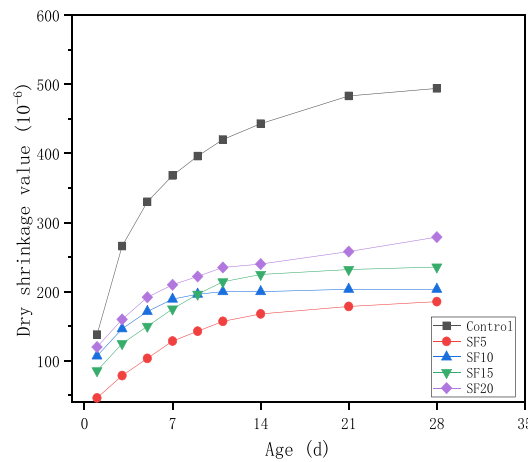


Figure 5. Effect of silica fume on mortar dry shrinkage

3.2. Effect on the compressive strength and flexural strength of the mortar

In this subsection, the effects of different amounts of metakaolin (MK), fly ash (F), mineral powder (Slag), and silica fume (SF) on the compressive strength and flexural strength of the mortar are studied. The compressive strength and flexural strength of metakaolin monomix with different cement substitution rates (5%, 10%, 15%, 20%) for special mortar are shown in **Figure 6**.

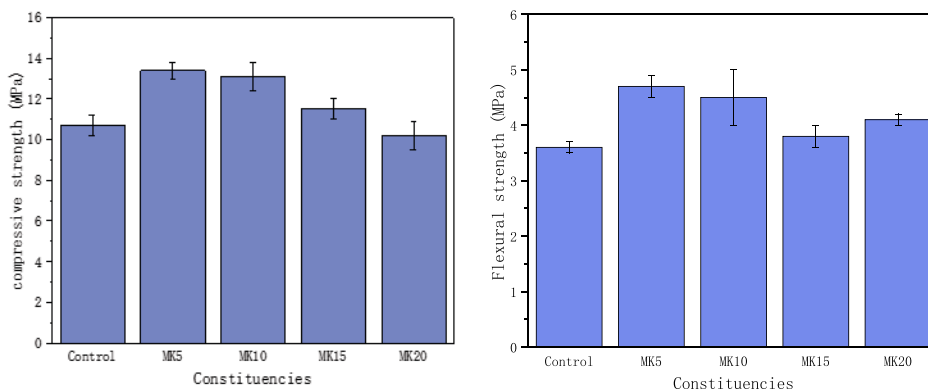


Figure 6. The compressive strength of different amounts of kaolin on mortar.

The left side of **Figure 6** illustrates the effect of metakaolin on the compressive strength of special mortar. It can be observed that after incorporating metakaolin, the compressive strength at 7 days initially increases and then decreases. When the cement substitution rate is 5%, the compressive strength reaches its peak at 13.4 MPa, representing a 25.2% increase compared to the control group. Additionally, the compressive strength of MK10 and MK15 increases by 22.4% and 7.5%, respectively, compared to the control group. However, when the metakaolin substitution rate reaches 20%, the strength begins to decline. The compressive strength of the mortar was reduced to 10.2MPa, which was 4.7% lower than that of the control group.

The right side of **Figure 6** illustrates the effect of metakaolin on the flexural strength of special mortar. It can be observed that as the metakaolin substitution rate increases, the flexural strength initially decreases and then rises. When the cement substitution rate is 5%, the flexural strength reaches its peak at 4.7 MPa, representing a 30.6% increase compared to the control group. Additionally, the flexural strength of the MK10, MK15, and MK20 groups increases by 25%, 5.6%, and 13.9%, respectively, compared to the control group. As the amount of metakaolin increases, the total heat of hydration of cement decreases. Additionally, since the particle size of metakaolin is larger than that of cement particles, the total porosity of the cementitious material increases with higher metakaolin content. This increase in porosity leads to a reduction in compressive strength, as observed in the MK20 group ^[11].

The compressive strength and flexural strength of fly ash with different cement substitution rates (5%, 10%, 15%, 20%) for special mortar are shown in **Figure 7**.

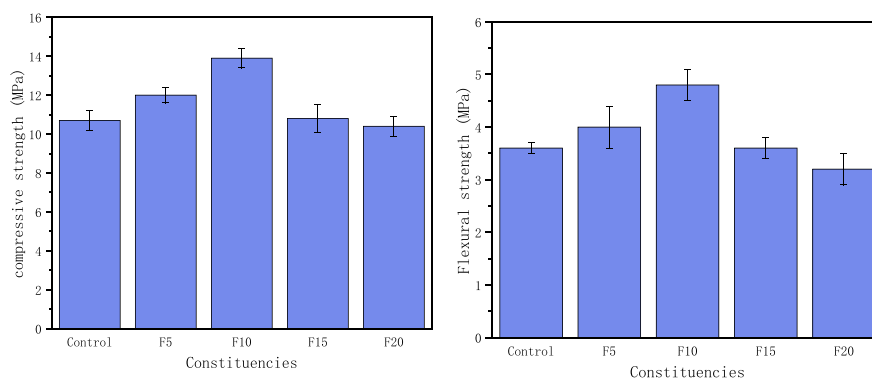


Figure 7. Effect of different amounts of fly ash on the compressive strength of special mortar.

The left side of **Figure 7** illustrates the impact of fly ash on the compressive strength of special mortar. As shown in the figure, after the addition of fly ash, the 7-day compressive strength initially increases and then decreases. The compressive strength reaches its peak at a cement substitution rate of 10%, achieving a maximum value of 13.9 MPa, with an increase of 29.9% compared to the control group. Additionally, the 7-day compressive strength of the F5 and F15 components is 12 MPa and 10.8 MPa, respectively. However, as the fly ash substitution rate increases to 20%, the compressive strength continues to decline. The compressive strength of the mortar was reduced to 10.4MPa, which was 2.8% lower than that of the control group.

The right side of the figure illustrates the effect of fly ash on the flexural strength of special mortar. As shown, with an increasing fly ash substitution rate, the flexural strength initially rises and then declines. The flexural strength reaches its peak at a 10% cement substitution rate, achieving a maximum value of 4.8 MPa, with an increase of 33.3% compared to the control group. However, as the fly ash substitution rate increases to 20%, the flexural strength of the F20 component reaches its lowest value. The cement content in the cementitious material was lower than that of the control group (11.1), resulting in a reduced amount of cement in the mixture. Additionally, the content of calcium silicate generated by the high-

alkali hydration reaction decreased, leading to a weakened secondary hydration effect of fly ash ^[12]. The compressive strength and flexural strength of mineral powder with different cement substitution rates (5%, 10%, 15%, 20%) for special mortar are shown in **Figure 8**.

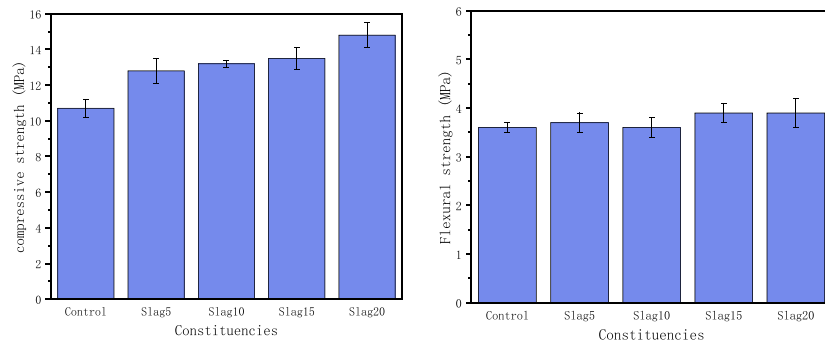


Figure 8. Effect of different amounts of mineral powder on the compressive strength of special mortar.

The left of **Figure 8** is the influence of mineral powder on the compressive strength of special mortar. The figure shows that after the addition of mineral powder, the 7-day compressive strength exhibits an overall trend. When mixed with cement at substitution rates of 5%, 10%, 15%, and 20%, the compressive strength of the Slag5, Slag10, Slag15, and Slag20 components reached 12.8 MPa, 13.2 MPa, 13.5 MPa, and 14.8 MPa, respectively. Notably, the compressive strength of the Slag20 component increased by 38.3% compared to the control group. The right side of the figure illustrates the influence of mineral powder on the flexural strength of special mortar. As shown in the figure, with the increase in the substitution rate of mineral powder, the flexural strength of special mortar exhibits a gradual upward trend. The maximum flexural strength of 3.9 MPa is achieved when the mineral powder is mixed at a 20% cement substitution rate.

In **Figure 9**, the compressive strength and flexural strength of fly ash with different cement substitution rates (5%, 10%, 15%, 20%) for special mortar are shown.

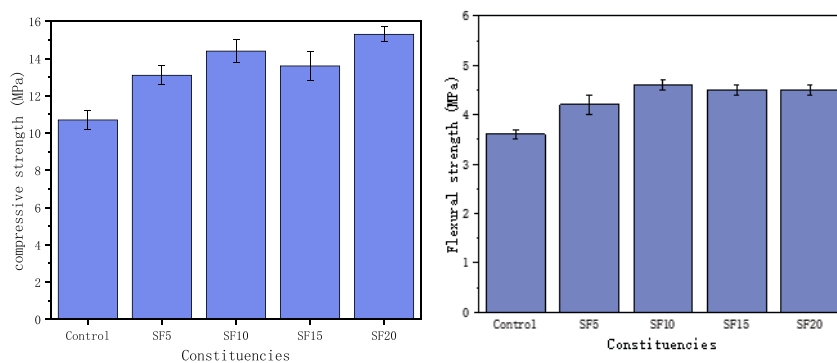


Figure 9. Effect of different amounts of silica fume on the compressive strength of special mortar.

The left side of **Figure 9** illustrates the influence of silica fume on the compressive strength of special mortar. As shown in the figure, after the incorporation of silica fume, the compressive strength at the 7-day age exhibits an overall increasing trend. The maximum compressive strength of 15.3 MPa is achieved when the silica fume substitution rate reaches 20%, representing a 43% increase compared to the control group. Additionally, the 7-day compressive strengths of SF5, SF10, and SF15 components are 13.1 MPa, 14.4 MPa, and 13.6 MPa, respectively. The right of the figure shows the effect of silica fume on the flexural strength of

the special mortar. It can be seen that with the increase of silica fume substitution rate, the flexural strength first shows a slight increase and is higher than that of the control group, while the highest flexural strength of the SF10 group is 4.6MPa, which is 27.8% higher than that of the control group.

4. Conclusion

To summarize, the high territory, fly ash, and silica fume have an inhibition effect on the drying shrinkage of mortar, while mineral powder will increase the drying shrinkage of mortar. The high territory in the mineral admixture has the best effect on the inhibition of mortar drying shrinkage. The 28-day dry shrinkage value of metakaolin with a content of 20% decreased by about 69% compared with the control group. The compressive strength and flexural strength of the mortar can be improved by adding a certain amount of mineral admixture, which increases the compressive strength by about 20%–40% and the flexural strength by about 20%–30% compared with the control group, though the improvement effect difference between different components is not large.

Funding

Hunan Provincial Department of Water Resources: Research on Formula Optimization and Performance Evaluation System of Ecological Concrete for River Water Quality Purification Based on the Dual Carbon Goal (Project No.: XSKJ2024064-44)

Disclosure statement

The author declares no conflict of interest.

References

- [1] Chang H, Li C, Wang X, et al, 2023, Effect of Composite Mineral Admixtures on Self-healing Properties of Mortar. *Material Reports*, 37(2): 58–64.
- [2] Zheng X, Zhou Z, 2017, Influence of Mineral Admixtures and Recycled Aggregate on Strength and Shrinkage of Cement. *Silicate Bulletin*, 36(1): 191–196.
- [3] Li K, Wei Z, Qiao H, et al., 2021, Research Progress of the Influence of Four Kinds of Admixtures on the Properties of Polymer Cement-based Materials. *Materials Review*, 35(z1): 654–661.
- [4] Yin Z, Zhang Q, Xu Z, et al., 2022, Research Progress and Trends of Polymer Cement Mortar. *Concrete and Cement Products*, 2022(8): 31–36.
- [5] Zhou Y, Dan H, Ma Z, 2024, Experimental Investigation on the Durability of Geopolymer Repaired Mortar Based on Metakaolin and Blast Furnace Slag. *Journal of Railway Science and Engineering*, 21(8): 3213–3224.
- [6] Liu Y, Wang J, Luo D, et al., 2024, Effects of Silica Fume and GGBS on Mechanical Properties of High Volume Fly Ash Mortar and Its Mechanism. *Silicate Bulletin*, 43(7): 2584–2594.
- [7] Xu Y, Xing G, Zhao J, 2023, Research Progress of Drying Shrinkage of Alkali Activated Slag Cement Based Materials and Corresponding Counter-techniques. *Materials Review*, 37(7): 81–91.
- [8] Liu H, Zhu B, Yuan J, et al., 2023, Study on the Impact of HTPP Fibers on the Mechanical Properties of Ceramsite Concrete. *Case Studies in Construction Materials*, 19: e2471.
- [9] Fang J, Zhou S, Yang Y, et al., 2020, Experimental Study on Mechanical and Drying Shrinkage Properties of High

Volume Fly Ash Cement Mortar. *Concrete*, 2020(6): 130–133.

- [10] Zeng J, Fan Z, Wang S, 2014, Comparative Research on Effect of Metakaolin and Silica Fume on Mortar Drying Shrinkage. *Journal of Wuhan University of Technology*, 36(6): 115–120.
- [11] Ye Z, Liu S, 2024, Study on Mechanical Properties of Alkali-excited Mineral Powder-sulfoaluminate Cement. *Journal of Heilongjiang Institute of Technology*, 38(5): 39–45.
- [12] Kong M, Cui Y, Li H, et al., 2024, Effect of Double-doped Fly Ash and Silica Fume on the Mechanical Properties of Mortar Under Ultra-low Temperature Environment. *New Building Materials*, 51(9): 30–34.

Publisher's note

Bio-Byword Scientific Publishing remains neutral with regard to jurisdictional claims in published maps and institutional affiliations.

Discussion on Smart Strategies for Barrier-Free Design of Outdoor Spaces in Healthcare and Wellness Buildings in Chongqing

LinYE Gao^{1*}, Haihe Zhao²

¹Chongqing Institute of Engineering, Chongqing 400056, China

²China Southwest Architectural Design and Research Institute Corp. Ltd., Chongqing 401120, China

*Corresponding author: LinYE Gao, 280121923@qq.com

Copyright: © 2025 Author(s). This is an open-access article distributed under the terms of the Creative Commons Attribution License (CC BY 4.0), permitting distribution and reproduction in any medium, provided the original work is cited.

Abstract: With the gradual deepening of aging, the barrier-free design of outdoor spaces in healthcare and wellness buildings is crucial to the quality of life for the elderly in their later years. The mountainous terrain of Chongqing poses higher requirements for barrier-free design. This paper analyzes the barrier-free needs of the elderly, systematically reviews the current status of barrier-free design in Chongqing's healthcare and wellness buildings, and proposes targeted smart strategy suggestions from four aspects: barrier-free transportation space, activity space, landscape sketches, and place spirit, combining regional characteristics. These suggestions aim to improve and enhance the quality of the elderly care environment in Chongqing.

Keywords: Integration of medical and nursing care; Healthcare and wellness buildings; Outdoor spaces; Barrier-free design; Smart strategies

Online publication: April 7, 2025

1. Introduction

According to the seventh population census conducted by the National Bureau of Statistics in 2021, China's population aged 60 and above accounts for 18.7% of the total population, with those aged 65 and above accounting for 13.5%. In Chongqing, these percentages are 21.87% and 17.08%, respectively, indicating a higher degree of aging than the national average. In the face of this aging situation, Chongqing is committed to building an integrated elderly care service system that coordinates home, community, and institutional care, and combines medical and healthcare services. This aims to enhance the sense of gain, happiness, and security for the elderly.

The integration of medical and nursing care refers to the combination of medical and health services with elderly care services. It targets elderly people who live at home, in the community, or institutions, and provides them with the necessary medical and health services based on daily care^[1]. Medical-nursing integrated healthcare buildings are comprehensive elderly care facilities that combine medical and nursing care services.

They provide integrated living, cultural entertainment, rehabilitation training, and medical care services for the elderly.

Market research statistics show that if the conditions of healthcare facilities are well-established, more than half of the respondents are willing to accept institutional care, and another third do not rule out the option of institutional care. Furthermore, the main considerations for choosing healthcare facilities are the level of medical care and environmental facilities. Field research has found that the elderly people living in these institutions are generally aged 70 and above, and a high proportion of them are disabled or semi-disabled. Therefore, barrier-free design in elderly care facilities is a key aspect of their environmental space quality.

2. Barrier-free design

Barriers can be classified into many types, including behavioral, psychological, language, and intellectual barriers. Barrier-free refers to the elimination or reduction of such barriers, and the essence of barrier-free design is to enhance accessibility^[2]. With the development of smart technology, barrier-free design is constantly incorporating intelligent elements, such as smart navigation systems and smart barrier-free facilities, further improving the service efficiency of environmental spaces. The barrier-free design of outdoor spaces in medical-nursing integrated healthcare buildings needs to fully consider the physical functions and behavioral abilities of the elderly. This will better meet their physical and mental needs and enable barrier-free use of environmental spaces.

3. Analysis of barrier-free needs for the elderly

With increasing age, the physiological functions of the elderly gradually decline. Their mobility, memory, and sensory perceptions such as vision, hearing, smell, and touch also deteriorate. Additionally, the flexibility of their hands and feet, as well as reaction speed, decreases. Simultaneously, the elderly are more prone to feelings of loneliness and loss, resulting in higher social and emotional needs. The famous American psychologist Abraham Maslow categorized human needs into five levels, from basic to advanced: physiological needs, safety needs, social needs, esteem needs, and self-actualization needs. Therefore, barrier-free design in outdoor spaces for the elderly should address their physical and mental characteristics to meet these needs.

3.1. Physiological barrier-free needs

The physiological barrier-free needs of the elderly arise mainly from the gradual aging of their bodily organs. For instance, as vision declines, the ability to distinguish objects diminishes. Hence, objects in the space should have high saturation, contrast, and recognizability. Reduced mobility requires simple and clear pathways, with ramps or stairs provided for elevated areas. Due to decreased sleep quality, a quiet spatial environment is essential. Moreover, considering memory decline, easily recognizable signs or symbols are necessary for navigation and recall.

3.2. Safety barrier-free needs

The elderly are more prone to safety hazards due to declining physical abilities. Thus, the spatial environment must address these safety concerns. For example, to prevent falls, furniture, structures, and fixtures should be arranged reasonably, avoiding sharp corners or protrusions. Anti-slip flooring and grab bars should be installed. Additionally, emergency rescue call facilities are crucial to provide timely assistance in case of health emergencies.

3.3. Social barrier-free needs

Retired elderly, especially those in institutional care, are more susceptible to loneliness due to a smaller social circle and separation from family. They require more social activities to enrich their lives. Therefore, the environment should provide ample social interaction spaces, such as entertainment areas, fitness zones, communication plazas, and horticultural experience areas. Alternatively, mixed communities can be established, where people of different ages reside, adding vitality to the elderly's lives.

3.4. Esteem barrier-free needs

As the elderly's self-care abilities decline, their inner need for esteem grows stronger. They hope to have their past achievements and experiences recognized and respected. They desire to maintain autonomy in life choices and decisions, and they yearn to be understood and heard. In outdoor space design, functional activity spaces or detailed designs should cater to these needs. For instance, providing quiet zones for meditation or solitude, and setting up spaces for lectures or performances to fulfill their exhibition needs. Additionally, accommodating the needs of wheelchair users by ensuring that road widths, ramps, and grab bars meet accessibility standards.

3.5. Self-actualization barrier-free needs

The self-actualization needs of the elderly represent the highest level of their spiritual demands. These include personal growth, realizing their own value, and gaining recognition. The environmental space should be designed accordingly, offering various learning opportunities and corresponding outdoor learning areas. For example, organizing literary study classes like those at Tianjin University for the Elderly, where they can gather, share their passions, and even publish their creative works. Moreover, interactive spaces such as gardens or vegetable patches can be established, allowing the elderly to contribute, experience the joy of labor, reap the harvest, and feel the happiness of achieving their value.

4. Analysis of the current status of barrier-free design in outdoor spaces of healthcare buildings in Chongqing

Barrier-free design originated in the 1930s, aiming to eliminate physical barriers in the built environment and enable equal and free access to various facilities and services for all^[3]. This design philosophy emphasizes a people-oriented approach, particularly considering the special needs of the elderly. Technical measures in outdoor spaces help older adults better engage with the landscape. Visits to integrated medical and nursing care facilities in Chongqing revealed that while there are corresponding barrier-free design measures, such as step-free design, double-layer handrails, spacious passageways, barrier-free walkways, and emergency call devices, the application of smart technology in this domain is still in its infancy, leaving significant room for improvement as barrier-free design evolves from the material to the spiritual level.

4.1. Material level

Firstly, hardware facilities are inadequate. Many elderly care facilities are renovated from old buildings not specifically designed for the physiological characteristics of the elderly, resulting in limited aging-friendly features in terms of spatial layout, scale, and environmental amenities. Secondly, outdoor spaces are cramped, restricting movement. For instance, the rehabilitation garden at Chongqing Longhu Senior Apartments is located on the rooftop, limiting accessible space, and vertical transportation is required for elders to reach it, reducing convenience and spatial experience. Furthermore, the spatial layout is simplistic, offering outdoor activities with limited functionality and aesthetic appeal, often featuring only hard paving without necessary

supporting facilities, leading to inefficient outdoor space utilization. In addition, the signage system is basic, relying primarily on traditional methods that are not clear or aging-friendly.

4.2. Spiritual level

Most facilities focus primarily on material care, such as daily living assistance and medical nursing, meeting basic needs while neglecting spiritual aspects. For example, landscape designs are often monotone, featuring simplistic planting and lacking cultural depth or humanistic care. Outdoor spaces for entertainment or collective activities are either limited or non-existent, reducing opportunities for relaxation, socialization, and enjoyment, thereby diminishing the outdoor environmental experience.

4.3. Smart technology application level

Chongqing has initially established the “Yu Yue - Elderly Care” smart platform, integrating functions such as welfare home management, smart management of elderly care institutions, and community services. A total of 1,308 elderly care institutions have been connected to video monitoring terminals. Some institutions have introduced smart devices like millimeter-wave radar digital healthcare solutions to monitor elders’ health status and activity trajectories in real-time, enhancing safety and convenience. Additionally, a 24/7 smart security system reduces accidental risks. While smart technology applications indoors, such as health monitoring, emergency calls, smart positioning, and intelligent access control, have proven effective, their outdoor implementation remains inadequate.

5. Smart strategy suggestions for barrier-free design in outdoor spaces of integrated medical and nursing care buildings in Chongqing

Outdoor spaces are an extension of indoor living, encompassing environmental elements like transportation spaces, activity areas, and amenities. Designing outdoor spaces for healthcare buildings is a comprehensive systems engineering task that should embody healthcare concepts while emphasizing ecology, functionality, culture, and humanity. The integration of smart technology can significantly enhance the experiential aspect of barrier-free design, creating a more convenient, comfortable, safe, and easily identifiable environment for the elderly.

5.1. Smart design of barrier-free transportation spaces

The organization of traffic flow in outdoor spaces of healthcare facilities should align with the physical and mental characteristics and needs of the elderly. Barrier-free access points, ramps, pathways, and other transportation spaces should be established, and smart technology should be employed to enhance the convenience, safety, and user-friendliness of these facilities.

(1) Barrier-free entrance and exit design

Given Chongqing’s unique mountainous terrain, there often exist height differences between indoor and outdoor spaces. In design, step-free entrances and exits, such as level access or equipped with smart ramps and automatic lifting platforms, can connect indoor and outdoor spaces. Smart sensor doors can facilitate access for wheelchair users or elders with mobility issues. Smart signage facilities, including voice guidance, touch screens, and Braille, can be installed to cater to diverse needs and aid elders in navigating spaces efficiently.

(2) Barrier-free ramp design

Ramps are common transportation spaces in Chongqing. In outdoor spaces of healthcare facilities,

ramps are often used to accommodate site height differences, better suiting the behavioral characteristics of the elderly. Ramps for wheelchair access should be designed in straight, segmented, L-shaped, or U-shaped configurations, avoiding curved designs. Ramp widths should accommodate wheelchairs or walking aids, typically being at least 1.2 meters wide, with a slope not exceeding 1:12. However, a 1:16 or 1:20 slope is ideal for safety and comfort ^[4]. Double-layer handrails can be installed on both sides to accommodate varying height requirements. Additionally, smart technologies like health monitoring and emergency call systems can be integrated to ensure timely assistance for elders.

(3) Barrier-free road design

According to accessibility standards, the minimum width of pedestrian roads should be no less than 1.2 meters to ensure smooth passage for wheelchair users. The ground pavement should have multiple characteristics such as slip resistance, stability, wear resistance, environmental friendliness, and aesthetics to avoid falls due to debris when elderly people are walking. At the same time, the deep integration of smart technology and humanized design will build a continuous, convenient, and safe transportation space system, connecting major functional areas such as medical care, rehabilitation, and elderly care. Adequate rest areas and smart auxiliary facilities will be provided, optimizing traffic flow and reducing cross-interference. The barrier-free road space can introduce a smart lighting system that automatically adjusts brightness based on ambient light, while being equipped with smart navigation and voice prompts to provide real-time guidance for the elderly. Additionally, the Internet of Things technology can be utilized to implement real-time monitoring and maintenance of road facilities, and emergency call systems can be installed to ensure a safe, comfortable, and barrier-free environment for the elderly.

5.2. Smart design for barrier-free activity spaces

Based on the diversity of travel needs and motivations, the types of activities that elderly people participate in also show diverse characteristics ^[5]. Elderly people of different ages, hobbies, and behavioral characteristics have varying ways of using space. Therefore, a scientific subdivision of the site can be adopted to construct small, functionally diversified venues, enhancing the participation and activity level of the elderly.

(1) Rest and socializing venues

According to research in environmental psychology, the optimal distance range for interpersonal communication is 1–3 meters, with 0.5 meters being a very close communication distance and 0.5–0.7 meters being a relatively close contact distance. Therefore, to meet the social and entertainment needs of the elderly, the design of rest and socializing spaces should be set at an optimal distance to promote social interaction and emotional exchange among them. For example, tall trees can be used to create a stable forest space, complemented by rich plant layers such as shrubs and flowers to form a natural and ecological environment. Spaces such as healing gardens, leisure plazas, meditation spaces, and therapeutic spaces can be provided to meet the diverse needs of the elderly. At the same time, the rest area can be equipped with smart seating, sunshade facilities, smart health detection equipment, emergency call systems, and fall alarm devices to enhance the sense of security and spatial experience for the elderly.

(2) Fitness activity venues

Fitness activity venues include fitness equipment areas, fitness trails, and ball sports venues. The site design should adhere to ecological principles, increase green coverage, and create a natural and comfortable environment. The site layout follows barrier-free design principles, ensuring that there

are no steps within the site, the slopes are gentle, and double-layer handrails are provided for easy and barrier-free use by the elderly. Combining smart technology, smart fitness equipment can be installed in the venue, which has functions such as heart rate monitoring and exercise data recording, helping the elderly better manage their health. Additionally, the venue can be equipped with landscape features and cultural display facilities with regional cultural characteristics, promoting sports culture or health and wellness knowledge, and enhancing the cultural identity of the elderly.

5.3. Smart design of barrier-free landscape features

Landscape features are indispensable elements of outdoor spaces, often serving as the finishing touch in landscape design and playing a pivotal role in outdoor spaces. As details of the environmental space, landscape features are the material carriers of the cultural heritage and spiritual civilization of the region, and an important way to showcase the regional character and unique charm. A successful landscape feature represents a microcosm of regional civilization construction, reflects the style and landscape characteristics of the region, enhances the inherent attractiveness and creativity of the region, and is a product that condenses regional culture. It includes structural features, sculptural features, natural scenery features, and public facility features.

Combining smart technology with barrier-free concepts in the design of landscape features can enhance the interactivity and fun of the space. Modern design techniques such as material innovation, technology integration, and lighting effects can be utilized in the design of landscape features, adding a sense of modernity and technology to them. Digital technologies such as AR (Augmented Reality) and interactive projections can be used to make the landscape features dynamically interactive ^[6]. The integration of technology and art, applying smart sensing technology and multimedia interactive smart features, creates landscape facilities that can interact with the elderly in real-time. These not only have decorative properties but also interact with the elderly through various means such as light, sound, and touch.

In outdoor spaces, smart seating that can automatically adjust temperature and height can be installed; sculptures equipped with smart monitoring screens can not only meet aesthetic needs but also monitor information such as air quality, humidity, and light in the area, allowing staff to better ensure environmental quality; smart pavilions or corridors can be arranged, utilizing energy conversions such as solar and wind power for smart switching, providing a comfortable environment in both winter and summer; smart medicine boxes that emit voice prompts can be placed in the space to remind the elderly to take medication on time; other small facilities such as sensor-activated trash cans, light and shadow interaction devices, and touch or sound-sensing devices can also be installed.

5.4. Smart expression of the spirit of barrier-free spatial places

In “The Spirit of Place: Towards a Phenomenology of Architecture”, Norberg-Schulz states, “The spirit of place is the fusion of the subjective consciousness space within a person’s heart and the objectively existing space. It refers to a sense of place atmosphere that people experience during their participation in activities, and a sense of belonging or identity that emerges from the place.” ^[7]. In the design of outdoor spaces for healthcare buildings, landscape storytelling can be employed to connect invisible perceptions such as time, events, experiences, and memories with specific sites. This links people’s experiences in the landscape into various interesting stories, extending their memories of living places ^[8]. The design method of landscape storytelling is conducive to expressing the spirit of place, exploring the collision between the real environment and traditional or regional culture, enhancing the recognizability of space, and shaping an emotional home with a sense of familiarity, warmth, protection, and belonging. This tightly connects the site culture with the emotional needs of

the elderly.

Firstly, it is the expression of the landscape theme. The theme of a landscape space represents its core spirit and connotation. A specific theme can bring a certain cohesion to the landscape space. Thematic conception based on the history and cultural memories of the site can evoke perceptual resonance among the elderly. For example, in the outdoor space design of healthcare facilities, incorporating elements of local farming culture in Chongqing and setting up landscape nodes themed around farming tools can not only beautify the environment but also evoke memories of farming life among the elderly ^[9]. Secondly, natural or artificial elements such as terrain, plants, water bodies, small features, structures, and pavement can be selected to create a scenically integrated landscape space effect. Thirdly, smart technology can be integrated to facilitate the expression of the spirit of place. For instance, AR technology can be utilized to enhance the cultural display function of the site, allowing the elderly to immerse themselves in nostalgic scenes through virtual mapped landscapes, thereby enhancing their sense of participation and belonging.

6. Conclusion

In the digital era, the barrier-free design of outdoor spaces for healthcare buildings in Chongqing faces new opportunities and challenges. Smart technology can meet the potential needs of the elderly in terms of information access, facility usage, personalized demands, virtual experiences, data analysis, and facility management. Through smart navigation systems, voice interaction technology, personalized design solutions, augmented reality and virtual simulation technology, as well as data-driven decision support and intelligent management, the convenience and safety of barrier-free facilities can be enhanced. Additionally, it provides a scientific basis for design and management. In the future, with the continuous development and application of digital technology, the barrier-free design of outdoor spaces for healthcare buildings in Chongqing will become more intelligent, user-friendly, and convenient.

Funding

Research Fund Projects of Chongqing Institute of Engineering: Research on the Intelligent Design of Indoor and Outdoor Spaces for Chongqing's "Integrated Medical and Elderly Care" Health and Wellness Buildings in the Context of Digitization (2023xsky01)

Research on Spatial Syntax Parameters and Combination Patterns of Urban and Rural Community Elderly Care Centers from a Multi-Dimensional Perspective (2024XZKY003)

Funding support: 2024 Curriculum Ideological and Political Demonstration Course Construction Project of Chongqing Institute of Engineering, "Residential Landscape Design" (Project Number: KC20240006)

Disclosure statement

The authors declare no conflict of interest.

References

- [1] Promoting the Integration of Medical and Elderly Care to Achieve Healthy Aging, n.d., Economic Daily, viewed on February 25, 2025.
- [2] Gao L, 2022, Discussion on Barrier-free Design of Elderly Care Facilities Based on Humanized Considerations.

Modern Decoration, 499(2): 10–12.

- [3] Huang Z, 2023, Development and Strategies of Adaptive Design for Residential Spaces Under the Concept of Barrier-free Design. *Architecture and Culture*, 2023(7): 175–176.
- [4] Wan L, 2025, Analysis of Key Points in Barrier-free Design of Medical Buildings. *Housing and Real Estate*, 2025(02): 126–128.
- [5] Fang T, 2024, Research on the Renewal Strategy of Barrier-free Environment in Old Communities from the Perspective of Aging Adaptation, thesis, Nanchang University.
- [6] Chen C, 2024, Research on Landscape Sketch Design Based on “Intangible Cultural Heritage” Culture - Taking Zhuhai Jinwan Sanzao Crane Dance as an Example. *Literature and Art Weekly*, 2024(13): 91–93.
- [7] Norberg-Schulz, 2010, *The Spirit of Place: Towards a Phenomenology of Architecture*, translated by Shi Zhiming. Huazhong University of Science and Technology Press, 2010: 186.
- [8] Potteiger M, Purinton J, 2012, *Landscape Narratives: Design Practices for Telling Stories*, translated by Zhang Nan, Xu Yuemeng, Tang Li. China Architecture and Building Press, 2012.
- [9] Hu Z, Gong W, 2024, Landscape Narrative Design Strategy for Old Communities Based on Spatial Perception - Taking Zaojiaojing Community in Chongqing as an Example. *Urban Architecture*, 21(05): 57–60.

Publisher's note

Bio-Byword Scientific Publishing remains neutral with regard to jurisdictional claims in published maps and institutional affiliations.

Atomic-Level Understanding of Contact Potential of Quartz Surface

Lina Ma*

Qinghai Vocational and Technical University, Xining 810000, China.

*Corresponding author: Lina Ma, 13299888637@163.com

Copyright: © 2025 Author(s). This is an open-access article distributed under the terms of the Creative Commons Attribution License (CC BY 4.0), permitting distribution and reproduction in any medium, provided the original work is cited.

Abstract: Laboratory and field observations have suggested a correlation between contact dynamics and slow dynamics. The underlying mechanical mechanisms at the contact level require investigation at the nanoscale. This study uses molecular dynamics (MD) simulations to investigate the interactions between two quartz plates separated by a water film, focusing on the relationship between adhesion force and separation distance. The density and orientation angle profiles were calculated from simulation data to investigate the relationship between the interfacial structure of the water film and contact potential. The simulations reveal multiple metastable states of the contact potential, consistent with existing theoretical models. The results show that the contact force is influenced by the structure of the water film, including oscillation forces and stratification. This provided verification and development for existing theoretical models based on metastable contacts

Keywords: Quartz; Molecular simulation; Adhesion; Multiple metastable states; Slow dynamics

Online publication: April 7, 2025

1. Introduction

The softening of near-surface space is caused by strong ground motion generated by large earthquakes. From a physical perspective, near-surface softening and healing are controlled by the dynamic elastic properties of the shallow geomaterials, characterized by strong nonlinear elasticity, stress-strain hysteresis, and slow dynamics, associated with long-term healing processes. The dynamic elastic properties of geomaterials are mainly determined by the contact between grains. For near-surface consolidated geomaterials under low confining pressure, contact mechanics between grains is primarily related to surface energy^[1,2]. Therefore, the investigation of surface force and energy on the interface is significant in explaining phenomena during strong earthquakes, such as long-time relaxation and slow dynamics^[3,4].

The surface force was first incorporated into the contact deformation analysis between grains by Sharma *et al.*^[5]. The existence of a second equilibrium state (metastable state) was theoretically proposed and connected to the hysteresis effect, further confirmed by Smith *et al.* and Averbakh *et al.*^[6, 7]. Our group proposed a theoretical contact model between mineral grains in geomaterials containing multiple metastable contacts at slight separations

due to the oscillatory hydration interaction. It was used to explain the two-stage recovery process of the site shear-wave velocity after a strong earthquake ^[8].

In this study, MD simulation is used to study the thickness of the equilibrium water film between the planes of amorphous quartz particles and obtain the equilibrium thickness and separation force curve. Meanwhile, the density and orientation angle profile are studied to investigate the relationship between the interfacial structure of water film and contact potential.

2. Models, methods, and simulation details

2.1. Construction of the hydroxylated quartz surfaces

A quartz lamella is constructed in the following fashion. Firstly, an α -quartz cubic periodic crystal was built using Materials and Processes Simulations (MAPS) crystal builder. The quartz crystal cell used for simulation was obtained from crystallographic structure databases. After that, the crystal was cleaved to obtain the surface. Considering the widespread existence of water in near-surface geotechnical materials, the quartz surface shall be hydroxylated. The annealing process was applied to turn the crystalline quartz into amorphous quartz. The bulk and surface properties of quartz system are greatly influenced by the annealing procedure. To obtain an amorphous silica slab for simulation with correct structural properties, a fairly high temperature of 4000 K was chosen for annealing. The steps were shown in **Figure 1**.

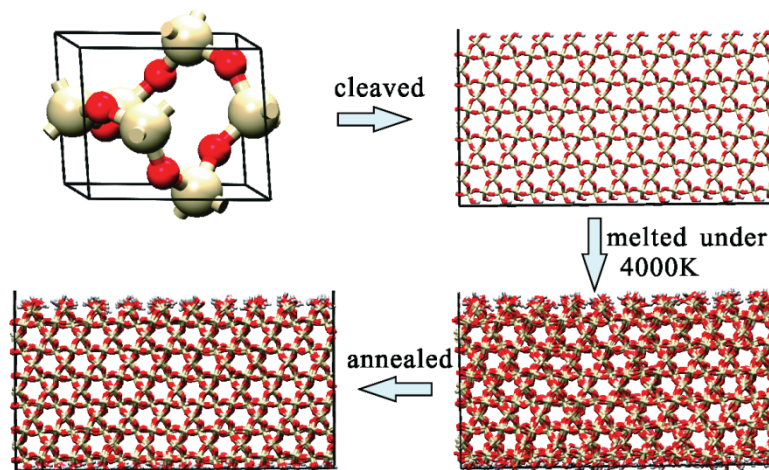


Figure 1. The construction process of quartz slab.

2.2. Construction of contact model

Considering the existence of water film, the slab-on-slab geometry was adopted instead of the conventional ball-on-slab model to control the number of water molecules confined within the slabs under periodic boundary conditions. **Figure 2(a)** illustrates the simulation system used for studying the relationship between adhesion force and separation distance on the nanoscale contact of quartz surfaces. Detailed heights of each portion are shown in **Figure 2(b)**. Our research chose amorphous quartz due to its wide distribution on rock and soil ^[9].

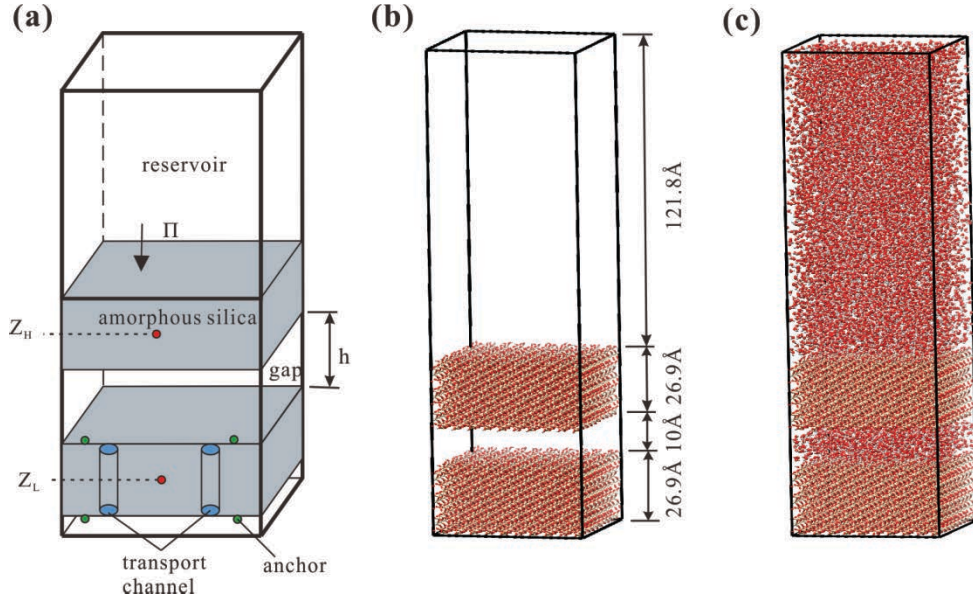


Figure 2. (a) schematic diagram of contact model. The pressure is applied to all atoms in the top quartz slab; due to the squeeze effect, the water molecules will migrate between the interlayer and reservoir through the channels till the applied pressure is balanced by force between the two slabs. (b) contact model without water. (c) contact model filled with water

2.3. Force fields

Simulations were performed with the extended Amber force field, as implemented in the large-scale atomic/molecular massively parallel simulator (LAMMPS) [10, 11]. Considering that the materials involved in the simulation are mainly quartz and water, the parameter set developed by Emami *et al.* was employed [12].

2.4. Simulation settings

Initially, the upper quartz slab was placed above the substrate at h , beyond the expected equilibrium gap. As simulation starts, the top slab moves toward the substrate until equilibrated. Due to the uneven water film, the following formula was used to calculate the effective thickness.

$$h = \int_{Z_L}^{Z_H} \frac{\rho_W(z)}{\max(\rho_W(z))} dz \quad (1)$$

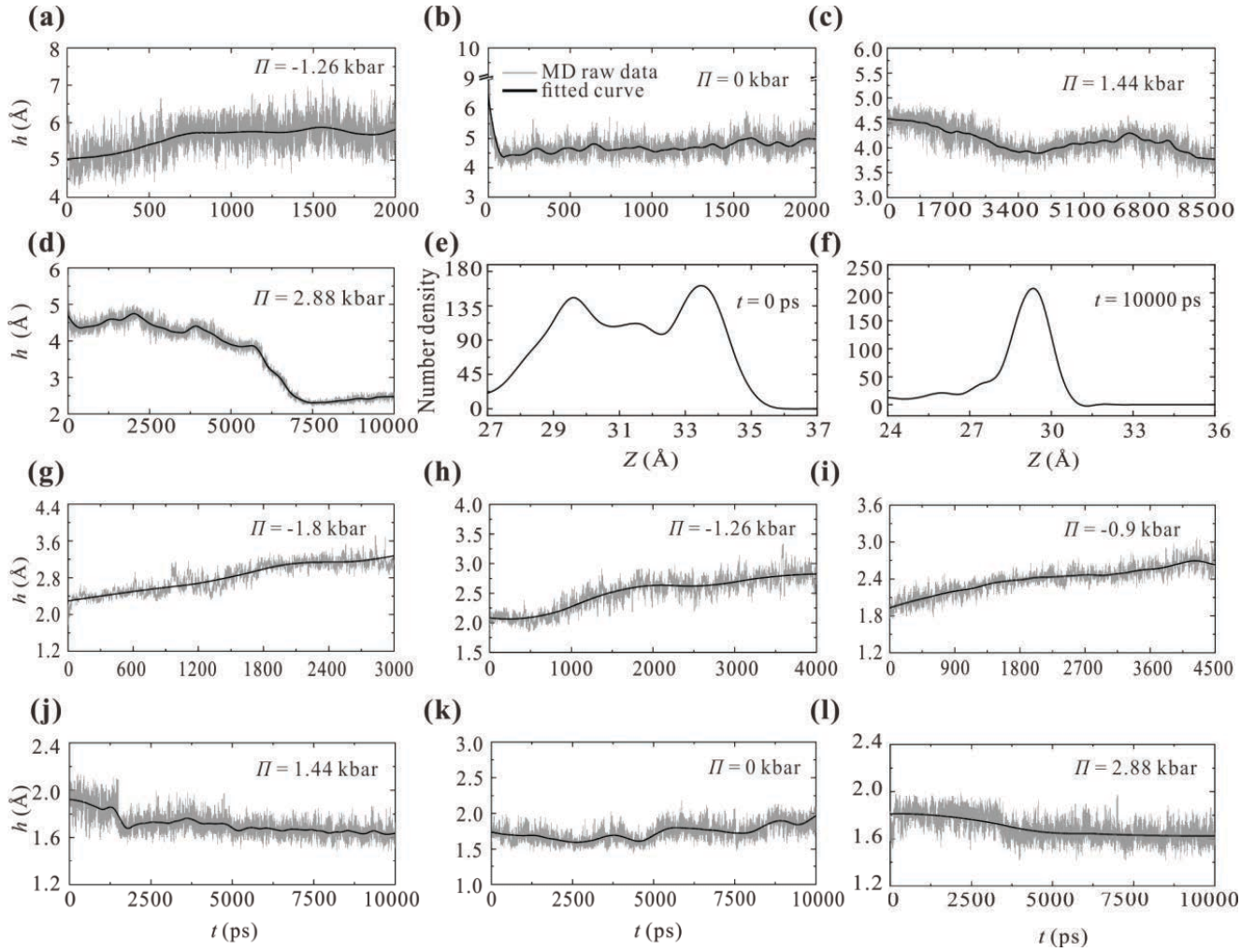
Among them, Z_H , Z_L are the barycentric coordinates of the top and bottom quartz slab respectively. $\rho_W(z)$ is the number density of water molecules in the z -direction.

3. Results and discussion

Although the theoretical model proposed by our group fits well with the two-stage recovery process of the site after a strong earthquake, the relationship between thickness and separation force within 1 nm still lacks verification from atomic level. Therefore, it is necessary to study the contact potential between quartz surfaces with nano water film using MD. In this study, the force-distance curves were shown in **Figures 3** and **4**.

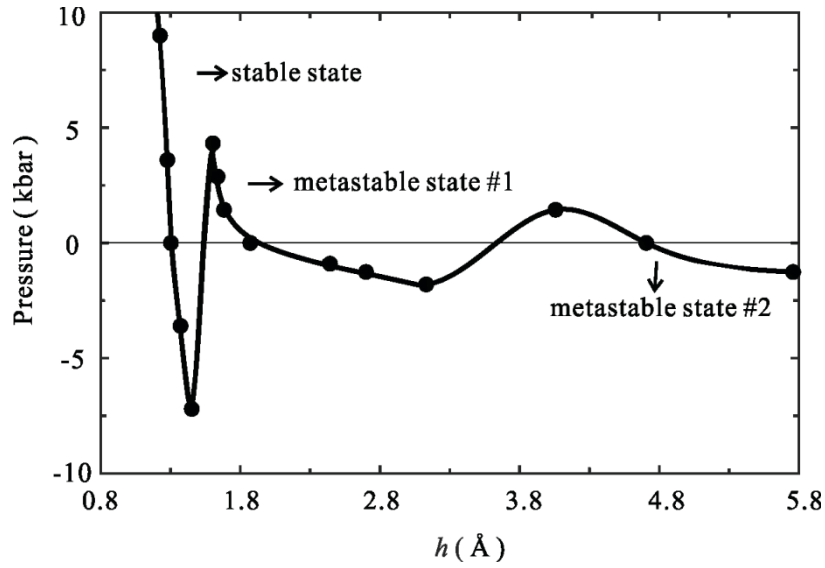
Figure 3 shows the time changes of h under different pressure. In **Figures 3(a)** and **3(b)**, the contact system reached equilibrium without a trend of change. The effective thickness h for applied pressure was calculated by averaging the stable section. As shown in **Figure 3(c)**, the equilibrium under positive pressure took more time than under negative pressure, due to the repulsive interaction between the slabs. Although the h fluctuated after

equilibrium, the unchanged position of the top slab confirmed the fact of equilibrium. **Figure 3(d)** showed an irreversible drop of h under 2.88 kbar, indicating a state change. Further confirmation in the density profile was shown in **Figures 3(e)** and **3(f)**. **Figure 3(g)-(l)** showed the time changes of h in the new state (the first metastable state). The effective thickness h decreased with the increase of positive pressure, while it increased with the rise of negative pressure.



Figures 3. The time changes of h in different simulation conditions. The gray and black lines represent raw data of MD and its fitted curve. According to their states, (a)–(c) refers to the time changes of h for the second metastable state; the shift from the second metastable to the first metastable state was shown in (d)–(f), (g)–(l) refers to the time changes of h under different pressure for the first metastable state.

So far, the stable and metastable states were obtained through the process above. The relationship between contact force and effective thickness is shown in **Figure 4**. In addition to the first global minimum, there were another two local minimums in the force-distance curve, indicating the existence of multiple metastable states on the contact of quartz particles in the presence of nanometer water film.



Figures 4. Dependence of the pressure on water layer thickness.

The contact relationship had a double sigmoidal shape. The existence of these states indicated the multiple metastable contacts of quartz with the presence of nano water film. **Figure 5** illustrates the spatial distribution and orientation of water molecules at the interface between two quartz plates.

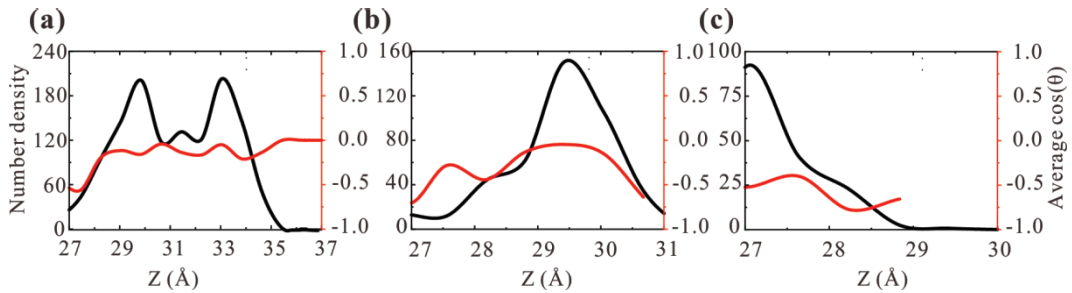


Figure 5. Profiles of density and average cos of orientation angle for the metastable and stable state: (a) For the second metastable state; (b) For the first metastable state; (c) For the stable state

Previous research indicates that water layers between solid surfaces exhibit density oscillations, which may contribute to the multi-stable states of the contact curve. The density profile of the second metastable state shown in **Figure 5(a)** shows two peaks and a middle platform, dividing the water layer into three regions: a lower adsorption layer from 27 Å to 30.65 Å, a stable layer from 30.65 Å to 32.25 Å, and an upper adsorption layer from 32.25 Å to 35.45 Å. The peaks indicate repulsion and attraction between water molecules and the quartz surface. A smaller peak in the stable layer suggests the presence of oscillation forces, consistent with experimental data on mica. The orientation angle profile shows no dominant orientation, indicating minimal polarization force contribution.

In the first metastable state in **Figure 5(b)**, the density profile has a single peak shifted to the right, likely due to transport holes on the lower surface. The distances from the peak to the upper and lower surfaces are 2.42 Å and 1.87 Å, respectively. The orientation angle profile shows a clear orientation angle, with water molecules gradually pointing toward the lower surface. In the stable state shown in **Figure 5(c)**, the density profile decreases monotonically without peaks, indicating that the force between surfaces is primarily Van der Waals. The

correlation between the density profile peaks and the multi-stable states of the contact curve highlights the role of oscillation forces in the interaction between quartz surfaces.

In **Figure 6**, the density profiles have the same double-peak shape under different pressures for the second metastable state. When the positive pressure was applied, the width of the profile decreased from 9.25 Å to 7.56 Å, but the distance between peaks and quartz surfaces did not change. Similarly, the negative pressure increased in the middle stable zone. So, for the second metastable state, the applied pressure mainly led to the change of the stable layer in the middle of the water film and had little effect on the adsorbed layer on the two sides.

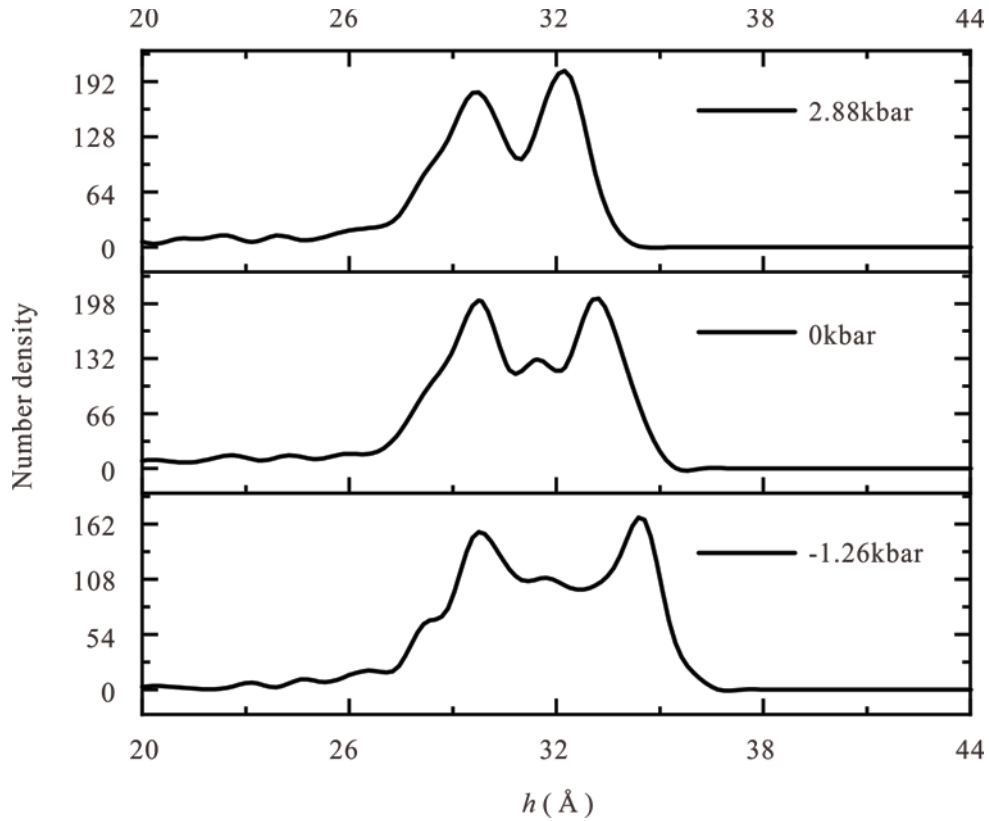


Figure 6. Evolution of density profile under different pressure for the second metastable state.

4. Conclusion

A general model is established to obtain the contact potential between quartz surfaces with nano water film using MD simulations. The contact potential is underpinned by the Lennard-Jones potentials between two quartz and solvation forces related to the structure of the water film. Multiple minima of contact curves are revealed by simulation results, indicating the multiple metastable states of contact potential between quartz. The results agree with the previous atomic microscope tests. Still, the simulation showed that the position of the stable state was closer to the surface, probably due to the difference between the slab and probe. Considering the characteristics of Lennard-Jones potentials, the multiple metastable states are mainly caused by the nano water film between quartz. Density profiles confirm the existence of oscillation force and the stratification of confined water. Due to the consistency of layer number and state, density profiles of different states reveal the relationship between layered water film and metastable states. In addition, the orientation angle profiles show that the polarization force contributes little to the contact force. These provide a preliminary reference for modeling the contact relationship of quartz slabs in the presence of nano water film.

Disclosure statement

The author declares no conflict of interest.

References

- [1] Clark VA, Tittmann BR, Spencer TW, 1980, Effect of Volatiles on Attenuation (Q^{-1}) and Velocity in Sedimentary Rocks. *Journal of Geophysical Research: Solid Earth*, 85: 5190–5198.
- [2] Lebedev AV, Ostrovsky LA, 2014, A Unified Model of Hysteresis and Long-Time Relaxation in Heterogeneous Materials. *Acoustical Physics*, 60: 555–561.
- [3] Zaitsev VY, Gusev VE, Tournat V, et al., 2014, Slow Relaxation and Aging Phenomena at the Nanoscale in Granular Materials. *Physical Review Letters*, 112(10): 108302.
- [4] Shokouhi P, Rivière J, Guyer RA, et al., 2017, Slow Dynamics of Consolidated Granular Systems: Multi-Scale Relaxation. *Applied Physics Letters*, 111(25): 251604.
- [5] Sharma MM, Tutuncu AN, 1994, Grain Contact Adhesion Hysteresis: A Mechanism for Attenuation of Seismic Waves. *Geophysical Research Letters*, 21(21): 2323–2326.
- [6] TenCate JA, Smith E, Guyer RA, 2000, Universal Slow Dynamics in Granular Solids. *Physical Review Letters*, 85(6): 1020.
- [7] Averbakh VS, Lebedev AV, Maryshev AP, et al., 2009, Observation of Slow Dynamics Effects in Nonconsolidated Media Under In Situ Conditions. *Acoustical Physics*, 55(3): 211–217.
- [8] Wang S, Zhuang H, Zhang H, et al., 2021, *Nature Communications*, 12: 1.
- [9] Liang L, Xiong J, Liu X, 2015, Investigation of Pore Structure and Fractal Characteristics of Organic-Rich Yanchang Formation Shale in Central China by Nitrogen Adsorption/Desorption Analysis. *Journal of Natural Gas Science and Engineering*, (22): 62–72.
- [10] Cornell WD, Cieplak P, Bayly CI, et al., 1996, A Second Generation Force Field for the Simulation of Proteins, Nucleic Acids, and Organic Molecules. *Journal of the American Chemical Society*, 118(9): 2309.
- [11] Plimpton S, 1995, Fast Parallel Algorithms for Short-Range Molecular Dynamics. *Journal of Computational Physics*, 117(1): 1–19.
- [12] Emami FS, Puddu V, Berry RJ, et al., 2014, Force Field and a Surface Model Database for Silica to Simulate Interfacial Properties in Atomic Resolution, *Chemistry of Materials*, 26(8): 2647–2658.

Publisher's note

Bio-Byword Scientific Publishing remains neutral with regard to jurisdictional claims in published maps and institutional affiliations.

ISSN (ONLINE): 2208-3537

ISSN (PRINT): 2208-3529



Journal of Architectural Research and Development

Focus and Scope

Journal of Architectural Research and Development is an international peer-reviewed and open access journal which is devoted to establishing a bridge between theory and practice in the fields of architectural and design research, urban planning and built environment research.

Topics covered but not limited to:

- Architectural design
- Architectural technology, including new technologies and energy saving technologies
- Architectural practice
- Urban planning
- Impacts of architecture on environment

About Publisher

Bio-Byword Scientific Publishing is a fast-growing, peer-reviewed and open access journal publisher, which is located in Sydney, Australia. As a dependable and credible corporation, it promotes and serves a broad range of subject areas for the benefit of humanity. By informing and educating a global community of scholars, practitioners, researchers and students, it endeavors to be the world's leading independent academic and professional publisher. To realize it, it keeps creative and innovative to meet the range of the authors' needs and publish the best of their work.

By cooperating with University of Sydney, University of New South Wales and other world-famous universities, Bio-Byword Scientific Publishing has established a huge publishing system based on hundreds of academic programs, and with a variety of journals in the subjects of medicine, construction, education and electronics.

Publisher Headquarter

BIO-BYWORD SCIENTIFIC PUBLISHING PTY LTD

Level 10

50 Clarence Street

Sydney NSW 2000

Website: www.bbwpublisher.com

Email: info@bbwpublisher.com

OUR JOURNALS



The *Journal of Architectural Research and Development* is an international peer-reviewed and open access journal which is devoted to establish a bridge between theory and practice in the fields of architectural and design research, urban planning and built environment research.

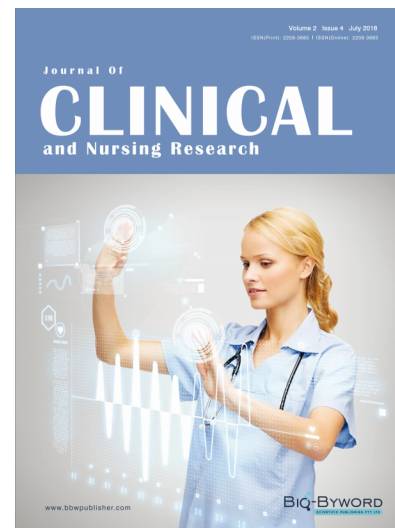
Topics covered but not limited to:

- Architectural design
- Architectural technology, including new technologies and energy saving technologies
- Architectural practice
- Urban planning
- Impacts of architecture on environment

Journal of Clinical and Nursing Research (JCNr) is an international, peer reviewed and open access journal that seeks to promote the development and exchange of knowledge which is directly relevant to all clinical and nursing research and practice. Articles which explore the meaning, prevention, treatment, outcome and impact of a high standard clinical and nursing practice and discipline are encouraged to be submitted as original article, review, case report, short communication and letters.

Topics covered by not limited to:

- Development of clinical and nursing research, evaluation, evidence-based practice and scientific enquiry
- Patients and family experiences of health care
- Clinical and nursing research to enhance patient safety and reduce harm to patients
- Ethics
- Clinical and Nursing history
- Medicine



Journal of Electronic Research and Application is an international, peer-reviewed and open access journal which publishes original articles, reviews, short communications, case studies and letters in the field of electronic research and application.

Topics covered but not limited to:

- Automation
- Circuit Analysis and Application
- Electric and Electronic Measurement Systems
- Electrical Engineering
- Electronic Materials
- Electronics and Communications Engineering
- Power Systems and Power Electronics
- Signal Processing
- Telecommunications Engineering
- Wireless and Mobile Communication

